Investigation into synthetic protease-sensitive hydrogels as siRNA nanoparticle delivery vehicles.

Emma Doubell

DBLEMM001

SUBMITTED TO THE UNIVERSITY OF CAPE TOWN

In fulfilment of the requirements for the degree MSc (Med) Biomaterials

Faculty of Health Sciences

UNIVERSITY OF CAPE TOWN

Supervisor: Associate Professor Neil H Davies

Cardiovascular Research Unit, Department of Surgery

Date of submission: 19 February 2018

Declaration

I, Emma Doubell, hereby declare that the work on which this dissertation/thesis is based is my original work (except where acknowledgements indicate otherwise) and that neither the whole work nor any part of it has been, is being, or is to be submitted for another degree in this or any other university.
I empower the university to reproduce for the purpose of research either the whole or any portion of the contents in any manner whatsoever.

Signature: Signed by candidate

Date: 19 February 2018

Abstract

RNA interference (RNAi) is receiving increasing attention as a form of gene regulation able to temporarily silence gene expression through post transcriptional mechanisms. RNAi agents have shown promise in targeting a range of ailments from cancers to myocardial infarction. However, RNAi based therapeutics have not passed the clinical trial stage of development, in part due to lack of optimal delivery mechanisms.

One means towards improving delivery is the development of localised and sustained delivery systems for the RNAi molecule. Such approaches are important as it has previously been found that systemic delivery often leads to off target effects and rapid clearance. The aim of this project has been to assess the utility of an enzymatically degradable polyethylene glycol (PEG) hydrogel as a localised delivery vehicle. Enzymatically degradable PEG hydrogels that rely on cellular invasion for their degradation might enable the release of entrapped RNAi agents to surrounding cells as well as transfection of invading cells.

The cationic polymer poly(ethyleneimine) (PEI), was used as a tool to investigate the PEG hydrogel as a localised delivery vehicle. Thus, an initial objective of this study was the establishment and characterisation of the PEI/siRNA nanoparticle technology in our group. siRNA was found to be fully complexed at a PEI nitrogen to siRNA phosphate ratios of 5:1 and higher. A 10:1 ratio and higher were able to protect the siRNA from RNases present in serum for 7 days with up to 65% of RNA still intact. A 40:1 ratio was found to be cytotoxic. A 20:1 ratio was found to be the most effective at gene knock down and determined to be optimal.

As there is a relatively limited volume available in the PEG hydrogel system used here for loading with PEI/siRNA nanoparticles, a study was conducted to assess the maximum concentration of siRNA at which effective nanoparticles could be formed. Somewhat unexpectedly it was found that at a concentration of 7.5 µM siRNA, nanoparticles showed a significant 40% reduction in transfection efficacy of cells cultured in 2D. This finding for PEI nanoparticles indicating a limitation in the dosage attainable in the PEG hydrogel system.

The influence of PEG encapsulation for PEI/siRNA nanoparticles on RNase protection was assessed by exposing hydrogels with entrapped nanoparticles to serum RNases. The PEG hydrogel was found to significantly improve PEI based protection from RNase degradation in the initial 24 hours and this

protection persisted for up to 5 days. PEI/siRNA nanoparticles were retained after encapsulation within PEG hydrogels for up to 7 days whilst siRNA alone was entirely released after 24 hours. It is possible that this is a limitation of the system.

A 3D invasion assay was developed to more closely mimic the *in vivo* scenario where cells could invade a PEG hydrogel with entrapped nanoparticles but are not initially exposed to high concentrations of nanoparticles prior to hydrogel polymerisation. The assay involved the formation of dermal equivalents (cells entrapped within contracted collagen) that were encapsulated within a PEG hydrogel. Cells were observed invading the hydrogel within 1 hour of polymerising and continued to do so for up to 7 days. Invading cells were seen to take up the fluorescent siRNA although this uptake was scant and challenging to quantify. When commercial cell death siRNA sequence nanoparticles were encapsulated, a trend towards higher death levels was observed.

In conclusion, PEI/siRNA nanoparticles and related RNAi based assays have been formally established in our laboratory and can be used in the future for other applications. A 3D cell invasion assay was developed which more closely mimics the *in vivo* scenario where hydrogels bearing siRNA are polymerised within tissue. The increased RNase protection though relatively slight is important for the use of hydrogels as localised delivery depots in an *in vivo* environment. Potential dose limitations of the PEG hydrogel system when using PEI nanoparticles and their apparent very tight encapsulation in the PEG hydrogels suggests the need for modifications of both nanoparticles and hydrogels to optimise efficacy. Future investigations into scaffold based localised siRNA delivery should be facilitated by the methodologies and assays established in this study.

Acknowledgements

I would like to thank my supervisor, Associate Professor Neil H. Davies, for the patience and guidance that he has given me over the years, especially during the final stages of my write-up.

Helen Ilsley, thank you for always supporting me and for being my “Work Mum” during my period in the Cardiovascular Research Unit (CVRU). My Mum and I appreciate this support very much.

To the members of the Polymer Lab, thank you so much for always being kind and supportive, and for answering my endless questions. To all of my laboratory mates in the Biology Lab, a special thanks for tolerating my pedantic requests and my very particular nature. I would especially like to thank Carla Gustafsson for helping me with both my lab work and my write-up: your assistance has been invaluable!

I have been very lucky to have enjoyed the tremendous support from many members of the CVRU, in particular Raymond Michaels and Paul Human. Paul has given me much guidance and statistical assistance, for which I am tremendously grateful.

Finally, I would like to say a huge thank you to my Mum, Dad, Spencer, Jane and Denver and other members of my family for tolerating my crazy requirements and helping me wherever possible.

Table of contents

List of tables

List of figures

List of Appendices:

List of Abbreviations

Arginine-Glycine-Aspartat amino-acid sequence	RGD
Diethyl Pyrocarbonate	DEPC
Destabiliased Green Fluorescent Protein	deGFP
Dimethyl Sulfoxide	DMSO
Dulbecco's Modified Eagle's Medium	DMEM
Deoxyribonucleic acid	DNA
Epidermal growth factor	EGF
Foetal Bovine Serum	FBS
Litre	L
Micrograms	µg
Micro RNA	miRNA
Milligram	mg
Millilitre	ml
Nano moles	nmol
Nitrogen to Phosphate	N:P
Phosphate buffered saline	PBS
Iso-osmotic PBS	Iso-PBS
Penicillin / Streptomycin	P/S
Polyethylenimine	PEI
Poly(ethylene glycol)	PEG
Revolutions per Minute	RPM
Ribonucleic acid	RNA
RNA interference	RNAi
Room temperature	RT
Sodium Bicarbonate	$NaHCO_3$
Sodium Dodecyl Sulfate	SDS
Sodium Hydroxide	NaOH
Sulfhydryl	SH
Triethanolamine	TEOA
TRIS / Borate / EDTA	TBE
Tris / EDTA	TE
Vinyl sulfone	VS
Water	H_2O

1. Literature Review

1.1 RNA interference (RNAi)

In recent years interest in the use of RNAi as an alternative therapeutic for disease has grown. It offers researchers the opportunity to exploit endogenous pathways to combat disease. RNAi involves the posttranscriptional gene silencing of a target sequence including those targets previously considered "undruggable"[1]. The silencing of target sequences can take the form of either irreversible cleavage of the mRNA strand or the prevention of its translation to protein.

Although originally observed in plants[2], RNAi was first fully described in the nematode worm, *Caenorhabditis elegans*, in the late 1990's by Andrew Fire and Craig Mello[3]. In their study they observed a reduction in endogenous protein production in *C. elegans* after introducing long double stranded RNA molecules.

Since its discovery, RNAi has become increasingly used as a research tool investigating gene function, but of at least equal importance is its potential as a new therapeutic approach[4]. Over the last decade the number of RNAi related patents has increased drastically, with nearly 500 patent applications as well as issued patents pertaining to the use of one form of RNAi alone annually[5], demonstrating the potential for RNAi as a therapy.

1.1.1 RNA interference structure and mode of action

The suppression of gene translation is activated by the presence of either endogenous or exogenous double-stranded RNA (dsRNA). Micro RNAs (miRNAs) are the body's endogenous regulators of gene expression, and have been found to be important regulatory factors in both animals and plants[6]. They are non-coding strands of 21-24 base pairs in length and have the ability to silence multiple different mRNA sequences due to having partial homology with many target sequences. Short hairpin RNAs (shRNAs) are in essence exogenous in their origins, however they are synthesised endogenously. They are transcribed from plasmid DNA (pDNA) which has been introduced into the cell's nucleus often via a viral vector. Small interfering RNAs (siRNA) are usually synthetically derived double stranded RNA sequences of similar length to miRNA which may be introduced into the cells cytoplasm via a vector. siRNAs can be synthesized or produced via different methods: chemical synthesis, *in vitro* transcription, enzymatic digestion of double stranded RNA, and finally transfection of a pDNA encoding shRNA which are then converted to siRNAs[7]. Both siRNA and shRNA are designed to have

full complementarity with a target mRNA sequence. A high degree of strand specificity or homology can result in the immediate irreversible cleavage of the target mRNA while incomplete homology often results in translation repression[8].

These differing forms of RNA are also related to each other when their processing in the cell is compared. They are all processed in virtually the same way but enter the pathway at different stages (Figure 1). miRNA genes are transcribed usually by RNA polymerase-II to form primary miRNA (pri-miRNA) transcripts containing a stem-loop. The stem-loop is recognised by Drosha, an RNase III like enzyme, in the nucleus[9,10]. Drosha processes the transcript into pre-miRNAs, an approximately 60-70 nucleotide long stem loop which has 3' overhangs with hydroxyl-termini and 5' phosphates[9]. Pre-RNA are then transported out of the nucleus by Exportin-5 where they are cleaved by Dicer into dsRNA to become functional miRNA[8]. The dsRNA is then dissociated by the incorporation of the antisense strand, known as the guide strand, into the RNA induced silencing complex (RISC), a multi-protein complex including Argonaut 2 (Ago2), which then binds to complementary target mRNA sequences at the 3'-unstranslated region (UTR). Ago2 is an RNase that is the catalytic element of the RISC[11]. However, it is often the case that miRNA binding takes place with incomplete homology and therefore elicits translation repression whereby the strands lack complementarity at the cleavage site thereby blocking the so called "slicer activity" observed during direct cleavage of a target strand[12]. As such miRNA can lead to translational repression, as well as mRNA degradation by deadenylation, decapping or exonuclease action and in a very few cases where there is a high degree of complementarity, mRNA cleavage by AGO protein[13–15].

When plasmids encoding shRNA are introduced into the cell and transcribed, the resulting transcripts form stem-loop structures known as pre-shRNAs or pre-miRNA mimics that are transported out of the nucleus into the cytoplasm in the same manner as pre-miRNAs. They are then processed by Dicer into siRNA which is then further processed into single stranded RNAs (ssRNA) and incorporated into the RISC to induce silencing of mRNA target sequances[8,16]. The siRNA directs the RISC to the target mRNA sequence. Ago2, cleaves the target sequence 10 nucleotides from the 5' end of the strand[17]. Once cleaved the mRNA sequence is released and the guide strand is free to bind another mRNA. A drawback to the use of shRNAs in the clinic is the use of pDNA. pDNA requires nuclear shuttling in order to function. This is often achieved with viral vectors which have their own set of associated shortcomings which will be briefly discussed later. With the use of DNA there is also a risk of insertional mutagenesis which is not a risk associated with RNA present in the cytoplasm.

siRNAs can be introduced via multiple methods, how it is introduced to the cell determines at which step in the process it enters – either in the nucleus in the form of shRNA as described above or directly into the cytoplasm. Delivery of siRNAs directly to the cytoplasm negates the need for nuclear shuttling as the siRNA enters the pathway after processing by Dicer and before cleavage by Ago2.

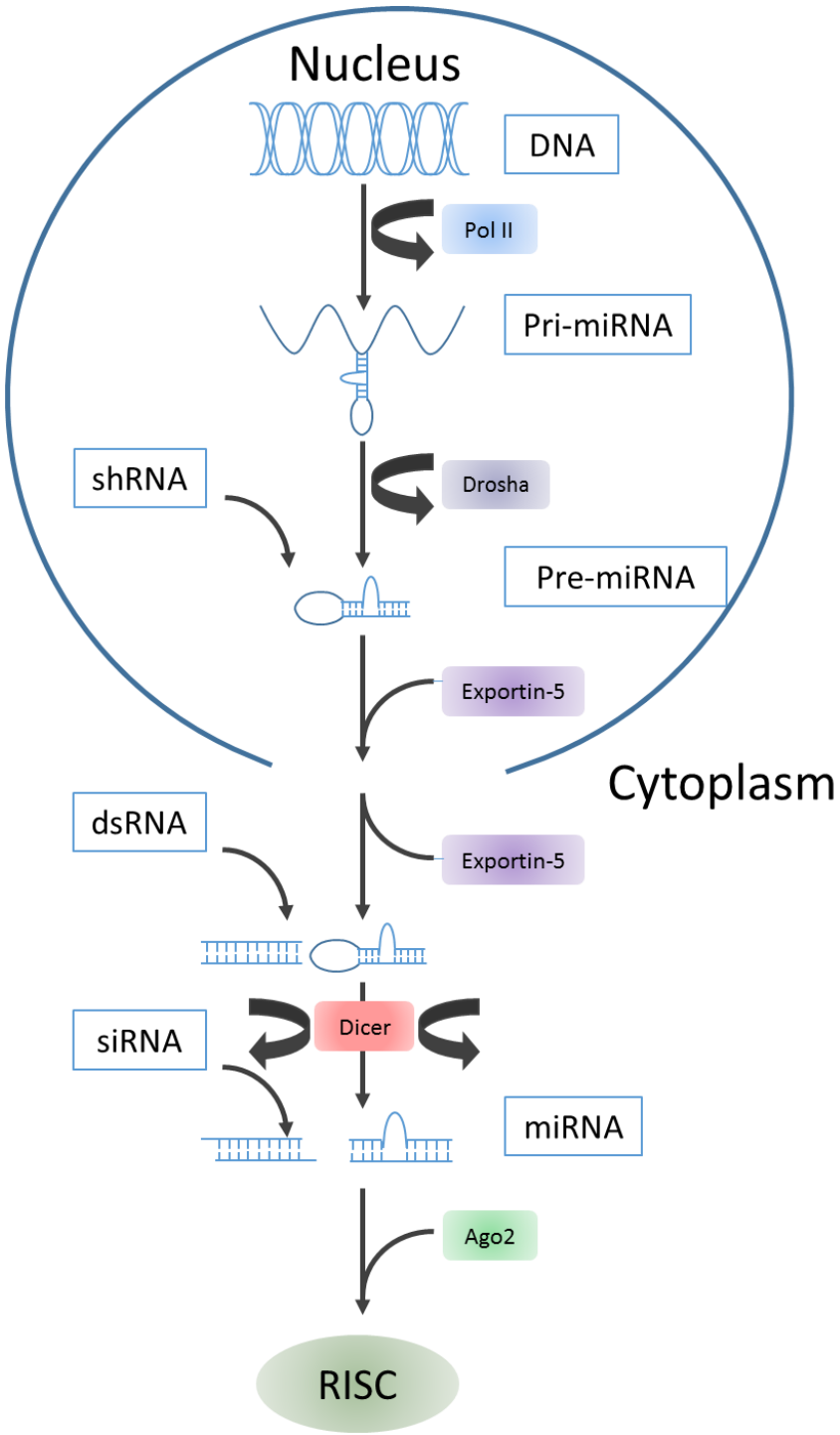

Figure 1: RNAi pathway. *RNAi pathway illustrating the different points at which the various forms of RNAi oligonucleotide enter the pathway to elicit gene silencing. Figure adapted from siRNA Versus miRNA as Therapeutics for Gene Silencing[13] and RNAi the Natural Way[18].*

1.2 RNA interference: challenges to translation to the clinic

Despite much promise as a therapeutic, one of the major constraining factors to the use of RNAi in a clinical setting is its delivery into the cell. Both intracellular as well as physiological obstacles prevent the efficient delivery of RNAi molecules and need to be overcome before its use as a therapeutic can be fully realised. In order to initiate the RNAi pathway, the RNAi molecule needs to be transported to the cytoplasm, to the RNAi machinery so as to induce silencing of the target mRNA. RNAs are negatively charged due to their phosphate backbones and as such cannot easily pass through the cellular membrane – which is of similar charge – without some form of transport vehicle aiding in its delivery[19,20]. Furthermore, RNA molecules are hydrophilic and too large to readily diffuse through the hydrophobic lipid bilayers of the cell membrane[21]. Moreover upon cellular uptake, RNAi molecules need to escape degradation in the endo-lysosome. Therefore, any delivery agent used should aid in RNAi agent transport across the cell membrane and in endo-lysosomal escape. When delivering RNAi systemically, physiological barriers need to be considered. RNAi molecules are subject to degradation by nucleases and it has previously been reported that RNAi molecules have a half-life of less than 1 hour in serum[22]. Other concerns also include the possibility for off target effects, rapid clearance from circulation and localisation to the liver and kidneys[23], the potential of overwhelming the endogenous machinery used to process the double stranded RNA[24], and inducing an innate immune response[25–28]. As such, much of what is delivered never has an effect on the target site[29]. The delivery concerns mentioned above are very similar for both siRNA and miRNA[13].

1.2.1 Delivery methods

A variety of approaches towards achieving gene expression regulation have been utilised. These approaches have been designed to overcome some of the aforementioned barriers to RNAi delivery, and include the use of biological vectors, RNA modification, high repeated doses of RNA and RNA incorporation into nanoparticles.

1.2.1.1 Viral vectors

Viral vectors encoding shRNA have been used for a number years to induce RNAi[13] and overcome many of the obstacles described above for the delivery of RNAi oligonucleotides. They have advantages in that they have the ability to efficiently enter the host cell and integrate into the genome which results in prolonged silencing[4,30]. They are also not prone to degradation, therefore the RNA is protected until transcribed. The studies below are examples of some of the successes which have been reported using viral vectors but associated dangers are also highlighted.

Their utility in identifying therapeutically useful miRNA sequences for myocardial infarctions has recently been demonstrated in a mouse model. In a study conducted by Eulalio *et al*[31]., a high-throughput functionalised screening of miRNAs was performed to determine which miRNA sequences, if administered, would induce cardiac regeneration in the form of cardiomyocyte proliferation. They were able to identify forty miRNA sequences which increased DNA synthesis and cytokines in neonatal cardiomyocytes, two of which, hsa-miR-590 and hsa-miR-199a, were selected for further testing. An adeno-associated virus (AAV) vector expressing the selected strands was injected into the peri-infarct zone of female adult CD1 mice that had undergone permanent left anterior descending coronary artery ligation. Echocardiography assessment indicated that the left ventricular ejection fraction, fractional shortening, end-systolic anterior wall thickness, as well as other associated parameters were significantly maintained compared to controls' measured over 60 days. Infarct size was also significantly reduced (± 15% smaller compared to non-treated controls).

Viral vectors have reached the clinical trial stage for the delivery of siRNA ex vivo[32], whereby cells are modified and then reintroduced into the patient. In one such pilot study, five patients being treated for AIDS-related non-Hodgkin's lymphoma (NHL) received autologous CD34+ haematopoietic progenitor cells (HPC)[33]. The study aimed to use RNAi based gene therapies to control HIV infection and demonstrate persistence for a number of months post treatment. Autologous HPCs were transduced with a self-inactivating lentiviral vector which encoded a siRNA that targeted chemokine receptor 5 (CCR5). CCR5 is an endogenous chemokine receptor in CD4+ T-cells and is a co-receptor for HIV-1 infection but is not an essential component for normal T-cell function, rendering it an ideal anti-HIV target. After receiving chemotherapy, patients were infused with the transduced cells. Patients responded positively to treatment with no short term toxicity concomitant with genetically altered cells being reported. They were able to demonstrate siRNA expression in human blood cells for up to 24 months post treatment, indicating the feasibility of RNAi for treatment of HIV in the future.
Follow up clinical trials[34] using similar methodology reported a similar safety profile and the feasibility of treatment was confirmed, however, none of the results achieved could conclude that therapy resulted in an improved disease state. The small number of patients enrolled in their clinical trial also did not allow for a true demonstration of safety with respect to possible genetic mutations.

However, despite these types of positive outcomes, there are many potential side effects associated with viral based delivery including mutagenesis, immunogenicity and the potential for there to be a continuous cellular presence of RNAi which in many cases is not desirable[35,36]. This is indeed the case when using vectors such as AAV's and retrovirus's. Long term silencing of some mRNA targets is

advantageous in certain pathological scenarios including the treatment of HIV, for many other diseases however, once a patient has recovered the silencing of a given mRNA sequence is no longer required.

Although many positives can be taken from the above studies safety concerns should still be noted. The risks associated with using viral vectors are highlighted in a study in which a viral vector was used to deliver a transgene. In the study, CD34+ bone marrow cells from five boys with X-linked severe combined immunodeficiency were transduced *ex vivo* using a defective retroviral vector[37]. Initially it was reported that there were no adverse effects due to the treatment. Later however, it was reported that one of the participants suffered adverse effects and developed acute lymphoblastic leukaemia as a result of participating in the trial due to an insertional mutagenesis event[38]. This finding raises concern with approaches such as the one detailed above in the clinical trial on AIDS related NHL.

1.2.1.2 Naked and modified siRNA

Though as detailed above, there are several obstacles facing the successful delivery of naked siRNA, there are many studies that have utilised this approach. Included below are studies where naked siRNA has been delivered *in vivo*, where it was either injected systemically or directly into the target organ. Some tissues have been found to internalise naked siRNA at a much higher level compared to others, these include the eye, central nervous system and lung, making direct delivery possible[39]. Naked siRNA is also considered to have a better safety profile compared to viral vectors as well as being more easily produced and therefore scalable.

High doses of unmodified siRNA have been rapidly injected into the blood vessels (described as hydrodynamic injection) of mice[40–43]. Rapid injection of a large volume is said to increase the permeability of endothelium and the cell membranes of parenchyma cells[44].

In a study looking at the use of siRNA as a potential treatment for hepatitis, hydrodynamic tail vein injection was employed to deliver siRNA against the *Fas* gene[42]. Fas is known to be a mediator of apoptosis in a broad range of liver diseases and it was postulated that inhibition of *Fas* would inhibit hepatocyte cell death and protect the liver from liver failure and fibrosis[45]. Using a Cy5-labelled *Fas* sequence they assessed hepatocyte uptake of the siRNA in mice. Twenty four hours post final treatment with 3 repeated high dose injections, uptake was assessed by flow cytometry and showed 88 ± 6% of hepatocytes to have taken up siRNA. Treatment with *Fas* siRNA led to an eight to tenfold reduction in levels of Fas mRNA as well as a reduction in the expression of Fas protein in hepatocytes

to almost background levels. The hepatocytes isolated from these mice were also found to be resistant to apoptosis when exposed to Fas-specific antibody.
Another study using hydrodynamic injection, investigated the use of siRNA in the treatment of acute liver failure in mice[43]. Caspase 8 was targeted as silencing of the caspase 8 gene inhibits Fas mediated apoptosis. They were able to demonstrate that treatment with siRNA was able to protect hepatocytes from apoptosis and therefore attenuate liver failure using this method of systemic delivery.

Age-related macular degeneration (AMD) is the breakdown of the eye's macula of the retina, which in some cases results from the abnormal growth of blood vessels and is often driven by vascular endothelial growth factor (VEGF). Elevated levels of VEGF are also associated with diabetic retinopathy[46], and retinopathy of prematurity[47]. siRNA has been used as a therapy in *in vivo* studies conducted in both mice[48] and primates[49] to down regulate VEGF expression. These studies showed that siRNA targeting VEGF resulted in a decrease in neovascularisation. In another study, siRNA was used to target VEGF, VEGFR-1, VEGFR-2 and a combination thereof, and also resulted in a significant reduction in neovascularisation[50]. These studies delivered the siRNA via direct injection into the eye, an otherwise isolated organ. A number of clinical trials have also been conducted and have reached phase I & II stages of development[24,32,51].

Though the above are very promising findings, there is a significant drive towards improving siRNA's half-life *in vivo*, its ability to cross the cell membrane, and to prevent immunogenicity via chemical modifications. Possible chemical modifications can be summarised into three different categories: internucleotide linkage modifications, sugar modifications, and nucleobase modifications (these include the incorporation of 2'-O-methyl and 2'-deoxy-2'-fluor groups)[52]. To improve the half-life of nucleotides in serum, modifications to the nucleotide linkages can be made in order to increase resistance to nuclease degradation. Sugar modifications made to the RNAi molecules can confer an increase in binding affinity for the target sequence. Modifications to the nucleobases can result in improved thermal stability and a reduction in immunogenicity.

The biodistribution and efficacy of systemically delivered RNAi molecules have been assayed in a number of studies. In one such study, Lewis *et al*[41]., employed hydrodynamic injection to co-deliver anti-luciferase siRNA with a firefly luciferase plasmid to determine if gene expression can be repressed in various organs. One day post injection the animals were euthanised and the organs collected for analysis. It was determined that luciferase expression was reduced by 80 – 90% relative to the luciferase plasmid alone in the liver, spleen, lung, kidney and pancreas. Not surprisingly these are all

well perfused organs. Braasch and colleagues[23] examined the distribution of modified siRNA. The group synthesised two siRNA molecules, the first with two phosphodiester modified strands (PO/PO) and the second with one phosphodiester strand and one phosphorothioate strand (PO/PS) in an effort to improve the pharmacokinetic properties of siRNA. The PO/PS strand showed higher levels of stability having remained intact for up to 72 hours in murine serum at 37°C relative to the PO/PO strand which was fully degraded after 24 hours. The strands were then further labelled with radioactive iodine. Mice were injected with the different formulations and the blood, liver, kidney, heart, spleen, lung, and brain were collected for analysis at various time points. Both the PO/PO and the PO/PS radiolabelled RNA were found to have preferentially accumulated in the liver and kidney over the course of the experiment. The levels of PO/PS in the blood were significantly higher than the PO/PO strand possibly due to superior stability. The PO/PS strand showed increased distribution to the lung, spleen, heart and brain compared to the PO/PO strand after 4 hours, although relative to other organs these were low. The levels of siRNA measured decreased after 24 hours in all the organs, but decidedly less in the liver and kidneys, and persisted for the full 72 hours of the experiment for both forms of siRNA. Treatment using naked siRNA delivered in this manner would therefore appear to be best suited to treat well perfused organs such as the liver and kidneys.

However, naked siRNA has its short comings that would make it less suitable for use in the clinic. As mentioned above naked RNAi oligonucleotides have difficulty crossing the cell membrane, a relatively short half-life in the blood due to the presence of RNases and systematically delivered siRNA is localised to the liver and kidneys and cleared from the system. Therefore high doses are required for there to be any noticeable effect[36,53–55] and this increases the chances of off target effects. While it is possible that dosages could be lowered by localised injection as opposed to systemic, alternatives are still needed.

1.2.2 Alternative vectors

Alternative vectors have been proposed to help overcome some of the limitations surrounding the use of RNAi oligonucleotides, such as the difficulty that RNAi molecules have crossing the cell membrane and the negative consequences of using viral vectors. Nanoparticle formulations have been proposed as a possible means to surmount both the physiological and intracellular barriers. These formulations interact with the siRNA in a number of ways including electrostatically binding, passively encapsulating, or covalently attaching to the siRNA to form usually slightly cationic complexes[53]. A plethora of formulations exist which include, cell penetrating peptides, cationic lipids, and cationic polymers.

The basic mechanism for cationic complexes to deliver RNAi cargo into the cell is as follows: The complexes bind to the cell surface via non-specific electrostatic interactions between the anionic cell surface and the cationic complexes and gain access to the cell via endocytosis or endocytosis like mechanisms[56]. Inside the endosome, the pH drops to 5.5 at which point some of the cargo escapes into the cytosol, the exact mode of endosomal or lysosomal escape differs depending on complex composition[56].

Below, studies that have investigated *in vivo* delivery with cationic vehicles are discussed with an emphasis placed on cationic lipids but more especially on cationic polymers as a cationic polymer was selected for use in this project. Multitudes of examples exist for each of the below sub headings, targeting a wide range of disease conditions, and are therefore too numerous to all be included here. Studies were selected as examples of the complexities and the delivery considerations involved in selecting a delivery vehicle, was made.

1.2.2.1 Peptides

Cationic cell-penetrating peptides (CPP) also known as peptide transduction domains are short strands of approximately 30 amino acids which are arginine- and/or lysine-rich[57]. The ability of some proteins to enter cells was first reported in the HIV Tat protein towards the end of the 1980's[58,59]. They are able to deliver the siRNA via direct penetration and/or existing endocytotic pathways which in general terms is a two-step process involving endocytic entry followed by endosomal escape[60]. The process can be activated via electrostatic interactions with cell surface proteoglycans or by direct interaction with the plasma membrane[61]. Endocytosis for CPPs and its cargo is via pinocytosis which can be further divided into four pathways: macropinocytosis, clathrin-mediated endocytosis, caveolae/lipid raft-mediated endocytosis, and clathrin/caveolae-independent endocytosis. The specific pathways utilised are related to the chemical and physical properties of the peptides and their cargo[62].

As with other nanoparticle formulations to be discussed later, various CPP formulations have been used to deliver siRNA to a range of targets[60] including those involved in cancer[63,64] and HIV[65]. In 2016 Welch et al[66]., reported on their use of a disulphide-constrained cyclic amphipathic peptide for the delivery of siRNA to cells in both *in vitro* and *in vivo* conditions. They were able to form non-covalent peptide siRNA complexes able to deliver siRNA into the cytoplasm. They demonstrated functional knockdown of the target gene expression of thyroid transcription factor-1 (TTF-1), a master regulator of cells in the thymus and lung, in human epithelial cells and mice when delivered locally.

Approximately 85% TTF-1 inhibition was achieved in A549 cells (human lung adenocarcinoma) and 40% in H441 cells (also human lung adenocarcinoma). In an *in vivo* experiment, whole lung expression of TTF-1 was analysed and it was found that TTF-1 protein levels were lower in mice treated with the peptide formulation with TTF1 siRNA compared to peptides formed with scrambled siRNA controls. Despite this success their complexes showed instability and over a period of 24 hours were unable to protect the siRNA from degradation by RNases present in FBS. It was therefore concluded that the siRNA-peptide formulations were best suited for *in vitro* delivery and localised *in vivo* delivery but that they were not well suited to systemic delivery.

There have also been concerns around the use of CPPs including cytotoxicity and immunogenicity which are caused by the disruption of the cell membrane[67]. The findings in the above study would also indicate that the use of CPPs is cell specific as they are not able to achieve the same levels of post transcriptional silencing in the H441 cell line compared to the A549 cell line. Other concerns regarding their use is the formation of insoluble aggregates - due to covalent interactions between the anionic siRNA and the cationic CPPs - which renders them ineffective and is an issue which is considered pivotal if CPPs are to be used succesfully[68–71].

1.2.2.2 Cationic lipids

First developed for gene delivery in 1987[72], the use of cationic lipids has grown considerably[73]. Cationic lipids contain a positively charged polar headgroup which is linked to a hydrophobic domain rendering them amphiphilic[56]. They are often combined with a neutral helper lipid to form liposomes. When the liposomes interact with siRNA they form what are referred to as lipoplexes and are also sometimes known as lipopolyplexes especially when there is an addition of a polycation[74,75]. Structurally the lipoplexes have multiple lipid bilayers with the RNAi molecules located between adjacent layers. Lipopolyplexes differ in that the RNAi molecules are located at the core within a polymer complex[75].

To gain entry into the cell the lipoplexes bind to the cell membrane via non-specific ionic interactions[76–78]. Endo-lysosomal escape is initiated by destabilisation of the endosome by the cationic lipid. Once inside the endosome the cationic lipoplexes form ionic pairs with the anionic lipids of the endosome membrane which results in siRNA release from the lipoplex and destabilisation of the membrane leading to siRNA release into the cytoplasm[79,80].

Sheng and colleagues[81] synthesised a lipid based nanoparticle using a natural steroid diosgenin cationic lipid (Diosarg) to which they added a 1,2-dioleoyl-sn-glycero-3-phosphatidylethanolamine

(DOPE) (a neutral lipid often used as a helper lipid) head group (Diosarg-DOPE). They showed that the addition of DOPE resulted in improved siRNA internalisation compared Diosarg alone. Diosarg-DOPE (1:1, 1:2 and 2:1)/ Cy3-siRNA nanoparticles displayed 1.77, 2.10 and 2.77-fold increases in siRNA internalisation compared to Diosarg/Cy3-siRNA complexes alone measured by flow cytometry. Warashina et al[82]., developed a novel cationic lipid based formula called YSK12-C4 to which they added a multifunctional envelope-type device (MEND) – also a lipid based nanoparticle – to target dendritic cells (DCs). Scavenger receptor class B type 1 was selected for gene knockdown experiments as it is an endogenous gene in bone marrow DCs. Their YSK12-C4 formulation achieved more than 90% knockdown compared to RNAi max which achieved a mere 57% in vitro. Both of these groups showed promising results, both having reported low cytotoxicity and high levels of transfection while only Warashina et al., demonstrated in vivo gene knockdown achieving significantly higher levels of gene silencing relative to the commercially available Lipofectamine RNAiMAX.

In another study Lee *et al.*,[83] developed a neutral nanoparticle termed small lipid nanoparticles (SLNPs) which were made of the cationic cholesterol derivative – mono arginine-cholesterol – and the neutral helper lipid DOPE as the major constituents and, a small amount of PEGylated phospholipid mixed with siRNA, for systemic delivery of siRNA for cancer treatment. Nanoparticles were between 45 and 52 nm in size and displayed low cytotoxicity both *in vitro* and *in vivo*. After 6 hours in 30% FBS at 37°C, 75% of the encapsulated siRNA was still present and 40% after 24 hours while naked siRNA was completely degraded within 3 hours. Kinesin spindle protein was targeted for efficacy experiments as it plays an important role in mitosis and is overexpressed in cancer cells. Its inhibition has been found to result in mitosis cessation and cell death. Gene silencing of 75% at a 1:1 (siRNA:SLNPs) molar ratio, and 68% at a 1:2 ratio was observed in PC-3 human prostate cancer cells. In the presence of serum the efficacy was markedly reduced at approximately 51% for the 1:1 ratio. In a prostate cancer mouse model the preferential accumulation of their siRNA-SLNPs at the target site (the tumour) was found after systemic injection and tumour growth was dose-dependently inhibited. Tumour growth was inhibited by 81% in mice who received a high dose treatment while mice receiving a low dose showed tumour growth inhibition of 58% relative to the saline controls.

Various other lipoplex formulations have also been used to target solid tumours and were able to demonstrate a reduction in tumour size[84–87]. Others have used lipoplex formulations which they applied directly to a target area and were able to effectively silence herpes proteins and protect mice from being infected with herpes simplex 2 virus[88]. They have also been used to deliver siRNA to a range of other targets with beneficial outcomes including preventing sepsis development[89], and reducing

low density lipoprotein (LDL) and serum cholesterol levels[90]. Lipids therefore hold a great deal of potential However, it has also been previously reported that lipids can induce an immunological response[91].

1.2.2.3 Cationic polymers

Cationic polymers, like cationic lipids above, were originally introduced for gene delivery as far back as 1987[92], since then they have been used for both *in vitro* and *in vivo* delivery of nucleic acids[56]. A variety of cationic polymers have been fabricated from both naturally and synthetically derived materials including; dendrimers, poly(L-lysine) (PLL), cyclodextrins, chitosans and poly(ethylenimine) (PEI). The polycationic polymers form nanoparticles, also known as polyplexes, with nucleic acids by electrostatic interactions between the positively charged functional groups – often amines – and the negatively charged phosphate groups present in nucleic acids producing a particle with either a positive or neutral charge. Cationic polymers are able to form relatively small nanoparticles with oligonucleotides, a favourable characteristic for gene transfer.

Some cationic polymers are able to successfully deliver their cargo to the cytoplasm via the proton sponge effect which improves endosomal release[79,93–95]. Polyplexes which have a high buffering capacity are able to stop the acidification of endosomes. This in turn increases the influx of protons and counter ions inside of the endosome. The increase in counter ion concentration leads to osmotic swelling, followed by membrane rupture and release of the siRNA into the cytosol[96,97].

Compared to cationic lipids, cationic polymers do not have a hydrophobic domain and are completely soluble in water[56]. They also have an advantage in that they are more easily and more economically produced, can be synthesised to different specifications, including the addition or substitutions of functional groups, and can form smaller nanoparticle complexes. As such a variety of structures are possible, and polymers used can be synthesised to various specific lengths and geometries (linear or branched). Due to the potential for modification, the use of these cationic polymers holds promise for the future. This is because any potential disadvantages associated with the use of some of these polymers, including cytotoxicity and weak electrostatic interactions between the siRNA and polymer, have the potential to be overcome as research in the area grows.

1.2.2.3.1 Poly(L-lysine)

Poly(L-lysine) (PLL) is a first generation cationic polymer, that is biodegradable – a favourable characteristic to have in vivo[56]. PPLs of different molecular weights are produced by the cationic polymerisation of lysine N-carboxy anhydrides[98,99]. Often, owing to poor delivery, PLL is modified with PEG[100], mesoporous silica[101] and dendrimers[102] in order to improve this[99,103].

In one such study PLL was modified with a sixth generation dendrimer before being complexed with siRNA to treat hypercholesterolemia in *in vivo* studies[102]. The PPL molecule termed KG6 was used to deliver siRNA targeting Apolipoprotein B (ApoB) (an essential protein for the formation and secretion of very low density lipoprotein and LDL during the metabolism of cholesterol) to hepatocytes *in vivo*. KG6 siRNA complexes were delivered to healthy mice via intravenous injection and a reduction of ApoB mRNA was observed in a dose dependent manner, with an up to 50% reduction in the mice receiving the highest dosage compared to control mice 24 hours after delivery without hepatotoxicity. Improvement in hypercholesterolemia was also observed after treating Apolipoprotein E (important for catabolism of triglycerides-rich lipoproteins) deficient mice with KG6 anti-ApoB siRNA.

Though successful examples of its use are reported, such as above, it should be noted that, compared to other cationic polymer transfection agents, PPL complexes have very low transfection capabilities due to being ineffective at endosomal escape (even with modifications, due to a lack of primary amines[97]) and are rapidly removed from circulation as they bind to plasma proteins[56]. Even when modified their oligonucleotide cargo is often subject to degradation in media containing serum[97,104].

1.2.2.3.2 Dendrimers

Dendrimers are synthetic polymers made up of multiple covalently bonded branched monomers forming a spherical shape. They consist of an inner core and an increasing number of radially attached branches emanating from the core. Each new layer of branches is termed a “generation” and is built up by the addition of methyl acrylate and amines[105]. The higher the number of branches, and therefore the generation, the higher the number of surface groups and charge density which offers the potential for multiple interations[53,56,95]. Cationic dendrimers have amine surface groups which assist with complexing the anionic RNAi molecule and aid in resisting degradation by nucleases. The amines also facilitate endosomal escape via a proton sponge effect[95].

Poly(ethylene) glycol monomethyl ether was used to modify fifth and sixth generation (G5 and G6) poly(amidoamine) (PAMAM) dendrimers and investigated for intramuscular siRNA delivery[106]. Their PEGylated G5 and G6 dendrimers were shown to be stable over 4 hours in RNase A compared to the uncomplexed siRNA which was degraded within 5 minutes. The PEGylated forms of both the G5 and G6 dendrimers were significantly less cytotoxic compared to unmodified dendrimers and were able to achieve significantly higher levels of FITC siRNA internalisation in primary vascular smooth muscles cells (VSMC) (5-7 fold higher) and macrophage cells (26-27 fold higher) compared to a commercially available transfection reagents. Efficacy experiments targeting GFP expression were conducted by co-delivering pEGFP with anti-GFP siRNA to 293 A cells. The G5 PEGylated dendrimer achieved the highest levels of GFP inhibition (66%) which was equivalent to that achieved with the commercial transfection reagent, Lipofectamine 2000. *In vivo* experiments were conducted in GFP transgenic mice as well as in neonatal C57BL/6 mice. C57BL/6 mice were injected in the quadriceps with Ad-GFP 2 hours prior to injection with dendrimer complexes. A 55% reduction in GFP expression in mice anti-GFP siRNA complexed with G5 or G6 PEGylated dendrimer was observed in the neonatal mice while a 44% reduction was observed in the GFP transgenic mice.

Although dendrimers can be manufactured to exact molecular weights, sizes and geometries and can be designed to achieve targeted drug delivery, concerns around toxicity and high manufacturing costs exist[95,107]. Despite this they have been used to modify other nanoparticle formulations such as PLL and cyclodextrins.

1.2.2.3.3 Cyclodextrins

Cyclodextrins (CDs) were originally used for pDNA delivery but were later re-optimised for siRNA delivery and have made it to the clinical trial stage for the treatment of cancer[108–110]. They are cyclic oligosaccharides which come in three forms; α, β and γ-CDs, however β-CD is most commonly used for delivery[111]. The β-CD are composed of seven glucose units connected by α-1, 4-linkages[4]. They have been favoured due to low cytotoxicity levels and lack of immunogenicity. CD molecules have a hydrophilic outer surface and hydrophobic core which can encapsulate the RNAi molecules for delivery, a process mediated by amidine functional groups[109]. The further addition of imidazole functional groups aids in endosomal escape and therefore enhanced delivery[112].

Although unmodified CD particles have been used for *in vitro* testing it was found that for *in vivo* studies chemical modifications to the CD molecules were necessary to assist with siRNA complexation, and to prevent aggregation thereby prolonging systemic circulation[22,113]. Many studies conducted

around the use of CDs for siRNA delivery have centred on cancer associated targets[108,110,114–117]. Other diseases and targets include acute colitis[118] and Huntington's disease[119], the central nervous system[120] and the liver[121].

In a recent advance in the use of this polymer, and an example of a modified CD, Guo and collegues[115] developed an antibody targeted CD based nanoparticle to selectively down regulate leukemic stem cells, in patients with acute myeloid leukaemia (AML)[122]. CD was modified via PEGylation for stabilisation, and the addition of an antibody for IL-3 receptor α-chain (a receptor highly expressed in target cells). siRNA targeting bromodomain-containing protein 4 (BRD4) (a therapeutic target of AML[123]) was encapsulated with the modified CD nanoparticles and used to transfect KG1 cells (an AML cell line). BRD4 mRNA expression was inhibited by 40% compared to the control while protein expression was inhibited by approximately 50% compared to the control. Cells treated with the CD nanoparticles displayed significantly higher levels of cell death (approximately 40%) compared to cells treated with negative control siRNA. The therapeutic potential of CD delivery of siRNA was further assessed *ex vivo* using primary culture leukocytes from newly diagnosed and relapsed AML patients. The mRNA and protein levels of BRD4 in leukocytes from newly diagnosed patients were reduced by approximately 40 and 45% respectively and were able to demonstrate myeloid differentiation, a reduction in myeloid blast proliferation and induce leukaemia apoptosis.

1.2.2.3.4 Chitosans

Chitosan is a polysaccharide derived from the deacetylation of chitin found in either fungi or the shells of *crustaceae*. Chitosan is a copolymer of β-(1,4)-2-acetamido-D-glucose and β-(1,4)-2-aminoD-glucose[124]. A naturally occurring cationic polymer, chitosan has formed the basis of some hydrogels[125] and has been used in nucleic acid delivery[126–129]. Chitosan based nanoparticles are considered favourable carriers due their high positive charge, biocompatibility, and low levels of cytotoxicity and immunogenicity[129,130].

Chitosans have been used successfully to silence target genes both *in vitro* and *in vivo*[4]. Targets of chitosan siRNA formulations include CDX2 factor which is involved in gastrointestinal maintenance[131], targets associated with cancers[132–135] such as galactin 1 which is associated with tumour progression, platelet-derived growth factor B in a rabbit iliac artery injury model[136], as well as genes associated with neuroregeneration[137] and brain endothelial cells[138].

Sadreddini *et al*[132]., looked at the potential of delivering both doxorubicin (DOX) – a drug used in chemotherapy – and siRNA in combination, for the treatment of colorectal cancer. The group combined carboxymethyl dextran (CMD) with chitosan to form DOX-snail siRNA CMD-Chitosan nanoparticles (ChNP). The Snail family of transcription factors are mediators of epithelial-mesenchymal transition that has been shown to down regulate E-cadherin – an adhesion protein which is anti-tumourgenic. CMD is an anionic derivative of dextran which allows for the addition of chemical conjugates such as drugs. The authors report that their nanoparticles were stable, after placing samples in FBS or heparin to represent physiological conditions. The authors were also able to demonstrate that their nanoparticle was able to achieve significantly higher levels of drug and siRNA delivery in an acidic environment compared to a neutral one, much like one would find in a tumour.

Chitosans have many favourable characteristics such as being both biocompatible and biodegradable[139–141]. However, unmodified chitosans are also considered to have poor solubility at physiological pH, low buffering capacity and have previously been considered to have low *in vivo* stability and inadequate intracellular release[139]. Therefore, as with many of the other formulations highlighted here, modifications are required to improve *in vitro* delivery as was done by Sadreddini *et al*[132].

1.2.2.3.5 Polyethylenimine (PEI)

Polyethylenimine (PEI) is a commercially available cationic polymer also originally used to deliver pDNA[142], but has subsequently been used to deliver siRNA[143–145] as well as other oligonucleotides[142,146]. It is considered the gold standard[147,148] amongst polymer based delivery systems and other non-viral vectors and delivery methods are often modelled on PEI due to its success both *in vitro* and *in vivo*[142,147–150]. It is generally accepted that PEI mediated siRNA entry is via clathrin mediated endocytosis, although like CPPs (section 1.2.2.1) above, this can vary depending on the physiochemical properties of the complex[151]. PEI is also understood to escape lysosomal degradation which is believed to be one of the main obstacles to overcome in cellular delivery of nucleic acids[93,152]. This occurs via the proton sponge mechanism, PEI has a buffering capacity due to protonation of the amines allowing it to regulate the pH inside endosomes[93]. The buffering capacity of PEI results in osmotic swelling and leads to the endosomes rupturing causing the release of the siRNA into the cytoplasm[93].

PEI has been used to deliver DNA and or siRNA to a range of targets including cancer cells[153–158], the central nervous system[159,160], the pulmonary system[161,162] and cardiomyocytes[145,163,164] and has been extensively used *in vivo*[155,156,159,160,162,163,165–167].

PEI is made up of repeating units composed of an amine and two aliphatic carbons. As such it is available in different geometries and sizes. Broadly, the different structures can be summarised as being low or high molecular weight and linear or branched. Kwok *et al*[144]., conducted a comparative study of linear (L-PEI) and branched (B-PEI) PEI to determine if the optimal criteria for delivery of siRNA and pDNA were the same as it is often the case that a selected vector for siRNA is chosen based on its effective pDNA delivery. Multiple aspects were considered including the binding and dissociation properties, the size and surface charge, internalisation, and efficacy. Polyplex formation is according to the ratio of nitrogen in PEI to phosphate in siRNA (N:P). It was determined that the optimal formulation for siRNA was B-PEI (20:1) while for pDNA L-PEI (10:1) was found to be optimal after comparing the various factors. For pDNA L-PEI was able to achieve higher levels of transgene expression, smaller size and lower surface charge compared to B-PEI. However, the B-PEI DNA was considered to be more stable (determined by heparin dissociation assay). At a ratio of 20:1, B-PEI to siRNA gene inhibition of approximately 60% was observed while at the same ratio for L-PEI there was no effect. B-PEI-siRNA complexes were also considered more stable, and smaller compared to L-PEI-siRNA. Similar results have been reported about the lack effectiveness when using L-PEI to deliver siRNA[94].

Structural difference between the pDNA and siRNA as well as between the L-PEI and B-PEI could explain the differences seen in delivery. siRNAs are smaller and more rigid structures compared to pDNA. The branched nature of the B-PEI could present more favourable complexing options for the siRNA which the L-PEI does not possess. By contrast, the larger structure of pDNA is better suited to complexation with linear PEI. Similar observations have been made with high (more flexible structure) and low (more rigid structure) molecular weight chitosans[168]. Another possible factor which could influence cellular uptake of siRNA and indicate why the 20:1 ratio was found to be optimal is the amount of free PEI available, as it has previously been shown that the presence of PEI in excess facilitates uptake[169–171].

Some have modified PEI complexes in order to improve transfection capabilities and *in vitro* and *in vivo* safety profiles. This includes modifications to aid cell entry and endosomal escape, cell targeting and particle stability, as well as decrease levels of cytotoxicity and improve delivery to target cells. Lowering the charge of complexes with modifications such as hyaluronic acid (HA) can improve toxicity but also help in cell targeting and PEI modified in this manner has been shown to improve *in vitro* silencing and reduce protein binding[53].

Hong et al[164]., had promising results using a linear PEI modified facial amphipathic deoxycholic acid(DA-PEI) to deliver siRAGE (siRNA RAGE) targeting receptor for advanced glycation end-products (RAGE), a known anti-inflammatory target, to rat cardiomyocytes. Their nanoparticle was shown to have low cytotoxicity and were able to successfully transfect rat cardyomycyte cells (H9C2). Under hypoxic conditions, they demonstrated a reduction in apoptosis compared to non-treated cells with 80% of non-treated cells exhibiting apoptotic nuclei versus 21% of treated cells. In *in vivo* experiments, nanoparticles were delivered via 3-intra-myocardial injections 1 hour prior to occlusion of the left descending artery of the heart. They were able to demonstrate a reduction in RAGE expression using siRAGE/DA-PEI in the ischemic myocardium and a reduction in infarct size and fibrosis in myocardial ischemic tissue pre-treated with siRNA/DA-PEI.

Wang and colleagues[145] modified PEI with hydrozide groups (PEI-HYD) – to neutralise the charge – and RGD (PEI-HYD-RGD) – a cell binding peptide – for siRNA delivery into an adult zebrafish heart injury model. Results were compared to unmodified PEI as well as siRNA alone. In *in vitro* experiments using HUVEC cells, both nanoparticles displayed no cytotoxicity with cell viability being maintained at increasing concentrations of polymer while unmodified PEI was considered toxic at all concentrations measured. They also looked at siRNA internalisation as well as the efficacy of transfected siRNA. Their PEI-HYD was the most efficient and they were able to demonstrate siRNA delivery to the cell and localise it to the cytoplasm surrounding the nucleus whereas transfection using the PEI or PEI-HYD-RGD was more homogenously spread throughout the cytoplasm. During *in vivo* assessment however, their hydrazide modification fell short and was not as efficient at delivery as compared to their PEI-HYD-RGD modification. The PEI-HYD-RGD was able to deliver higher levels of Cy5-labeled siRNA into the heart of zebrafish, and was also able to achieve higher levels of silencing. The unmodified PEI while superior to naked siRNA, uptake levels were still significantly lower than the PEI-HYD-RGD. This study suggests that use of a neutral or slightly positive (± 10 mV) polymer should be further explored for delivery.

As is evidenced here, many polymers both natural and synthetic exist which can and have been exploited for oligonucleotide delivery. PEI is one of the most widely used molecules due to it's effectiveness at delivering RNAi molecules and is commonly used *in vivo*[165,172]. However, high levels of cytotoxicity have also been reported limiting its progression as a therapeutic delivery vehicle[13,173]. Potential modifications can be made to improve not only the cytotoxicity but also improve transfection[13,145].

1.3 Scaffolds for localised sustained delivery

As outlined above, systemic delivery is plagued by two major issues namely degradation by ribonucleases and rapid clearance to the liver and kidneys[23]. Furthermore the potential for other complications including immunogenicity and toxicity, the potential for aggregation and undesirable accumulation, and off target gene silencing can also complicate delivery. Naturally these factors have a very unfavourable impact on the ability to deliver sufficient dosages of RNAi oligonucleotides at the desired target sites in the body. One approach by which this goal can possibly be achieved is through the systemic delivery of very high dosages. However, this strategy significantly elevates the potential for undesirable off target effects, both at the level of non-target tissue / organs and also non-target mRNA sequences. It has been shown that the down regulation of off target sequences occurs at moderately high dosages and that low dosages are required to offset this undesirable consequence[174]. It is the appreciation of this delivery problem that raised interest in the use of scaffolds, in particular hydrogels, as a possible means by which localised and more efficacious delivery might be relatively simply realised[10,54].

1.3.1 Biomaterials used for scaffold based delivery

Biomaterials are materials which are biologically compatible and may be made from either a synthetic or biological material. They can be used throughout the body as part of an implant or biological device as well as on their own. They can also be specifically designed to either work alone or in synergy with a complex system via interactions with living components to control any therapeutic or diagnostic procedure where they are used[175].

Depending on the material used in these scaffolds, the structural and functional characteristics can be manipulated to display different properties based on a given need. This is determined by the final clinical application of a given scaffold and the chosen form of release. A selected scaffold needs to be compatible with both the site of delivery and the RNAi agent it is to deliver. During fabrication of the scaffold containing RNAi molecules, the methods used must form the scaffold without damaging the RNAi therapeutic. Any potential protection the scaffold provides from nuclease degradation in addition to that from systemic clearance would also be of benefit. A biodegradable scaffold is desirable as it would eliminate the need to remove the scaffold post treatment and as such improve a patient's prognosis[54]. The most necessary characteristic is for the fabrication or implantation of the scaffold not to be the cause of more harm at the site of implantation.

Biomaterial based scaffolds which have been used for RNAi delivery include hydrogels, surface coatings, fibres, and microspheres. The main focus of this work is toward the use of hydrogels to deliver RNAi therapeutics, however the potential of other biomaterial based scaffolds will also be discussed briefly below.

1.3.1.1 Surface coatings

There is potential to be found in modifying the surfaces of implants to deliver therapeutics, as surfaces of pre-existing devices or implants can be easily modified with a multi- or single-layered film or hydrogel to release RNAi molecules. The coating of surfaces with RNAi therapeutics can be employed to enhance the therapeutic potential of surgical implants or other devices implanted into the body – including to aid in device tolerability. RNAi molecules as well as other therapeutics have been incorporated into surface coatings to induce gene silencing[176–179], and treat ailments including bone defects[180], and others[180–183] with beneficial therapeutic outcomes.

Joddar *et al*[179]., incorporated siRNA into dopamine coated stainless steel surfaces. The aim was to eventually develop a method for RNAi delivery from stainless steel surgical implants such as intravascular devices. Stainless steel discs were submerged in a solution of dopamine, at either acidic pH to form a monolayer or at a basic pH which resulted in a multilayer both with exposed amine groups before discs were coated with various concentrations (0.3 – 10 µM) of anti-luciferase siRNA. Both surface coatings were able to retain similar amounts of siRNA compared to untreated surfaces of control discs (optimum concentration of 0.625 µM siRNA). They were also able to achieve both localised and sustained delivery of siRNA for at least 7 days on both forms of coated surface *in vitro*, and demonstrated reduced cytotoxicity compared to traditional transfection methods using Lipofectamine. Discs were then coated with Egr-1 siRNA, a transcriptional regulator of many genes involved in cell migration and mitogenesis in smooth muscle cells which are important factors in atherosclerotic lesion formation[184]. In an experiment to mimic the elution of siRNA from a stent *in vivo*, human aortic smooth muscle cells (HAoSMC) were seeded in 24-well plates, allowed to grow, before placing a coated stent centrally in the well. They were able to show a significant reduction of Egr-1 protein expression and proliferation inhibited in HAoSMCs for both surfaces compared to cells treated with scrambled siRNA eluted from either surface or bare discs.

Castleberry and colleagues[185] used a technique where they assembled layer-by-layer ultrathin polymer films, on oxygen plasma treated sutures, with siRNA incorporated within. Hydrolytically degradable base layers of Poly 2 (a polycation) and dextran sulfate were formed by submerging the sutures in

alternating solutions of the two using a slide stainer. A similar process was followed to form alternating layers of chitosan and siRNA for the siRNA incorporation layers. In this study they used this technique to coat commercially available silk sutures with siRNA to promote wound healing in a third-degree burn model in rats. siRNA targeting connective tissue growth factor (CTGF), was targeted. CTGF is known to interact with transforming growth factor-beta (TGFβ), which has previously been shown to be associated with increased fibrosis, when upregulated[186]. They were able to demonstrate CTGF inhibition (approximately 36% compared to controls) which resulted in the altered expression of genes associated with scar formation. There was also evidence of tissue remodelling, and a reduction in scar formation.

This approach certainly has promise in optimising responses to implanted devices or in wound healing. However, due to their nature, the use of these kinds of films is somewhat limited as they are not injectable. The need to place some sort of implant also may not be as easily achieved in less accessible organs.

1.3.1.2 Electrospun NanoFibres

Electrospun nanofibres offer another alternative for siRNA delivery. Electrospinning is a versatile process which offers the researcher the possibility to produce wafer thin scaffolds made up of continuous fibres. Using this technique it is possible to produce scaffolds of nanofibres which resemble the structure of the extracellular matrix. It is also possible to orientate the specific fibres and alter the pore and fibre size depending on a given need. They have a high surface area to volume ratio, resulting in many cellular attachment sites which allows for a high degree of cellular and drug interactions[187]. The successful release of siRNA from electrospun nanofibres scaffolds has been examined. These include fibres made using poly(caprolactone) (PCL) and Poly(ethylene) glycol (PEG),[188] copolymers of PCL and ethyl ethylene phosphate (EEP),[189] and poly(D,L-lactic-co-glycolic acid) (PLGA)[126].

In an *in vitro* study, Low *et al*[190]., used PCL in combination with polydopamine (PD) to form scaffolds in to which they incorporated anti-REST siRNA (REST is a transcriptional regulator for many neuronal specific genes, which control the expression of ion channels, synaptic vesicles and neurotransmitters[191,192]) with the aim of increasing differentiation of stem cells into neuronal cells. Further exploitation of the scaffold was leveraged by the provision of topographical cues that might enhance stem cell differentiation towards neural cells. Briefly, PCL was electrospun into scaffolds, and then soaked in PD for four hours, siRNA was then complexed with the commercially available Lipofectamine RNAimax before being incorporated into PD-fibre scaffolds which were then lyophilised

overnight. The scaffolds were coated in laminin (protein found in basal lamina of epithelia) before being seeded with murine neuronal progenitor cells (NPCs). They were able to transfect cells with siRNA using their PD-fibre scaffolds and demonstrated enhanced neuronal differentiation by topographical effect and gene knock down *in vitro*. Also using NPCs, they demonstrated REST silencing for up to five days. They were also able to show, that in combination with gene knock down, the topographical cues provided by the scaffolds resulted in significantly higher levels of NPC neuronal commitment, and lower levels of glial cell differentiation. This demonstrates the potential synergy that can exist between RNAi therapeutics and delivery method.

Nanofibre scaffolds such as these are not injectable, thus this form of therapeutic delivery would be most suited as therapeutic patches for burn wounds or lesions. Another limiting factor of electrospun fibres is the lack of cell infiltration as well as scant mechanical strength for load-bearing applications[187].

1.4 Hydrogels

Hydrogels are highly hydrated structures at more than 90% water and are formed by covalent or non-covalent interactions between either synthetic or non-synthetic hydrophilic polymer chains. The hydrogels structure is similar to that of the extracellular matrix (ECM), making them compatible for use in many tissue types. Hydrogels have long been recognised and utilised as very engineerable localised drug depots[193]. The tuneable nature of their chemistry allows the release of the drug by the biomaterial to be finely controlled through parameters such as steric entrapment and chemical drug-scaffold interactions. Additionally, the scaffolds can be engineered such that their rate of release can be altered by biological stimuli such as pH[194–196] and cellular degradation[197]. Their hydrophilicity also allows for potentially facile incorporation of hydrophilic oligonucleotides. As such, they are considered to be a good candidate for biomedical applications including as eluting reservoirs for RNAi oligonucleotides as well as other therapeutics[54]. The use of hydrogels overcomes many of the drawbacks associated with systemic delivery including the need for high repeated dosages, toxicity, and undesired accumulation. By localising treatment using a hydrogel, drug retention and release to a target area are promoted and in doing so, the concentration required for a given therapeutic to be effective is reduced[198,199].

Material selection is an important aspect to consider to achieve localised RNAi delivery. As previously mentioned hydrogels are composed of either synthetic or non-synthetic polymers. Non-synthetic or naturally derived materials include collagen, fibrin, chitosan and hyaluronic acid (HA). These materials have often been used to form hydrogels as they are biocompatible and either are part of or have

similar properties to that of the naturally occurring ECM[200]. These naturally derived hydrogels are also favoured for their intrinsic cellular interactions and cell facilitated degradation[54,200]. However, it is difficult to manipulate their specific properties and, due to their biological origins, they run the risk of inducing an immune response limiting their use in the clinic[201].

Synthetic hydrogels are highly attractive due to their reproducibility and modifiability. Examples of synthetic hydrogels include PEG, poly(ethylene oxide) (PEO), and poly(vinyl alcohol) (PVA). Synthetically derived hydrogels lack the intrinsic cellular interactions seen in non-synthetic hydrogels, and often require modification to render them more cell compatible.

In many instances it is often desirable that the hydrogel is degraded once the RNAi oligonucleotides have all been delivered. The crosslinking methodology can also alter the degradability of the hydrogel and in turn influence the release rate. Hydrolytically degradable crosslinks allow for the gradual breakdown of the hydrogel. In a more sophisticated approach, enzymatically degradable crosslinks can be used that allow for cell dependent degradation of the gel[197,201–203]. Control of the monomer size and extent of crosslinking will regulate pore size and allows for further control of release rates by steric hindrance. This also allows for the control of mechanical parameters such as stiffness. It can certainly be envisaged that consideration of both delivery rates and the mechanical nature of the hydrogel will be important in instances such as delivery to the heart after myocardial infarction[204]. A gel that can relieve stress and also control the release of a cardioprotective siRNA would be desirable.

The method of delivery can also be selected; gels can either be injected or surgically implanted. Injectable hydrogels can be administered in a minimally invasive way. Surgically implanted hydrogels are formed prior to implantation in a controlled environment and as such they do not run the risk of diffusing away from the target site or undergoing gelation prematurely which could result in delivery failure.

1.4.1 *In vitro* analysis of RNAi delivery using hydrogels.

Understanding release kinetics of and cellular interactions with hydrogel based delivery systems are essential in furthering their development. In addition, assessing the bioactivity of any RNAi oligonucleotides which may be enmeshed should be considered.

Krebs *et al*[205]., were the first to report on the localised and sustained delivery of siRNA in vitro. They employed three different hydrogels which were all biodegradable and potentially injectable for their

experiments. These hydrogel formulations were a calcium crosslinked alginate, photocrosslinked alginate, and collagen. They used a siRNA targeting destabilised Green Fluorescent Protein (deGFP) (half-life of approximately 2 hours, versus enhanced GFP which has a half-life of 24 hours) for their experiments. The group reported sustained release of siRNA of approximately one week for the alginate based hydrogels and approximately two weeks for the collagen gels. The photo-, and calcium crosslinked alginate gels released the most siRNA in that order, followed by the collagen. They noted that the addition of chitosan or PEI to the calcium crosslinked alginate reduced the release rate. Bioactivity of released siRNA was assayed by co-culture using transwells. Cells expressing deGFP were seeded in a monolayer while hydrogels containing siRNA were suspended above in the permeable transwell. The released siRNA inhibited GFP expression by 80% compared to the no treatment controls. The ability of incorporated siRNA to transfect cells entrapped within the same hydrogel was assessed in the photocrosslinked alginate and collagen gels. Briefly, the different formulations were mixed with anti-deGFP siRNA and deGFP cells before gelling. After 3 days significant GFP inhibition was recorded for both gels, however after 6 days GFP expression for the photocrosslinked gel had increased while in the collagen hydrogel it continued to inhibit GFP expression at 6 days. This is in accordance with the results of their release profile experiments as collagen was able to sustain release for a longer period. However, it should be noted that mixing the cells and gels together in this manner is not a true reflection of *in vivo* conditions. By mixing the cells together with the siRNA before gelation, there is substantial risk of transfecting cells prior to polymerisation of the hydrogel. Under true *in vivo* conditions this would not be the case as the siRNA would need to be released by the hydrogel, or cells would have to first invade the hydrogel before coming into contact with the siRNA.

The differences in release profiles noted in the above study were attributed to the highly anionic charge of the alginate polymer and the probable repulsion of the anionic naked siRNA. In a follow up study by members of the same group, they noted that release of siRNA from alginate and collagen hydrogel systems was not easily controlled and that it was necessary to develop a hydrogel that would allow for better controlled, localised and sustained delivery of siRNA[206]. A photo cross-linked dextran hydrogel, into which they covalently incorporated the cationic polymer LPEI via biodegradable ester linkage, was developed to enable modifiable controlled degradation[206]. Release rate was determined by hydrogel concentration, 8% w/w hydrogels degraded and released the siRNA over 9 days whilst 12% w/w hydrogels degraded and released the siRNA over 17 days. The bioactivity of released anti-deGFP siRNA was assessed by transfecting cells with siRNA eluted and collected after 3, 7 and 14 days. deGFP inhibition was reported of approximately 90, 60 and 75% when using siRNA collected after 3, 7 and 14 days respectively. Aggregation has been reported to occur for PEI nanoparticles[56]. The surface charges, particles including PEI have previously been reported to aggregate in a time dependent

manner[56]. This time dependent aggradation has previously been reported to occur at a faster rate for LPEI than for BPEI[207]. These are important considerations as with aggregation comes an increase in particle size which affects the ability of the nanoparticle complex to deliver the siRNA. Complexes should be between 50 to 200 nm in order for internalisation via endocytic pathways to occur[208,209]. This does not appear to have played a role here and maybe due to its conjugation to dextran.

Similar experiments were also conducted using PEG hydrogels which formed via thiol-acrylate reactions thereby removing the need for photo-polymerisation, and avoiding potentially harmful exposure by the incorporated cells and other biologically active factors[210]. Here PEI (25 KDa Branched)/siRNA nanoparticles were formed prior to being incorporated into the PEG hydrogels using anti-GFP siRNA. The PEG hydrogels were crosslinked using another PEG containing sulfhydryls at the termini. Every 5 days releasate was collected and replaced. Cells were treated with releasate collected on the final day (day 42) before complete gel degradation due to hydrolysis as well as with freshly prepared PEI/siRNA complexes. The expression of deGFP after treatment with the releasate and freshly prepared particles was silenced to 10-25% of untreated cells, indicating that bioactivity was maintained. It is perhaps surprising that PEI aggregation did not play a role here. The overall aim in this study was to use the siRNA containing hydrogels to promote osteogenic differentiation of mesenchymal stem cells (MSCs). Following on from the release studies the group formed nanoparticles using anti-Noggin siRNA and miRNA-20a which were delivered separately or in combination to encapsulated MSCs in an effort to promote osteogenic differentiation. Noggin is an antagonist of bone morphogenetic proteins (BMP) -2, -4, -5, -6 and -7 and its expression is promoted by BMPs via negative feedback. miRNA-20a down-regulates the expression of peroxisome proliferator-activated receptor gamma (PPAR-ϒ), a negative regulator of BMP-2. A significant reduction in Noggin mRNA levels was observed at all time points measured over 28 days. PPAR-ϒ expression remained unchanged in the anti-Noggin siRNA group, but was significantly lower in the miRNA-20a group and combination treatment groups at 7 and 14 days, while only the miRNA20a group remained significantly low at 28 days. Mineralisation of hydrogels was determined and a higher calcium content was found in the combination groups and anti-Noggin siRNA groups. The group was able to engineer a hydrogel which was shown to release siRNA in a sustained manner and which can be used to control stem cell fate.

As previously discussed hydrogel systems can be designed to respond to different external environmental stimuli such as temperature, light, enzymatic activity, electricity and pH to promote RNAi elution. Huynh and co-workers[211] incorporated an aminoethyl methacrylate, a cationic

molecule, into an acrylated PEG hydrogel. Particle release could be controlled by exposing the hydrogels to various degrees of light and exposure time. They found that by applying UV light to a photolabile hydrgrogel they could increase the rate of siRNA release and that by varying the exposure time and intensities the rates of release could be altered. They also found that UV exposure for different lengths of time and at different intensities did not affect the bioactivity of the released siRNA. Another group employed radiofrequency and critical temperatures to stimulate release by crosslinking N-isopropylacrylamide and acrylamide with bis-acrylamide in the presence of APS/TEMED[212]. Above certain critical temperature the hydrogels turns to liquid thereby releasing its payload. To this end magnetic PEG-disulphate particles and siRNA were co-encapsulated within the hydrogel, radiofrequency was then used to heat the particles to a temperature above the critical temperature resulting in gel liquidation and in turn siRNA release. Temperature controlled release has been achieved by entrapping polyplexes in a hydrogel composed of glycol chitosan, a water-soluble chitosan, and a benzaldehyde-capped tri-block copolymer of poly(ethylene oxide)-poly(propylene oxide)-poly(ethylene oxide)[213]. With these hydrogels, by varying the temperature the rate of polyplex release could be varied.

1.5 *In vivo* RNAi delivery using hydrogels

Evidence of the progression made from *in vitro* to *in vivo* application of RNAi based therapeutics harnessing hydrogel formulations for their localised, and sustained delivery is described below. siRNA in combination with hydrogel scaffolds has been used to treat a range of disease states including; cancer[214–219], inflammation[220–226], bone regeneration[227–229], and cardiovascular disease[230–232].

1.5.1 Cancer

Much of the research utilising hydrogels for RNAi delivery has been in cancer, most probably due to the large body of existing knowledge utilising siRNA as a cancer therapeutic.

In earlier work, advantage was taken of the fact that the polycation chitosan (1.2.2.3.4 Chitosans) in conjunction with glycerol-2-phosphate undergoes a temperature driven liquid to gel transition upon injection *in vivo*[214]. Fluorescently labelled siRNA delivered within the chitosan hydrogel was shown to be localised in a tumour to a higher degree after intra-tumoral injection in a mouse relative to siRNA alone. Efficiency of RNAi was determined using anti-transglutimase 2 (TG2) siRNA. TG2 has been found to be up regulated in tumour growth[233]. Injection with chitosan hydrogels resulted in significant inhibition of tumour growth for both melanoma (48%) and breast cancer tumours (66%) relative to

chitosan with control siRNA. In another example of hydrogels as potential multi-therapeutics, co-delivery with docetaxel resulted in even greater inhibition of tumour growth (72% and 92% reduction in melanoma and breast cancer tumours respectively). It was not clear however whether the siRNA was released from the chitosan hydrogel as chitosan/siRNA complexes.

Another group used polyplexes to form hydrogels for siRNA release[215–218]. In their initial work[215] PEI-poly(organophosphazene) (PP) was used to form thermally responsive hydrogels containing cleavable ester-linkages. PP was formed by combining a hydrophobic isoleucine ethylester, a hydrophilic amino PEG (for thermosesitivity) and cationic PEI (for gene delivery). At room temperature the PP formed polyplexes, while at 37°C a gel was formed. siRNA displayed a consistent pattern of release which was measured up to 28 days. Fluorescently labelled siRNA was used to show retention in mice tumours. Fluorescent signal was shown to be maintained for 21 days where as siRNA delivered alone had disappeared by day 7. Anti-Cyclin B1 (cell cycle regulator – the inhibition of which leads to cell cycle arrest) siRNA in PP hydrogel was shown to reduce tumour size after 4 weeks *in vivo* compared to controls (PBS, anti-cyclin B1 siRNA alone, and PP complexed with anti-GFP siRNA) which had no effect on tumour size.

In follow up studies the group formulated PP, with a range of different polymer and drug combinations aimed at the long-term localised delivery of siRNA to tumours. PP was modified with a folate (FPP) to form targeted micelleplexes[217]. The addition of the folate meant that micelleplexes selectively entered cancer cells over expressing folate receptors. The hydrogel, acting as a depot for sustained release targeted siRNA complexes, was administered by subcutaneous injection so that the released micelleplexes could enter the circulatory and lymphatics systems. In order to determine the targetability of this formulation, fluorescently labelled siRNA was injected into the opposite side of the mouse from the tumour in the right dorsal subcutis. By imaging the mice at predetermined time points, using an optical imager, it was found that when injected alone the siRNA was cleared from the system within a few hours, while the FPP and PP conjugated siRNA was found to be localised to the injection site for up to 10 days. Mice treated with FPP curiously had a reduced tumour size despite the fluorescent signal only being seen at the injection site. It was hypothesised that this was due to a relatively small amount of siRNA present in the tissue coupled with a signal which weakened overtime. They confirmed by dissecting the organs that the reduction in tumour size was due to the released micelleplexes with a significantly stronger fluorescent signal in the tumours of FPP injected mice compared to PP siRNA or siRNA alone treated mice. The therapeutic effect of the FPP was further assessed by forming micelleplexes with anti-VEGF siRNA. Mice which were treated with FPP displayed anti-tumour activity up to 3 weeks. Reduced VEGF expression was found only in mice treated with the

FPP. They also noted that once the hydrogel had fully degraded, the tumour began to increase in size. In order to compensate they increased the volume of injected hydrogel and reported anti-tumour effects were maintained for a longer period (30 days). This indicates a dose dependent effect of treatment and the need for a continual presence of treatment until the disease state can be cleared from the system completely.

Most recently published they have developed the dual delivery of docetaxel and siRNA using a ternary nanocomplex hydrogel[218]. PP and docetaxel were conjugated via hydrophobic interactions with the isoleucine moiety and siRNA targeting B cell lymphoma 2 (Bcl-2) (a gene known to be involved drug resistance and apoptosis[234]) was attached via ionic interactions with PEI at 4°C to form thermosensitive polymer/chemical drug/gene complexes. When injected directly into the tumour or at 37°C a hydrogel was formed. Again uncomplexed siRNAs were released in a burst release whereas complexed siRNA and docetaxel displayed a more gradual pattern of release over 40 days *in vitro*. siRNA was present up to 41 days *in vivo*, and tumour inhibition was maintained for 4 weeks following a single injection.

This group has also formed hydrogels from conjugating protamine CPPs to the carboxyl group of poly(organophosphazene) via an amide linkage without PEI[216]. Anti-VEGF siRNA was selected to target tumour growth. The group reported localisation of fluorescently labelled siRNA to the tumour site for 24 days using their hydrogel formulation while siRNA alone was cleared completely from the site within 48 hours. Tumour growth after 4 weeks following a single injection, with the anti-VEGF siRNA containing hydrogel, was found to be inhibited, with tumour volume of less than 600 mm^3 compared to controls which ranged from 1400 – 1000 mm^3 which included an anti-GFP siRNA conjugated to their hydrogel formulation, anti VEGF siRNA and a PBS only control.

The studies above illustrate how hydrogel-based delivery can be used to have beneficial outcomes in the treatment of cancers, and in particular how they can be used to localise chemotherapeutics to the target site thereby minimising the exposure of the rest of the body to the toxic treatment.

1.5.2 Inflammation

Hydrogels have also been assessed as potential delivery vehicles for siRNA oligonucleotides targeting a variety of mRNA sequences involved in inflammation [220–226]. Inflammation can play a major role in worsening the prognosis of many diseases state rendering it an important RNAi target.

Towards the treatment of inflammatory bowel disease (IBD), Laroui and colleagues[220] formed polyplexes with PEI and anti CD98 siRNA and encapsulated them in an alginate-chitosan hydrogel which they crosslinked with calcium and sulfate. CD98 is an important mediator of homeostasis and

the innate immune response in gastrointestinal tract and has been found to be up-regulated in those who suffer IBD[235,236]. Mice were given daily doses of the formulation via oral administration. The hydrogel selected was pH sensitive and therefore only released its payload in the colonic lumen at a pH range of 5-6. Weight loss, myeloperoxidase (MPO) activity (indicator of neutrophil infiltration into the colonic mucosa[237]), CD98 and pro-inflammatory cytokines mRNA levels were all assayed to determine the therapeutic effect of siRNA administered in this manner in a mouse model of colonic inflammation. Weight loss of 10% was seen in the no treatment control groups as well as the nanoparticle alone groups after 8 days while only a 3% loss was seen in hydrogel containing PEI/anti-CD98 siRNA. A fourfold reduction in MPO activity and a reduction in the mRNA levels of pro-inflammatory cytokines keratinocytes, interleukin 1β and 6 of 50, 50 and 33% respectively were reported in the hydrogel PEI/anti-CD98 siRNA group and are indicative of a reduction in inflammation.

A commercially available polyamidoamine dendrimer (Superfect™) was used to form polyplexes which were entrapped within collagen hydrogels[221]. pDNA was encapsulated into collagen microspheres which were also embedded in the collagen hydrogels with the polyplexes. Anti-interleukin-6 (IL-6) siRNA was co-delivered with pDNA encoding endothelial nitric oxide synthase (eNOS) (IL-6 inhibitor and pro-angiogenic factor) in an attempt to reduce the foreign body response seen in organs and transplants. Release experiments showed that release rates of the siRNA and pDNA were different, with the siRNA being released more rapidly (50% within 5 days) from the system compared to pDNA (< 20% within 5 days). This suggests potential for temporal control of delivery of the different components. Hydrogels were delivered via injection into the subcutaneous space prior to gelation. The authors reported reductions in inflammatory cells of 46 and 34% when IL-6 siRNA was delivered alone and in conjunction with eNOS pDNA at 7 days respectively. No significant change was reported when eNOS pDNA was delivered alone. At 14 days there was a significant increase in blood vessel density, however this was highest in groups treated with the pDNA alone which could be due to the more gradual release profile of the pDNA. A protein analyses was conducted on various inflammatory and angiogenic proteins and revealed an overall reduction in inflammatory cytokines and an increase of angiogenic factors expression. The results achieved here would indicate that hydrogels could be used, to regulate the foreign body response and promote the vascularisation of transplanted organs while decreasing inflammation.

The beneficial effect of Hydrogels delivering RNAi molecules on inflammation in wound healing models has also been reported. Zhao and co-workers[222] combine polyvinylpyrrolidone, polyvinyl alcohol, glycerol, water and siRNA (Entranster-R-coated, commercially available transfection agent), naked siRNA or saline in a vacuum mixer to form hydrogels which were poured into a siliconized

mould. The hydrogels were then transferred to medical non-woven fabric to form patches which were pasted onto hypertrophic scars of mice. Treatment with patches containing Entranster-R/TGFβ1-337 siRNA lead to a significant decrease in TGFβ1, scar volume and collagen content compared to controls. The orientation of collagen fibres in scars treated with the Entranster-R/TGFβ1-337 siRNA hydrogel patches were also found to more closely resemble a healthy dermis compared to controls.

Collagen type 1 which was cross-linked with 4-arm PEG with succinimidyl glutarate termini to form a hydrogel has also been used in a wound healing model[226]. miRNA-29B was incorporated into the hydrogel scaffold and placed on dermal wounds which had been created in rats. miRNA-29B was selected as it has previously been shown to; play an important role in fibrosis in many different tissues, to directly target fibronectin, collagen type I & III, and its down regulation or complete loss of expression has been observed in fibrotic tissue[238–242]. A significant reduction in wound contraction for all groups compared the no-treatment controls was reported. Rats which received 5 µg of miRNA displayed a significant increase in granulation tissue (highly vascularised, forms the surface for new tissue formation) compared to a lower dosage of 0.5 µg. A reduction in the ratio of collagen type I and III (an indication of stiffer, mainly type I collagen granulation tissue) was also reported for all groups, except the 5 µg miRNA group, compared to unwounded tissue.

1.5.3 Bone Regeneration

Hydrogels delivering RNAi agents have also been used to facilitate bone regeneration[227–229]. It has previously been reported that the use of hydrogel based scaffolds for bone repair has advantages over current treatments which include the use of metallic implants and bone grafts. These advantages include: they can be injected into inaccessible sites using less invasive techniques; can gel *in situ* and the fabrication of a patients specific implant is not needed as the injected gel can take the shape of the injury site[243].

Manaka *et al*.,[228] used poly-D,L-lactic acid-p-dioxanone- polyethylene glycol block co-polymer (PLA-DX-PEG), a biodegradable hydrogel to deliver anti-Noggin siRNA *in vivo* to enhance the effect of BMPs (factor that promotes bone and cartilage formation). The hydrogels were formed *ex vivo* with siRNA then surgically implanted into the left dorsal muscle pouches of mice to promote ectopic bone formation. Fluorescently-labelled siRNA was used to determine intracellular delivery and was found localised to cells adjacent to the implants. The fluorescence signal increased in a dose dependent manner and was significantly higher than the naked siRNA, which was delivered via direct injection into the muscle, however the signal decreased over time to undetectable levels at 7 days. To

determine the potential of ectopic bone formation due to enhanced BMP-2 presence, hydrogels containing recombinant human BMP-2 with and without siRNA were implanted. Two weeks post implantation the hydrogels had been completely replaced by new bone for both groups. They determined the mean size of the ossicles and calcium content, and found that the ossicles were significantly larger in the group of mice treated with both BMP-2 and siRNA and had significantly higher mineral content compared to the group which received BMP-2 alone. What is interesting to note about this study is the lack of cellular translocation vehicle for the siRNA. The authors suggest, based on previous reports, that the poly (D,L-lactide-co-glycolide), an amphipathic molecule, component of their hydrogel enters the cell via endocytosis through fluid-phase pinocytosis and escapes endo-lysosomal degradation to slowly release their contents into the cytoplasm[244,245].

A hydrolytically degradable hydrogel PEG-*b*-poly(lactide)-*b*-dimethacrylate (PEG-*b*-PLA-*b*-DM) has been used to deliver siRNA nanoparticles to promote bone fracture healing[229]. siRNA targeting WW domain-containing E3 ubiquitin protein ligase 1 (*Wwp1*) was selected as it has previously been reported that its down regulation promotes the rate of bone formation and bone mass[246]. A murine mid-diaphyseal femur fracture model was used to assess bone repair. siRNA was complexed with a diblock co-polymer consisting of dimethylaminoethyl methacrylate and propylacrylic acid into nanoparticles before being mixed with PEG-*b*-PLA-*b*-DM and lithium arylphosphate (a photo-initiator of gelation). Hydrogels were crosslinked *ex vivo* using UV light and surgically implanted at the fracture site. Nanoparticles delivered via hydrogel were localised to the fracture site for 3 weeks while nanoparticles that were injected into the site had been cleared from the site within 3 days. *In vivo* gene silencing was determined using quantitative real time PCR. Levels of *Wwp1* in fractures which received anti-*Wwp1* siRNA delivered by hydrogels were reduced to 23% of untreated control groups. At the same time those genes which are associated with bone growth were also upregulated including osteocalcin, collagen type 1 and alkaline phosphatase. Fracture healing was assessed by the presence of calcified bone callus. Calcified calluses were reported in 11 out of 12 mice treated with anti-*Wwp1* siRNA nanoparticle hydrogels 3 weeks post treatment (compared to 6 out of 12 for the control), while one out of 12 untreated mice displayed evidence for callus formation. Histological analysis confirmed accelerated fracture healing in treatment groups compared to the no treatment control groups. Callus area and cartilage formation was increased in the treatment group at 14 days and by 21 days had significantly less unimineralised cartilage and larger bone area relative to the untreated control groups.

These studies illustrate the potential for using degradable hydrogels to deliver siRNA in order to promote bone growth and healing however, gels in both studies were formed *ex vivo* and implanted.

Since the gels were surgically implanted the potential benefits of the gel taking the form of the injured area were not realised or examined. Photocrosslinking hydrogels *ex vivo*, followed by surgical implantation or for that matter injecting hydrogels and photocrosslinking *in vivo* are not always viable options in area of bone that are hard to reach. Further research using in situ forming hydrogels not dependent on photocrosslinking may hold great potential in this area.

1.5.4 Cardiovascular Disease

Hydrogel based delivery of RNAi therapeutics have also been used towards the treatment of cardiovascular disease[230–232]. Pullulan, a naturally occurring polysaccharide that is considered nontoxic, non-immunogenic and is biodegradable was used to coat carotid stents to prevent restenosis – a complication of coronary stent implantation – via inhibition of MMP2[230]. Elevated levels of MMP2 have previously been associated with increased restenosis[247]. Pullulan was functionalised by grafting of diethylaminoethylamine groups to form a cationised pullulan hydrogel that would be able to complex with siRNA via electrostatic interactions to form nanoparticles. The hydrogels were physically crosslinked with sodium trimetaphosphate. Kinetic studies were conducted to determine siRNA retention and found that 20% of siRNA was released from the cationic pullulan after 1 hour, whereas the neutral pullulan stents eluted 100% of siRNA in less than 10 minutes. For *in vivo* experiments, a balloon catheter was used to induce right carotid abrasion in a rabbit model. The cationised pullulan hydrogel coated stents were then implanted 15 days post injury. Using Tamra-tagged siRNA, they were able to show siRNA internalisation in the carotid artery 24 hours after implantations, and silencing of MMP2 was reported (approximately 28%). Functional outcomes such as arterial flow were either not assessed or not reported on.

For the delivery of siRNA into the myocardium, PEI (section 1.2.2.3.5) has been modified in order to fulfil the dual role of as a transfection agent and as a component of the hydrogel[232]. PEI was modified with β-cyclodextrin (CD) and triethylamine to form CD-PEI. An 8-arm PEG-maleimide was modified by reacting it with 1-adamantanethiol via Michael addition to form Ad-PEG. Hydrogels could form through guest-host interactions between CD and adamantane. To encapsulate the siRNA, polymers were mixed with the siRNA to form polyplexes which at higher concentrations formed shear thinning hydrogels through a guest-host interaction. Sustained release of siRNA was observed from the siRNA/CD-PEI/Ad-PEG system at a constant rate over a two week period (less than 10%). Hydrogels containing fluorescently labelled siRNA were injected into the left ventricle of rats which were sacrificed after 24 hours to determine localisation. The fluorescent signal was localised to the site of injection. GFP expressing rats were used to determine efficacy of siRNA delivered from within this

hydrogel system. Rats were injected with the hydrogel formulations containing either an anti-GFP siRNA or a negative control siRNA into the left ventricular wall and were sacrificed 24 hours or 7 days post injection. In rats sacrificed 24 hours post inject a 40% drop in GFP expression was reported and this reduction was maintained for 1 week.

In another study, targeting fibrosis in the ECM, miRNA-29B was incorporated into hyaluronic acid which was modified with thiols and cross-linked with PEG diacrylate to form a hydrogel[248]. Their hydrogel, which is polymerised in 20 minutes at room temperature, was injected into the peri-infarct zone of mice that had undergone left anterior descending artery ligation. miRNA-29B was selected for delivery as its down regulation in the peri-infarct zone has previously been shown to contribute to fibrosis[242]. Myocardial function was tested at 2 and 5 weeks post infarct and significant improvement was recorded for ejection fraction at both time points relative to control mice which received a scrambled miRNA sequence. A significant improvement in fractional shortening and fractional area change was also reported at the 5 week time point compared to the scrambled control group. No significant difference in scar size was reported for either group. However, a significant reduction in elastin expression in the peri-infarct zone and a trend towards increased vascularisation in both the peri-infarct zone and the centre of the infarct in mice treated with the miRNA29B relative to controls was reported.

The above studies demonstrate the feasibility of delivering RNAi molecules via a hydrogel system to achieve a therapeutic outcome via sustained localised delivery. This potential has been illustrated by anti-tumorigenic effects, mediation of inflammation, and improved bone healing and cardiac outcomes *in vivo*. They have also been shown to have beneficial outcomes in wound healing experiments demonstrating improved scar healing[222,226]. This highlights the scope of applications possible using a hydrogel system in this manner. As well as being able to both sterically and covalently entrap nanoparticles, hydrogels can also have cell adhesion sites allowing for cell migration and entrapment and can be used to co-deliver other therapeutics.

1.6 Enzymatically degradable hydrogels

Enzymatically degradable hydrogels which have the ability to form crosslinks spontaneously without the need of an external light source have the potential to allow for delivery of RNAi oligonucleotides in scaffolds that are injectable and permit cell based release of siRNA. A synthetic peptide cross-linked hydrogel based system (poly(ethylene glycol) (PEG)) is one such hydrogel option. The potential and versatility of using these types of PEG hydrogels is discussed below.

PEG hydrogels have been designed to have the ability to form spontaneously at physiological temperature and pH via Michael type addition reaction without the formation of by-products[249]. A Michael addition reaction is a nucleophilic reaction whereby a nucleophile is added onto unsaturated esters[250]. Briefly, PEG monomers with branched structures can be constructed with vinyl sulfones at their termini. Vinyl sulfones are able to very specifically covalently bind to thiols via the Michael addition reaction[251]. Thus these branched PEG molecules can be cross-linked with any molecule containing at least two thiol moieties [203,251]. As a consequence thereof, a peptide containing two cysteine residues when added stoichiometrically to a PEG vinyl sulfone mixture can cause polymerisation of the hydrogel. Furthermore, the peptide sequence can be synthesised such that they contain proteolytic recognition sequences[201]. With the incorporation of such peptides as crosslinkers, the hydrogel becomes enzymatically degradable and can regulate cellular ingrowth to be dependent on cellular based proteolysis[201–203].

These types of hydrogels have shown utility in a range of therapeutic areas inclusive of bone growth[201,252], angiogenesis[197] and myocardial infarction[253–255]. Bone formation was enhanced in a rat cranial model by the sustained delivery of BMP-2. Increased blood vessel growth was found in hydrogels containing covalently linked VEGF and importantly release of VEGF was found to be contingent on cellular invasion. Cellular invasion and migration was also shown to be dependent on the presence of cellular adhesion peptides such as RGD that were attached covalently through cysteine residues[201,202]. The rate of cellular invasion can also be controlled in these hydrogels, both *in vitro* and *in vivo* by simple titration of the degradability of the peptide crosslinking sequences[203].

Our group has investigated the ability of these hydrogels to biomechanically support the infarcted heart after cardiac injection[253,254]. The delivery of the hydrogel was shown to reduce wall thinning in the infarcted wall of the heart, thus reducing the mechanical stress experienced by surviving cardiomyocytes. This was found to result in reduced functional damage. Though, these findings are promising, they are not sufficient as a therapy for infarction, and the delivery of bioactive modalities has begun to be assessed. Importantly for the work described in this thesis, the PEG hydrogels were shown to be able to entrap and localise growth factor containing microspheres in the infarcted rat heart[255]. Coacervates of heparin and poly(ethylene argininylaspartate digylceride) were formed that contained the factors Sonic Hedgehog and IL-10 that were approximately 1 µm in diameter. These coacervates were sterically entrapped and the combination of coacervates and hydrogel were found to improve the functional outcome in infarcted rat hearts relative to the individual components.

For the *in vivo* studies highlighted above 8-arm PEG hydrogels were used while *in vitro* studies have also been conducted, for which a 4-arm PEG hydrogel was employed[202,203,253–255]. The *in vitro* studies demonstrated how cellular ingrowth in the hydrogel could be controlled by varying peptide crosslinker used to polymerise the gel[202,203]. Regulation of tissue ingrowth was also demonstrated *in vivo* by surgically implanting PEG hydrogels, polymerised within highly porous polyurethane discs, subcutaneously in a rat[203].

Thus these enzymatically degradable hydrogels have shown potential in a variety of therapeutic arenas and are able to sterically entrap microspheres that contain bioactive agents. This could also be exploited to entrap nanoparticles containing siRNA conjugates. The work in this thesis describes the initial experiments directed towards their further exploitation as RNAi molecule delivery vehicles.

It is hypothesised that the entrapment of PEI/siRNA nanoparticles within PEG hydrogels will allow for the transfection of invading cells and that the PEG hydrogel will increase the stability of siRNA particles.

1.7 Aims

The fundamental aim of this project is to assess the potential of using a PEG hydrogel to localise delivery of PEI/siRNA nanoparticles. Enzymatically degradable PEG hydrogels have previously been shown to allow cellular invasion and have been used as depots for the controlled release of a variety of drugs and proteins. PEI was selected for entrapment within the enzymatically degradable PEG hydrogel as it is considered a gold standard for nanoparticle based delivery of siRNA. .

A prerequisite is the establishment of the required techniques for PEI/siRNA nanoparticle formation and optimisation in our laboratory. To achieve maximum transfection a nanoparticle formulation needs to meet certain criteria listed below. Nanoparticles or polyplexes are formed based on a ratio between amine nitrogen's of the PEI to the phosphates of the siRNA (N:P ratio). It is necessary to assay a range of these ratios for complexation, stability, cytotoxicity, and transfection capability.

Prior to assessing the efficacy of hydrogel based delivery of RNAi therapeutics *in vivo*, it is necessary to optimise and characterise aspects such as the release and bioactivity of entrapped nanoparticles in *in vitro* models that resemble the *in vivo* scenarios as closely as possible.

A secondary aim of this project is the establishment of an *in vitro* RNase protection assay for encapsulated nanoparticles. siRNA oligonucleotides are subject to degradation by RNases present both *in vitro* and *in vivo*. PEI nanoparticles are widely reported to protect their siRNA cargo from RNases. The influence of PEG encapsulation on PEI based RNase protection still requires assessment.

These hydrogels are enzymatically degradable, and thus allow for cell-directed invasion. Upon implantation, these hydrogels will be invaded by cells from surrounding tissue and it is therefore necessary to develop a 3D RNAi assay which properly mimics this *in vivo* environment. A variety of cellular entrapment techniques will be assayed for entrapment and invasion potential.

The objectives of this project can be summarised as follows:

1. Determine the optimal ratio of PEI to siRNA (N:P) for delivery of siRNA in terms of:
    - Complexation
    - Stability
    - Cytotoxicity
    - Transfection
2. Entrapment and release of nanoparticle formulation within PEG hydrogels
    - Influence of 3D encapsulation on RNase degradation
3. Development of a 3D cellular invasion assay for the assessment of siRNA delivery *in vitro*

2. Materials and Methods

A detailed list of all reagents and equipment used can be found in Tables A1.1 – A1.3 of the Appendix (section A1). The recipes and other instructions for buffers and other reagents which are commonly used can be found in section A2 of the Appendix, Tables A2.1 – A2.4.

2.1 Tissue Culture

HT1080 cells were used for all tissue culture experiments. HT1080 cells are a fibrosarcoma line from a 35 year old human male. Cells were never used above passage 20 (P20). All tissue culture related work was conducted in a Bio-Hazard Laminar Flow Hood. All surfaces and containers entering the hoods were first sprayed and wiped down with 70% ethanol.

Prior to working in tissue culture with cells, MCDB-131 or Dulbecco's Modified Eagle's Medium (DMEM) media was prepared. Before working with cells, MCDB-131 or DMEM, Foetal Bovine Serum (FBS) and Penicillin / Streptomycin (P/S) was removed from 4˚C fridge and allowed to warm to room temperature on the bench or in a 37°C water bath. Media containing FBS was prepared fresh on the day of use in 50 ml Falcon® tubes. FBS was added at a concentration of 10% (v/v) while P/S was added to a concentration of 1% (v/v) (100 U penicillin/ml and 100 µg streptomycin/ml). P/S was added to all media involved with the routine passaging and thawing of cells, however, it was not present in experiments involving cells.

2.1.1 Thawing of Cells

Cells were removed from cryostorage, thawed at room temperature and the contents added to a T75 cm^2 or a T25 cm^2 flask containing 12 ml or 5 ml 20% (v/v) FBS media respectively. Cells were seeded at a maximum density of 20 000 and a minimum density of 6500 cells per cm^2. The flask was then placed in the 37°C, 5% CO_2 incubator overnight after which time the media was replaced with fresh 10% media.

2.1.2 Passaging of Cells

When cells were 70 - 90% confluent they were passaged. The media was removed and discarded and cells washed 2X with 5 to 8 ml iso-PBS. The washed cells were then incubated with 5 ml of trypsin in the 37°C, 5% CO_2 incubator. Once the cells were detached the trypsin was deactivated with 5 ml MCDB-131, 20% FBS media. The solution containing the detached cells, media and trypsin was then

pipetted into a 50 ml Falcon® tube and centrifuged for 3 minutes at 1 500 revolutions per minute (RPM). After centrifugation was complete, and the presence of a pellet confirmed, the supernatant was carefully discarded. The cells were resuspended in 1 ml MCDB-131 or DMEM, 10% FBS media. Between one fifth and half of the solution of media containing cells was added to a new flask containing media.

2.1.2.1 Cell Counting

For all experiments involving cells as well as cryopreservation, the cells were counted using a haemocytometer. To count the cells, 20 µl of the resuspended cell solution from section 2.1.2 was added to 20 µl Trypan Blue (0.4% m/v). The haemocytometer and cover slip were cleaned with 70% ethanol before adding 10 µl of the cell Trypan blue mixture directly under the cover slip. Grids 1, 2, 4 and 5 were counted, averaged and the number of cells per millilitre was determined as follows:

$$Average\ Number\ of\ cells\ counted\ \times\ 2\ \times 10'000 = Number\ of\ cells\ per\ millilitre$$

2.1.3 Cryopreservation of Cells

Stocks of HT1080 cells were cryopreserved. Cells were counted according to the above method (section 2.1.2.1) and frozen in stocks of 500 000 cells per vial. A volume of Media, 10% FBS containing 500 000 cells was added to 2 or 1.5 ml cryostorage tubes and placed on ice. To maintain cellular integrity cells were frozen in 7.5% (v/v) dimethyl sulfoxide (DMSO). An equal volume of MCDB-131, 10% FBS and 15% DMSO was then added drop wise to media containing cells and placed on ice. Cells were frozen overnight at -65°C in a polystyrene rack before being transferred to liquid nitrogen (-196°C) for long term storage.

2.2 siRNA/PEI Nanoparticle preparation

Nanoparticles were formed at a range of ratios and in varying concentrations, buffers and solutions depending on the experiment for which they were going to be used.

2.2.1 siRNA

Various siRNA sequences with and without fluorescent tags were used to form nanoparticles (Table 1). The type of siRNA used to form complexes was based on experimental requirements.

siRNAs arrived lyophilised from the respective suppliers and re-suspended in RNase free water which arrived with the siRNA. The siRNA was re-suspended to 100 µM and 20 µl aliquots were made and stored at - 20˚C.

Table 1: Summary table of the different siRNAs used to form nanoparticles complexes in this project.

Product name	**Modification**	**Molecular Weight**
AllStars Negative Control siRNA	AF 488	15 550.9 g/mol
AllStars Negative Control siRNA	AF 555	16107.1 g/mol
AllStars Hs Death Control siRNA	-	13 295.1 g/mol
Negative control siRNA	-	13299.9 g/mol

*AF = Alexa Fluor

2.2.2 Complex formation

Nanoparticle complexes were initially formed at a range of nitrogen to phosphate (N:P) ratios in order to determine which was optimal for siRNA delivery. The ratio is determined by the nitrogen within the PEI and the phosphate within the siRNA. PEI stocks of 4.3 mg/ml (0.172 mM PEI) were prepared in iso-PBS. A 0.172 mM solution of PEI is equivalent to 0.1 M nitrogen (100 nmol amine nitrogen per microliter)[256] while there are 3 nmol phosphate per microgram of siRNA[256]. This solution was then filter sterilised with a 0.20 µm syringe filter unit.

Nanoparticles were formed at N:P ratios of 0:1, 1.25:1, 5:1, 2.5:1, 5:1, 10:1, 20:1 and 40:1 in 20 µl solution as detailed in Table 2. After the addition of all the components, samples were incubated for 30 minutes at room temperature to allow for complex formation. Prior to each experiment a master mix of nanoparticles was made from which technical repeats were derived. Nanoparticles were always formed according to this protocol unless otherwise stated.

Table 2: Volumes according to which a single aliquot of nanoparticles of various N;P ratios were prepared.

Ratios N:P	Stock solution		Volume (µl)		
	PEI (µM)	siRNA (µM)	siRNA	PEI	Diluent
0: 1	0.0	1.5	10	0	10
1.25: 1	0.172	1.5	10	7.5	2.5
5:1	1.72	1.5	10	3.00	7.00
10:1	1.72	1.5	10	6.00	4.00
20:1	17.2	1.5	10	1.20	8.80
40:1	17.2	1.5	10	2.40	7.60

2.3 Assessment of Nanoparticle Formation

The optimal N:P ratio was determined by gel retardation, RNase protection, transfection efficacy and cytotoxicity assays.

2.3.1 Gel Retardation Assay – Agarose Gel Electrophoresis

This assay allows for the assessment of complex formation. The complexes were formed at a concentration of 0.75 µM siRNA in 20 µl NanoPure Water. A 4% agarose gel was made using 0.5X TBE buffer (Appendix A2). After complexation, 5 µl GoTaq Green containing GelRed nucleic acid stain was added to the samples and vortexed. Following vortexing, 12.5 µl (7.5 pmols) of the sample mix was loaded into the wells of an agarose gel. The gel was run at 80V constant for 30 – 35 minutes. The gel was visualised and quantified using an InGenuis3 gel documentation system & GeneSys image capture and GeneTools image analysis software. All quantification was conducted on raw images taken on the InGenuis 3. Any adjustments to band intensities were done to the entire gel image. For purposes of presenting the images in figures, empty lanes were removed.

2.4 Complex Stability Assays

In order to determine the stability of the nanoparticles and therefore their ability to protect the siRNA, they were exposed to RNases which are present in FBS[257].

2.4.1 Protection of siRNA from RNase present in Foetal Bovine Serum (FBS)[22,258,259]

After nanoparticle formation, an equal volume of FBS was added to each ratio sample so that the final concentration of FBS was 50%. Samples were kept at 37°C. At time points T = 1, 3, 6, 24, 72, 120 and 168 hours 20 µl of sample was removed and added to 5µl 2.5% SDS (0.5% final) and flash frozen in liquid nitrogen before being stored at -65°C. The SDS dissociates the nanoparticles and neutralises RNases present in the solution and was added to all samples including controls. Naked siRNA and 50% FBS served as controls and were frozen with SDS until the completion of the experiment.

Once all samples had been taken, the samples, including controls, were defrosted and subjected to gel electrophoresis (section 2.3.1). The results were quantified using GeneTools image analysis software and normalised to the naked siRNA control.

2.5 Cellular Transfection of siRNA

Unless otherwise stated, cells were seeded in a clear flat bottomed 96-well plate that was tissue culture treated and sterile, at a concentration of 6 000 cells per well in 200 µl, 10% MCDB-131 media and incubated overnight at 37°C. Cells were always seeded in the centrally located wells of the plate and not on the edge. This was done to avoid any variations in seeded cells due to evaporation in the outer wells, media or PBS alone was aliquoted into these wells instead. After overnight incubation nanoparticles were prepared for transfection experiments as described below.

2.5.1 siRNA transfection of cells

Cells were seeded a minimum of 24 hours prior to the commencement of the experiment. After 24 hours each well was viewed under a light microscope to determine if the cells were evenly seeded and of similar density in all of the wells.

After nanoparticle formation, each sample was diluted 1:5 in 10% FBS containing media and vortexed. The media was removed from the cells and the cells washed 1X with iso-PBS which was then replaced with 100 µl of each nanoparticles ratio. Samples were well mixed by pipetting up and down before being added to the cells. Each well then received an additional 100 µl media and placed in the 37˚C, 5% CO_2 incubator for 4 hours, occasionally shaking. After 4 hours had elapsed, media was removed and the cells washed 1X with iso-PBS before being replaced with 200 µl media. The cells were then incubated until assessment with CellTitre-Glo® (section 2.5.1.1).

2.5.1.1 CellTitre-Glo®

The efficacy of internalised siRNA as well as the cytotoxicity of PEI/siRNA nanoparticles was assayed using CellTiter-Glo® from Promega. The commercially available CellTiter-Glo® enables the user to determine cell viability by reacting with the ATP present in metabolically active cells. The addition of the CellTiter-Glo® reagents causes cell lysis and the release of ATP which reacts with luciferase to give a luminescent signal. Briefly, luciferin undergoes mono-oxigenation, a reaction which is catalysed by luciferase (in this case a proprietary thermostable luciferase – Ultra-Glo™ Recombinant Luciferase) in the presents of magnesium, ATP, and molecular oxygen to form the light generating oxiluciferin and other reaction products. This cell viability assay therefore can give you an indication of the number of viable cells present[260,261].

Both efficacy and cytotoxicity can be determined using this assay. Efficacy of delivered siRNA can be determined by using AllStars Hs Cell Death Control siRNA when formulating nanoparticles while cytotoxicity can determined by complexing negative control siRNA.

After thawing the CellTitre-Glo® reagents, CellTitre-Glo® Buffer was added to CellTitre-Glo® Substrate according to the manufacturer's specifications. An equal volume of reagent to media was then added to each well after which the plate was placed on an orbital shaker for 3 minutes to induce cell lysis. The plate was then incubated at room temperature to allow the luminescence signal to stabilise. After this 180 µl was removed from each well and placed in a corresponding well on an opaque, non-sterile, 96-well flat-bottomed plate. The tips were discarded and replaced between triplicates. Wells with media alone were used as blanks with CellTitre-Glo® reagent. The luminescence signal was then recorded using a luminometer which had the conditions for the CellTitre-Glo® installed.

2.5.1.2 Standard curve for determining number of cells

For every experiment in which Cell Titer Glo® was used, a standard curve was also constructed on the same day that the experiment was seeded. After cells had been seeded on the experimental 96-well plate, cells from the same flask were also seeded for a standard curve. This was done in triplicate, on an opaque, non-sterile, 96-well flat-bottomed plate. Cells were seeded from 0 to 40 000 cells per well in increments of 5000 cells, in 100 µl media. CellTitre-Glo® was then added according to the protocol in section 2.5.1.1.

2.5.2 Cytotoxicity and eficacy assay using CellTiter-Glo® Luminescent Cell Viability Assay

2.5.2.1 Cytotoxicity of PEI/siRNA nanoparticles

Cytotoxicity experiments were conducted. Nanoparticles were prepared using Negative Control siRNA as per section 2.5.1. Cytotoxicity and efficacy experiments were conducted in parallel. Therefore, cells used for this experiment were seeded on the same plate as those cells used for the efficacy experiment (section 2.5.2.2) with the same procedures followed.

2.5.2.2 Efficacy of internalised siRNA

PEI/siRNA (AllStars Hs Cell Death Control siRNA) nanoparticles were added to cells as per section 2.5.1 siRNA transfection. After removal of the nanoparticle containing media, the 96-well plate was then

returned to the 37˚C incubator for 48 hours as recommend by the manufacturers of the Cell Death siRNA. After 48 hours had elapsed, CellTiter Glo® assay was performed (section 2.5.1.1).

2.6 Zeta sizing and Zeta Potential Measurements

Nanoparticles were prepared as above in section 2.2.2 Complex formation in 1 ml. Both Zeta Potential measurements and size measurements were taken using a Folded Capillary Cell. Negative Control siRNA was used to form 1 ml of 20:1 PEI/siRNA nanoparticles. To form the nanoparticles, 500 µl DEPC treated H_2O containing 10 µg siRNA was added to 500 µl DEPC treated H_2O containing 600 nmols of PEI amine nitrogen. The final volume was therefore 1 ml (0.75 µM siRNA).

Readings were taken using the Zeta Sizer Nano ZS. Mark Houwink parameters were used to determine the complex size and laser Doppler anemometry with the Smoulchowski model was used to estimate zeta potential.

2.7 Maximal concentration for nanoparticle formation

Nanoparticles are formed on the basis of a molar ratio of nitrogen in the PEI to the phosphate in siRNA. While the molar ratio of nitrogen to phosphate remains constant, the concentration of nanoparticles per volume of solution can be altered to suit a given need. Due to concerns about the potential of nanoparticles to aggregate at higher concentrations a series of experiments was conducted to determine the maximal concentration of siRNA at which to form nanoparticles for an N:P ratio of 20:1.

2.7.1 Cytotoxicity and efficacy

The procedures followed in section 2.5.2 were used to assess the effect of increasing siRNA concentrations on nanoparticle efficacy and cytotoxicity. Formation of nanoparticles at the following concentrations of siRNA were assessed: 0.75, 1.5, 2.0, 3.0 and 7.5 µM siRNA. Transfection was carried out 0.075 µM siRNA final concentration.

2.7.2 Heparin Dissociation assay

The stability of complexes formed at a range of concentrations was determined by a heparin dissociation assay. Heparin can compete with the siRNA to bind to PEI resulting in complex dissociation. Heparin sodium stocks were made to a concentration of 5000 U/ml in DEPC treated H_2O.

The stocks were then diluted to 50 U/ml (0.05 U/µl) in iso-PBS. The various concentrations of siRNA were exposed to 0, 1, 2, 3, 4 and 5 U/ml heparin in triplicate.

Fluorescently labelled (Alexa Fluor® 488) siRNA was used to form 20:1 nanoparticles at the range of concentrations of siRNA described above (section 2.7.1), samples were aliquoted into an opaque flat-bottom 96-well plate. The samples were then further diluted with iso-PBS before heparin sodium was added to each concentration for a final volume of 100 µl. Although the complexes were formed at various concentrations the final concentrations in the wells was 0.15 µM siRNA. The samples in the wells were then mixed by shaking the plate for a minute before incubating for 10 minutes at room temperature. The fluorescence signal was then read at an excitation of 499 nm and emission of 519 nm using a fluorometer. A graph of relative fluorescent units versus the heparin concentration was plotted.

2.8 Hydrogel preparation

Polyethylene Glycol (PEG) (Mw: 20 KDa) hydrogels of varying percentages (m/v) were prepared using both 4-arm and 8-arm PEGs. Collagen gels (2 mg/ml) were also used in this project.

2.8.1 Poly(ethylene) Glycol preparation

Both 4-arm (20PEG-4VS) and 8-arm (20PEG-8VS) PEG monomers (Mw: 20 KDa) with vinyl sulfone (VS) termini were formed as previously described[251] by the polymer laboratory of the Cardiovascular Research Unit, UCT. Briefly, 20PEG-4VS and 20PEG-8VS were fabricated in dry Dichloromethane by deprotonating 20PEG-4OH and 20PEG-8OH using sodium hydride (NaH). Divinyl sulfone ($C_4H_6O_2S$) was next added in excess. Acetic acid (CH_3COOH) was used to quench the remaining NaH in the crude reaction mixture followed by three consecutive precipitations in ether.

Vinyl sulfones react with sulfhydryls via a Michael addition reaction. Thus if divalent sulfhydryl containing molecules are reacted with multivalent PEG-VS at stoichiometric amounts of sulfhydryls to VS termini, a hydrogel is formed. A matrix metalloproteinase 1 (MMP-1) recognition sequence containing cysteine residues (GCREGPQGIWGQERCG, 1732.91 Da) can thus be used to polymerise PEG-VS hydrogels. These MMP-1 peptide sequences are enzymatically cleavable by MMP-1 and other members of the MMP family[202]. Additionally, when cell adherence was required, an Arginine-Glycine-Aspartate (RGD) (GCGYGRGDSPG, 1025 Da) amino acid sequence containing a single cysteine residue was covalently bound to the hydrogel. RGD is a tripeptide which enables cell migration through cellular binding via integrin's[262].

The MMP-1 peptide and PEG were combined at a molar ratio of 4:1 (8-arm) or 2:1 (4-arm) MMP:PEG. For cellular experiments, RGD was added prior to the addition of other gel components at a molar ratio of 12.5:1, PEG:RGD. The RGD and PEG were incubated for 30 minutes in a water bath at 37°C prior to adding other components. These were then combined to form hydrogels with a final PEG concentration of 2, 3.5 or 4% (m/v).

The MMP-1 peptide sequence, RGD and PEG were both resuspended using triethanolamine (TEOA 0.3 M). The gels were made up to their final volumes using TEOA in order to have the correct final concentration of components before the addition of the MMP-1 peptide cross linker. An example of a 3.5% (m/v) 20PEG-8VS hydrogel and 20PEG-4VS hydrogel is given below (Table 3). When nanoparticles were added, they were added in the place of a portion of the TEOA.

Table 3: Components for a 3.5%, 100 ul hydrogel for both 4- and 8-arm PEGs.

		20PEG-8VS		20PEG-4VS	
Sequence	Components	Volume	Final concentration	Volume	Final concentration
1	PEG 20% (m/v)	17.5 µl	1.75 mM	17.5 µl	1.75 mM
2	RGD (0.1 mg/60 µl)	8.61 µl	0.14 mM	8.61 µl	0.14 mM
3	TEOA or iso-PBS	45.02 µl	-	59.45 µl	-
4	MMP-1 peptide (1 mg/23.8 µl)	28.87 µl	7 mM	14.44 µl	3.5 mM

2.8.2 Collagen Gel Preparation

Collagen gels were formed at a concentration 2 mg/ml using collagen derived from bovine skin or rat tail. When working with collagen it is important to work on ice at all times, as such all microcentrifuge tubes used as well as reagents were kept on ice. To make 800 µl of 2 mg/ml collagen gel, 533.34 µl of 3 mg/ml stock solution was combine with 45.25 µl 10 X DMEM (pH 7.4), 45.25 µl of a 23 mg/ml stock solution of $NaHCO_3$, 15.5 µl 0.36 M NaOH (occasionally additional NaOH was required), and finally 160.66 µl of 1 X DMEM (pH 10, 2.3 mg/ml $NaHCO_3$). Table A2.2 (Appendix A2) is a list of reagents used for collagen hydrogels and their preparation. Gels were allowed to polymerise for 30-45 minutes at 37°C.

The reagents were added sequentially ending with the NaOH. In order for the gels to be able to set, the final solution needed to have a red to pink colour – this colour (derived from phenol red present in the DMEM) indicates a pH between 7.5 and 8.0. At lower pH values gelation would not occur.

2.8.2.1 Dermal equivalent preparation

Collagen gels were prepared according to the above protocol (section 2.8.2). Gels were prepared with 40 000 cells entrapped per 40 µl collagen gel (1000 cells/µl). A volume of media containing the required number of cells was removed and placed in a 1.5 ml microcentrifuge tube and spun down into a pellet at 13200 rpm. Excess media was removed and replaced with the required volume of collagen (2 mg/ml) mix. The collagen cell solution was mixed thoroughly by pipetting and then aliquoted (40 µl) onto siliconized sterile petri dishes (3 cm) and allowed to set. Once set, 3 ml media was added to the petri dish and gels were detached from the surface using a sterile spatula. Using the same spatula the gels were moved into individual wells of a 24-well plate containing 10% DMEM and incubated for 48-72 hours at 37°C, 5% CO_2. These form dermal equivalents which are used in experiments described below (section 2.10.2).

2.9 Entrapment of nanoparticles within PEG hydrogels

Nanoparticles were formed at an N:P ratio of 20:1 (2 µM siRNA) and encapsulated within PEG hydrogels. The nanoparticles were added to the hydrogel mixture prior to polymerisation, samples were vortexed before aliquoting out 20 or 50 µl gels in a siliconised (Appendix A3) 24-well plate or surface or on Parafilm® within a petri dish and allowed to polymerise at 37°C. To compensate for the addition of nanoparticles an equivalent volume of TEOA was not added to the mixture.

2.9.1 Visualisation of encapsulated nanoparticles

Nanoparticles were formed using AllStars Negative Control siRNA which had been fluorescently tagged with an Alexa Fluor® 555 label. The fluorescent tag of the siRNA allowed for the visualisation of the entrapped particles. The final concentration of the siRNA within the hydrogel after entrapment was 0.75 µM.

The hydrogels were imaged and z-stacks taken using a Zeiss 510 LSM Meta with a solid state laser (excitation: 561 nm, emission: 500-550 nm) at 10X times objective magnification, 1X zoom.

2.9.2 RNase protection of entrapped nanoparticles

Nanoparticles were complexed using negative control siRNA. Nanoparticles were entrapped within a 20 µl 4% 8-arm PEG hydrogel at a final siRNA concentration of 0.75 µM siRNA. All gel and nanoparticle preparation was done in a Bio-hazard laminar flow hood using sterile buffers and consumables.
After the gels had set they were carefully removed (using a thin sterile spatula) from sterile Parafilm® and added to individual sterile 2 ml microcentrifuge tubes with 300 µl 50% FBS. These gels were then placed in a shaking 37°C incubator (50 rpm). For time point T0 the gels were not placed in FBS and frozen straight away. At T = 24, 72, 120 and 168 hours gels were removed from the 37°C incubator. At all-time points, including T0, gels were washed 1X using DEPC treated H_2O and flash frozen in liquid nitrogen before being placed in the -65°C freezer for storage so that no further degradation could take place. As an additional control 2 gels were also placed in 300 µl DEPC treated H_2O and incubated for 7 days. Non-encapusulated PEI/siRNA were processed as above in section 2.4.1.

The gels were thawed and then digested in 1 mg/ml proteinase K (10 mM pH 7.3 Tris-Cl, 1 mM $CaCl_2$) and 0.5% SDS (to dissociate nanoparticles) for 2 hours in a shaking 37°C incubator. The non-entrapped nanoparticle complexes in FBS were also treated with Proteinase K in the same way as the hydrogels. Agarose gel electrophoresis was used to analyse samples (2.3 pmols) as described above (section 2.3.1). The digested product from the T0 time point was always run alongside experimental samples and used as the 100% mark for quantification purposes.

2.9.3 PEI/siRNA nanoparticle and naked siRNA controlled release

Both PEI/siRNA nanoparticles and naked siRNA were entrapped within 4- and 8-arm 3.5% PEG hydrogels (section 2.8.1 and 2.9.2). Negative control siRNA was used to form nanoparticles (2 µM siRNA. The final concentration of siRNA for both complexed and non-complexed siRNA in the PEG hydrogels was 0.75 µM.

Polymerised hydrogels were removed from sterile Parafilm® (using a thin sterile / clean spatula) and placed in individual sterile 2 ml microcentrifuge tubes containing either nothing or 100 µl HBS elution buffer (25 mM, pH 7.4-7.5). The hydrogels placed in the empty microcentrifuge tubes were immediately frozen along with the extra nanoparticles and naked siRNA solutions which were prepared and stored at -65°C. The gels in elution buffer were placed in a shaking (50 rpm) 37°C incubator and washed for 1 hour (Time = 1 hour). After 1 hour incubation, they were removed and placed into new sterile 2 ml microcentrifuge tubes also containing fresh 100 µl 25 mM HBS elution

buffer. The Time = 1 hour microcentrifuge tube containing buffer was stored at -65°C. The process of moving the hydrogels, placing into fresh HBS and storing the elution buffer at -65°C was repeated at T = 24, 72, 120 and 168 hours. The hydrogels were placed in the initial "wash" buffer for one hour to remove any nanoparticles and siRNA which are perhaps not fully entrapped.

At the conclusion of the experiment, the hydrogels were defrosted and digested in Proteinase K according to the protocol outlined in section 2.9.2. The digested gels as well as the wash and elution buffers were analysed via gel electrophoresis (section 2.3.1). A standard curve was constructed using naked siRNA stocks and run alongside the buffer and digest samples.

2.10 3D Cellular invasion / migration

Cells were entrapped within hydrogels in order to assess cellular invasion and transfection of cells by the entrapped nanoparticles. Combination of PEG/PEG and PEG/collagen gels were assessed (section 2.8).

2.10.1 3D Cellular Invasion from a PEG Hydrogel into a PEG Hydrogel

Both 8-arm and 4-arm PEG hydrogels were used to assess cellular invasion and migration in a 3D environment. Varying percentages were tested. For the 8-arm gel, 2% (m/v) gels were prepared and for the 4-arm 3.5% (m/v). Flat-bottomed, non-tissue culture treated 96-well plates were siliconized prior to starting these experiments and were re-sterilised via gassing.

Gels of 3 µl and 50 µl, containing RGD, were prepared. For the 3 µl gels, cells were suspended in PEG gel solution at 40 000 cells/3 µl). Cells were mixed before being individually pipetted into separate wells in a 96-well plate and allowed to set. While the gels containing cells were allowed to set, the 50 µl PEG gels were prepared. The 50 µl gels were then added directly over the 3 µl gels and also allowed to set before adding 200 µl of 10% FBS MCDB-131 media. Epidermal Growth factors (100 ng / ml) were added to some wells every alternate day.

2.10.2 3D Cellular Invasion – From Dermal Equivalents into PEG Hydrogels

Prior to performing these experiments, 24-well plates were prepared by scoring them with a specially made in-house punch and then siliconizing and re-sterilising by gassing (Figure A3.1 of the Appendix).

Dermal equivalents were prepared according to the protocol in section 2.8.2.1. After 24-72 hours the dermal equivalents were removed from the incubator and carefully placed into PEG hydrogels using forceps. The gels were allowed to set for 25-45 minutes in the 37°C, 5% CO_2 incubator. Once set, 1 ml 10% FBS DMEM media was added to each well.

PEG hydrogels of 3.5% (m/v) were made using a 4-arm or 8-arm PEG as described above in section 2.8.1. Gels were prepared with and without nanoparticles added and the nanoparticles were formed using either AllStars Negative Control siRNA Alexa Fluor® 488 or 555, Negative Control siRNA or AllStar Hs Cell Death Control siRNA at a concentration of 2 µM siRNA. Once encapsulated the final concentration of siRNA inside the gel was 0.75 µM.

The following aspects of cell migration were assessed; ability of cells to invade from a collagen gel into a PEG hydrogel and the overall distance migrated, the ability of cells to migrate into gels containing nanoparticles was assessed for siRNA internalisation, and efficacy of entrapped nanoparticles once they have been internalised by invading cells. Methods for assessment are outlined below.

2.10.2.1 3D Cellular Invasion – measuring cellular migration

The same randomly selected segment of each well containing gel was imaged using a Nikon Eclipse Ti-S light microscope over a number of days to monitor cell migration. The same area was imaged at each time point. The images were analysed using Motic Image Plus 2.0 software to measure the distance which the invading cells moved. The distance from the furthest 6 cells to the edge of the dermal equivalent was measured and averaged. Accumulated distance was calculated and plotted against time.

2.10.2.2 3D Cellular Invasion – Internalisation

When using fluorescently tagged nanoparticles, gels were imaged using a Zeiss LSM510 Confocal microscope with ZEN 2009 software. Tile scan Z-stacked images were taken. ZEN 2012 (blue edition) was used to compile tile-scan Z-stacked images into compressed images. It was also used to assess internalisation of the fluorescently tagged siRNA. The Ortho (orthogonal projection) tool was used to view individual cells from the X-, Y- and Z-view in order to confirm transfection.

2.10.2.3 3D Cellular Invasion – Efficacy

Efficacy was determined using cell death siRNA nanoparticles. Wells were only imaged on the final day of the experiment, when cells were stained using LIVE/DEAD™ cell viability assay (section 2.10.2.3.1). Z-stacks were taken using a Zeiss Axiovert 200M Fluorescence microscope with a Zeiss AcioCam HRm monochrome camera AxioVision 4.8 software. The area imaged was selected using the green channel in order to avoid biased selection. Controls for this experiment were entrapped Negative Control siRNA nanoparticles and a non-treated group where no nanoparticles were added.

2.10.2.3.1 LIVE/DEAD® cell viability assay

The LIVE/DEAD® cell viability assay is a commercially available assay used to determine the number of living or viable cells present. The assay works based on plasma membrane integrity and esterase activity. It is a two-dye system that allows the user to visually distinguish between living and dead cells. Ethidium homodimer-1 (EthD-1) is a red fluorescent dye that indicates the loss of plasma membrane integrity. Calcein-AM is a green-fluorescent dye which is able to cross the plasma membrane and indicates the presence of intercellular esterase activity. Thus dead cells are red and live cells are green. The assay was adapted from manufacturers' guidelines for 2D to 3D and is outlined below.

To 10 ml of sterile PBS pH 7.4, 20 µl 2 mM EthD-1 (4 µM) was added and the solution vortexed before adding 5 µl of the 4 mM Calcein (2 µM). Media was removed from the wells and washed 1X with 1 ml sterile PBS. The PBS was then removed and replaced with 700 µl of the EthD-1 Calcein solution. The samples were then incubated for a minimum of 20 minutes and a maximum of 40 before imaging. Wells were stained in duplicates and just prior to imaging one pair of wells, the next pair was prepared by washing with PBS as above and then adding the EthD-1 Calcein mix to the wells for incubation. This process was repeated until all of the wells had been imaged. It has previously observed in our laboratory that after > 1 hour exposure to cells in a gel, EthD-1 gains access to live cells turning them yellow.

Z-stack images were taken of the wells using a fluorescent microscope after incubation. Images were taken using 10X objective magnification using Cy3 (red) and 10 Alexa Fluor 488 (green) reflectors. Both the exposure time and the size of the z-stack was optimised when the experiment was first conducted and all proceeding experiments were imaged with the same specifications. Exposure times were 687

ms and 205 ms for the Cy3 and 10 Alexa Fluor 488 channels respectively. The entire stacks comprised of 25 slices each 758 µm thick.

After imaging, individual images from Z-stacks were analysed manually using Zen Blue software. When analysing wells containing cell death siRNA, as previously mentioned, green cells represented those cells which are living and red cells represented dead cells. Zen Blue was used to mark each of the red cells and end up with a final count of number of dead cells. Results were normalised to wells containing non-treated cells.

2.10 Statistical analyses

STAT Plus was used for statistical analysis. Results are expressed as the mean and error bars are standard error of the mean (SEM) unless otherwise stated. Comparisons between more than two groups were analysed by analysis of variance (ANOVA) followed by the Tukey-Kramer post hoc testing. A probability value of less than 0.05 was considered to be significant. Though data is represented graphically as normalised where appropriate, statistical analysis was performed with original data.

3. Results & Discussion

The aim of this project was to determine the feasibility of using enzymatically degradable PEG hydrogels to localise delivery of complexed siRNA. Assays establishing the use of PEI to complex siRNA into nanoparticles and the techniques required for this were initially developed. Towards entrapment and delivery, various techniques were developed and assessed. The development of a 3 dimensional (3D) cellular invasion assay for the analysis and potential optimisation of siRNA delivery *in vitro* prior to *in vivo* work being conducted formed part of this assessment. Additionally, the potential for added protection via hydrogel encapsulation from degradation by ribonucleases was assayed. The results achieved, and the various techniques used are outlined below.

3.1 Establishment of PEI/siRNA nanoparticles

PEI/siRNA nanoparticles are formed based on a ratio of amine nitrogen's found on PEI to phosphates on the siRNA backbone known as an N:P ratio. The optimal N:P ratio with regards to the complexation, stability, cytotoxicity and internalisation was established.

3.1.1 Nanoparticle Formation

Nanoparticle formation was assessed via a gel retardation assay. Agarose gel electrophoresis was used to assess complex formation as it allows for the separation of non-complexed siRNA from complexed siRNA (Figure 2). There have been two proposed explanations given for the inability of polycationic complexed siRNA to migrate into an agarose gel. Firstly, elevated steric hindrance due to the increased size and/or changed structure of the nanoparticle complexes. Alternatively, when complexed the negative charge of the siRNA is negated by the positively charged PEI and as such the nanoparticle complex does not run towards the anode[94]. Of course these two mechanisms can both play a role.

Qualitatively, partial complexation was seen already from the lowest N:P ratio of 0.625:1 with complete complexation occurring at 5:1 (Figure 2a). Densitometric analysis confirmed this observation with N:P ratios of 0.625, 1.25 and 2.5:1 complexing 27, 58 and 96.5% of the siRNA respectively (Figure 2b). At 5:1 and higher 100% of siRNA was complexed. Though it might be postulated that all ratios below 5:1 needed no further characterisation as incomplete complexation was achieved, only the 0.625:1 ratio was excluded for further analyses in this section due to its inability to fully complex siRNA. Although all three of the lower ratios did not fully complex the siRNA and may thus not be expected to perform optimally for RNase protection and transfection efficacy, lower ratios have been assayed by others and found to be effective[263].

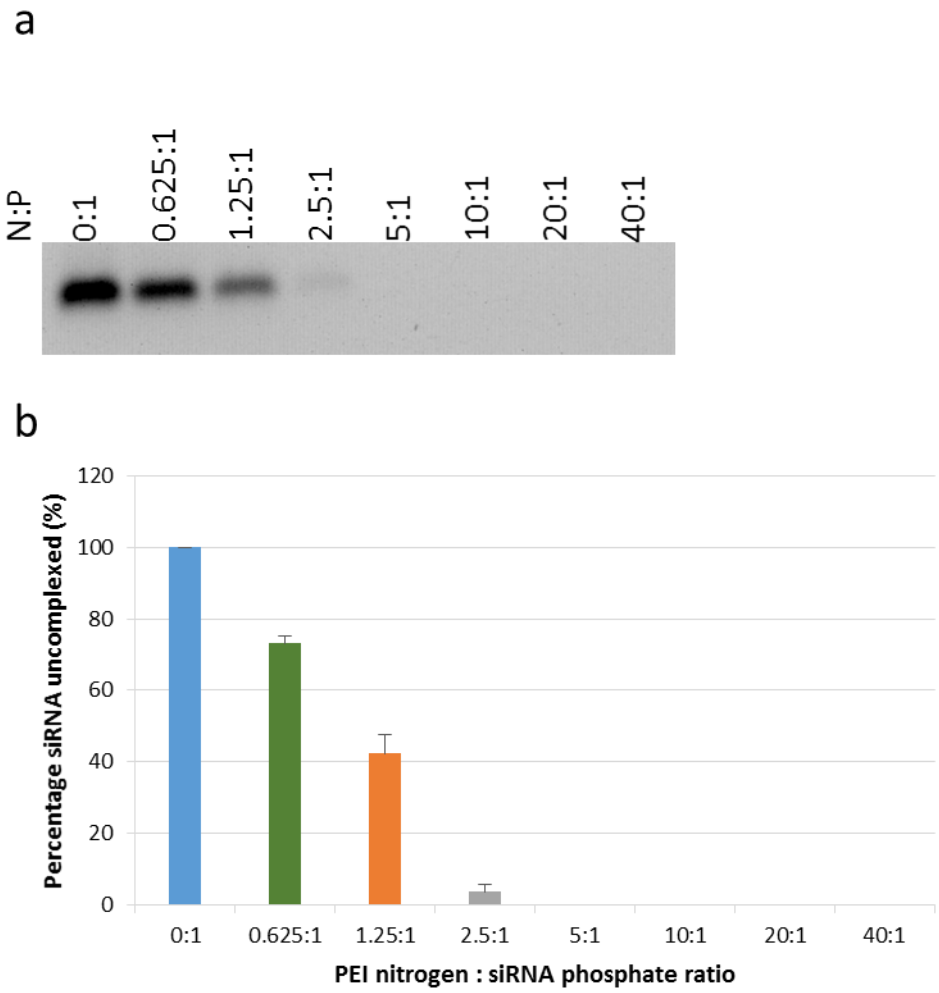

Figure 2: Gel Retardation Assay: *(a) PEI/siRNA complexes formed at a range of ratios resolved on a 4% agarose gel. (b) Densitometric quantification of gel retardation assay. Data was normalised to non-complexed siRNA. n = 2 (biological repeats).*

3.1.2. Complex Stability: Protection of siRNA from RNase Degradation

siRNA is subject to degradation by RNases found in serum and their inhibition has been previously shown to improve siRNA half-life[257,264]. RNA is more susceptible to degradation by ribonucleases than other nucleic acids. This is because DNA contains the sugar deoxyribose whereas RNA has the sugar ribose in its backbone. The ribose has a hydroxyl group in the 2' position of the pentose ring which renders the RNA more vulnerable to hydrolysis by serum nucleases[265,266]. Therefore an important aspect of complexation by polycations is their ability to potentially sequestrate the siRNA from degradation by serum RNases.

The ability of the various ratios of PEI:siRNA to protect the siRNA from RNases was thus assessed by incubating the nanoparticles in 50% serum[55,257,259,264] at 37°C over a period of 7 days. After incubation

the nanoparticles were disrupted by exposure to SDS and the relative amounts of siRNA assayed using agarose gel electrophoresis (Figure 3a).

After 1 hour incubation none of the uncomplexed siRNA (0:1) was still present in the samples. An unidentified contaminant that originates from serum can be observed running above the siRNA band but is well separated. The 1.25 and 2.5:1 ratios achieved the lowest levels of protection with 60 ± 5% and 40 ± 16% of siRNA being degraded within first 6 hours respectively (Figure 3b). The 1.25:1 ratio was 95 ± 3% degraded within the first 24 hours and by 72 hours had completely degraded. While the 2.5:1 ratio fared slightly better, after 72 hours 99% of siRNA had been degraded. The results achieved here were not unexpected as these ratios did not achieve complete complexation (section 3.1.1). The 5:1 ratio was the lowest ratio which achieved full complexation. After 72 hours, 18 ± 5% still remained but by 168 hours only a minimal 2 ± 1% remained. After 7 days, the 5:1 ratio had a lower level remaining than the adjacent ratio of 10:1. The 10, 20 and 40:1 ratios achieved the highest levels of protection after 7 days (Table 4) with increase protection proportional to PEI ratio.

Table 4: Percentage siRNA remaining per ratio after 7 days exposure to RNases present in FBS (± SEM) n = 3 (biological repeats)

	0:1	1.25:1	2.5:1	5:1	10:1	20:1	40:1
% siRNA	0 ± 0	0 ± 0	0 ± 0	2 ± 1	48 ± 9	53 ± 13	66 ± 12

As previously mentioned (section 1.2.1.2), high and repeated dosages of naked siRNAs have been used to deliver siRNA *in vivo*. This is partly due to rapid degradation by the ribonucleases present. It is therefore apparent that maintenance of dosage by increased protection is both important and desirable. The potential dosage reduction might reduce side effects. Previous studies have also demonstrated the vulnerability of uncomplexed and unmodified siRNA in serum and showed that even in a 1% solution of Foetal Calf Serum, the siRNA is fully degraded within 15-30 minutes[143,165]. To our knowledge RNase protection of polycationic complexed siRNA has not been examined beyond 24 hours[267]. A reduction in degradation observed here for up to 7 days is especially important in the context of scaffold based localised and controlled delivery of siRNA where longer persistence times would be desirable. Thus, the protection garnered to the siRNA by the higher ratios, where a substantial amount of siRNA is still available at 7 days, is promising. It has been proposed that encapsulation of nanoparticles in a scaffold may allow for further additional protection[226]. This aspect is examined in greater detail later.

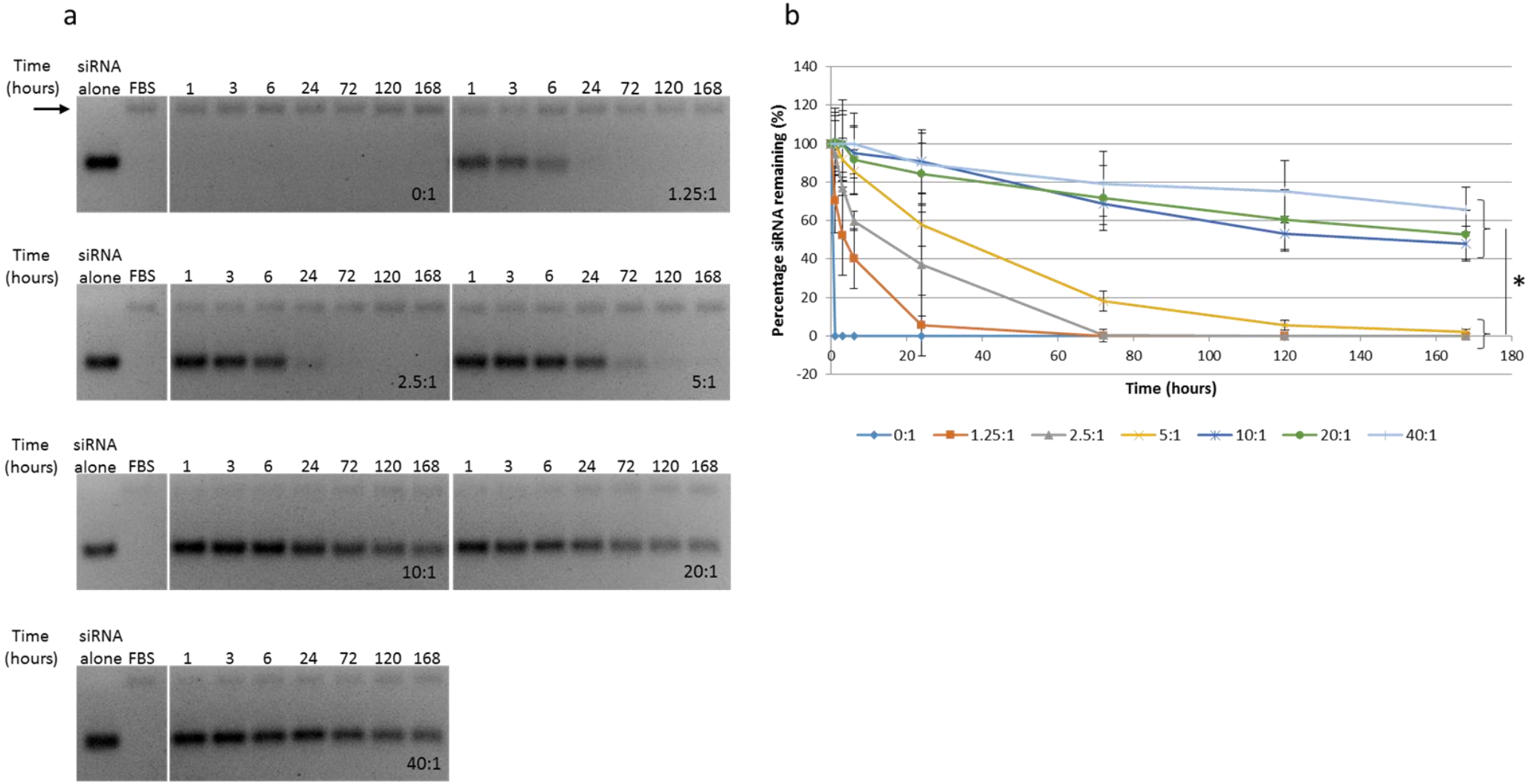

Figure 3: Ability of PEI to protect siRNA from degradation. *RNase degradation of siRNA was measured by exposing complexes to RNases present in FBS. (a) Samples were resolved of a 4% agarose gel. Qualitatively, the optimal ratio for protection from degradation appears to be from 10:1 and higher as siRNA is still present at 7 days. (b) Band quantification of the siRNA present from each of the respective ratios over time. At 7 days the 10, 20 and 40:1 ratios were able to protect the siRNA from degradation at a significantly higher level compared to the lower ratios of 0, 1.25, 2.5 and 5:1 (*p < 0.05). n = 3 (biological repeats). Arrow indicates serum contaminant.*

3.1.3 Cytotoxicity of PEI/siRNA ratios

As previously stated, PEI is a commonly used transfection agent however, it has also previously been reported as being cytotoxic[150]. Moghimi *et al*[268]., conducted a study to elucidate the cytotoxic effects of PEI and found that its use can cause membrane damage and induce apoptosis. A possible cause of the reported cytotoxicity is the PEI being in excess and it has been shown that partial purification of PEI nanoparticle complexes can result in a reduction in cytotoxicity[269]. However, with this reduction, a reduction in transfection efficacy was also reported[269]. As such in determining the optimal ratio of PEI/siRNA it is important to first determine the relative cytotoxicity of the PEI.

Negative control siRNA, was complexed with PEI to allow for the detection of cytotoxicity. This form of siRNA (a scrambled sequence) is reported by the manufacturers to have no known homology with any identified mammalian gene. Samples were analysed using the CellTiter-Glo® Luminescent Cell Viability Assay that determines the number of metabolically active cells present. The levels of ATP which are measured by the assay are generally considered to be directly proportional to the number of metabolically active cells[261].

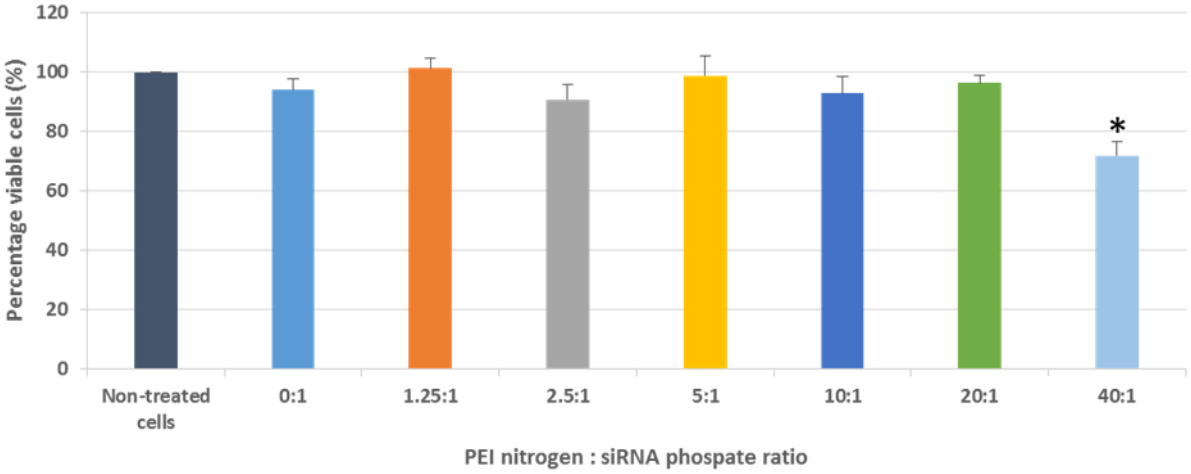

Figure 4: Relative cytotoxicity of a range of PEI/siRNA nanoparticles using Negative Control siRNA. *Cells were treated for 4 hours and incubated for a further 48 hours with media. Treated wells were normalised to non-treated wells and the percentage cells remaining determined 48 hours post transfection. (*p < 0.05 versus to the non-treated cells) n = 3 (3 technical repeats per biological repeat).*

Significant levels of cell death due to cytotoxicity were seen only at the 40:1 ratio (*p < 0.05 versus non-treated cells*) (Figure 4). There was no significant difference in the number of viable cells between ratios 0:1 (naked siRNA), 1.25:1, 2.5:1, 5:1, 10:1 and 20:1 compared to the control wells (non-treated cells). This result suggests that the 40:1 ratio is not optimal due to cytotoxicity.

3.1.4 Efficacy of siRNA transfection

The efficacy of delivered siRNA was determined using AllStars Hs Cell Death Control siRNA. Determining efficacy is essential as although there might be complexation (as determined by gel retardation assay, section 3.1.1), nanoparticles may be ineffective at delivering the siRNA across the cell membrane and releasing them into the cytoplasm.

AllStars Hs Cell Death Control siRNA is a commercially available siRNA that targets a range of ubiquitously expressed genes which are essential to cell functioning. This form of siRNA was selected as the cell death due to successful transfection is readily quantifiable with the CellTiter-Glo® assay (Figure 5).

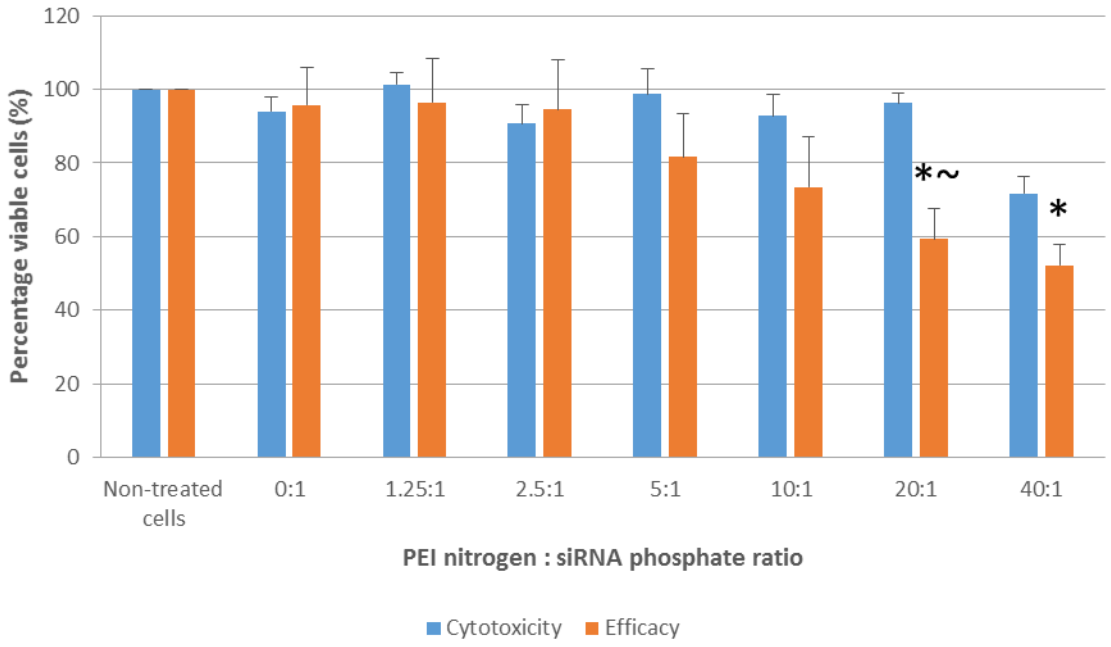

Figure 5: Measuring the efficacy of internalised siRNA and comparing efficacy with cytotoxicity. *AllStars Hs Cell Death siRNA was complexed at a range of N:P ratios in order to determine efficacy. Cell death was normalised to wells containing cells which were non-treated with nanoparticles. Results displayed allow for the comparison between cytotoxicity and efficacy to be easily made and to more clearly demonstrate the effectiveness of the delivery modality. (*p < 0.05 versus the non-treated cells) (~ p < 0.05 versus 20:1 ratio used to assess cytotoxicity) n = 3 (3 technical repeats per biological repeat).*

A trend was observed with an increase in cell death as the N:P ratio increases. As would be expected from the literature, no evidence of cell death was observed for the naked siRNA (0:1). This was also observed for the 1.25 and 2.5:1 ratios. The 5:1 ratio achieved on average approximately 20% cell death and the 10:1 27%. However, significantly higher levels of cell death were only observed for the 20:1 ratio and 40:1 ratio with a 40 and 50% decrease in cell viability (*$p < 0.05$ versus the non-treated cells*). Results were collated to allow for the easy comparison of efficacy and cytotoxicity. There was

significant difference in the levels of cell death seen in those wells treated with the 20:1 cell death siRNA ratio relative to the 20:1 negative control siRNA ratio (*$p < 0.05$ versus 20:1 negative control siRNA)*. However there was no significant difference seen when comparing the cell death siRNA and the negative control siRNA at the 40:1 ratio.

3.1.5 Selection of optimal ratio

The data analyses indicates that the 20:1 ratio is optimal. The higher ratios of 10:1, 20:1 and 40:1 were generally superior to the lower ratios. A significantly higher level of RNA was preserved from RNase degradation for the above ratios. The 40:1 ratio did have a relatively higher level remaining at 2 days compared to the 10:1 and 20:1 ratios. However, the 40:1 ratio showed significant levels of cytotoxicity. Effective gene knockdown is perhaps the most important consideration when determining an optimal PEI/siRNA formulation. Only the 20:1 and 40:1 ratios showed significant and relatively substantial levels of gene knockdown. The 20:1 was considered optimal as it is clear that a portion of the knockdown efficacy of the 40:1 ratio could be attributed to its cytotoxic effects. Additionally, the small increase in knockdown achieved by the 40:1 was not significantly greater than that by the 20:1. It should be noted that although the cell death siRNA allows for easy quantification, the results can be complicated by cytotoxicity. However, the outcome here was clear and additional experiments utilizing other assays such as anti-GFP siRNA were not considered necessary. Levels of cell death recorded at a ratio of 40:1 for the cell death siRNA treated wells versus the negative control treated wells were not significant, whereas for the 20:1 ratio these levels were significant. This would indicate that a large proportion of the cell death seen at a ratio of 40:1 was due to PEI toxicity rather than due to the action of the siRNA as seen for the 20:1 ratio.

It has been suggested that having PEI in excess, in other words free PEI, contributes to its efficacy as a delivery agent[169–171,269]. However, an overabundance of PEI leads to a higher degree of toxicity[171]. This could explain the differences seen in the ratios which achieved full complexation (Figure 2). The 5:1 and 10:1 ratios may have insufficient excess PEI whilst the 40:1 ratio too great an excess resulting in cytotoxicity. The 20:1 may have had an optimal excess. It is also possible that insufficient charge shielding occurred with the lower ratios resulting in inadequate cell ingress.

This work supports and corroborates the study of Kwok et al[270]. They too achieved full complexation from a ratio of 5:1 as determined by gel retardation assay (Figure 2). Unlike here where Cell Death siRNA was used to assay efficacy in HT1080 cells, Kwok and colleagues[270] used anti-luciferase siRNA in Neuro-2A luciferase expressing cells. Anti-EGFP siRNA was used as a negative control. The second

largest knockdown in luciferase expression (60%) was reported for cells treated with the 20:1 ratio. This is similar to the efficacy results achieved here as the 20:1 ratio also achieved the second largest levels of knockdown determined here by cell viability (Figure 5). While a larger decrease in luciferase was seen after treatment with the 40:1 ratio, this was attributed to cytotoxicity as a similar decrease in luciferase expression was also reported for cells treated with anti-EGFP siRNA at this ratio. Cytotoxicity assay confirmed this and cell death of approximately 20 and 40% was seen for both the 20:1 and 40:1 ratios. No noticeable cell death due to cytotoxicity was seen for the 20:1 ratio in this project. This could be due to HT1080 cells being a more robust cell-line compared to the Neuro-2A cells used in the Kwok study.

3.1.5.1 Nanoparticle characterisation: Size and zeta potential for 20:1 ratio

Subsequent to determining an optimal ratio, the size of PEI/siRNA nanoparticles formed at a ratio of 20:1 was determined by dynamic light scattering (Appendix A4). The mean size of the complexes was 74.165 nm with an average polydispersity index (PDI) of 0.1875. PDI is a measure of the particle size distribution. A PDI between 0.1-0.3 is considered good as it indicates a high proportion of particles are of similar size. The zeta-potential was measured at 56.7 mV $\pm$ 6.22 mV. Both of these are within range in order to achieve optimal delivery.

Complex size and charge can negatively impact on siRNA internalisation and are therefore important considerations. It has previously been suggested that in order to achieve non-specific uptake by clatherin coated pits, complexes should be between 50 and 150 nm in size, beyond which nanoparticles are unlikely to be passively endocytosed[265,271]. As with size, particle charge is important in order to promote cellular uptake. Negatively charged siRNA is not likely to be passively taken up by the negatively charged cell membrane. By donating an overall positive charge, siRNA internalisation is promoted, however, *in vivo* other complications which lead to nanoparticles aggregation could occur and should be considered. Physiological salt conditions could lead to a reduction in repulsive forces between nanoparticles resulting in aggregation and nanoparticle complexes too large to be internalised[272]. Another concern *in vivo* would be the interactions between complexes and negatively charged serum proteins[265].

3.2 Towards localised delivery

Enzymatically degradable PEG hydrogels have been shown to have a wide range of utility including growth factor delivery. More specifically with regard to siRNA delivery, these types of gels have been used as a therapeutic vehicle delivering microspheres containing growth factors[255]. They have been used to promote angiogenesis, bone growth, wound healing and also provide mechanical support to an infarcted heart. An advantage of the form of PEG hydrogel proposed here, for the localised delivery of siRNA, is that it is both injectable and self-polymerising. Their use negates the need for complicated surgical procedures that would otherwise be required to implant pre-fabricated hydrogels. This form of hydrogel also does not require an external light source for gelation to occur. Non-polymerised hydrogels can be delivered to otherwise hard to access areas via catheter where self-polymerisation can take place once delivered. As detailed above in sections 1.4.1 and 1.5, several forms of hydrolytically degradable and photocroslinkable forms of PEG have been explored as a means of siRNA delivery[211,229]. This study aimed to extend the repertoire of PEGs investigated for the delivery of RNAi particles to include Michael addition reaction based spontaneously polymerising and enzymatically degradable forms[201].

The fundamental aim of this project was to assess the feasibility of using enzymatically degradable PEG hydrogels to deliver siRNA complexed with PEI. After establishing an optimal ratio with which to formulate PEI/siRNA nanoparticle complexes, the formulation was then used to assess the PEG hydrogels utility as an RNAi delivery depot.

3.2.1 Optimal Concentration for nanoparticles

Various facets of nanoparticle entrapment and release were considered and examined. These included determining the optimal concentration of siRNA for nanoparticle formation. Due to the nature of PEG hydrogels, the volume of nanoparticles that can be added is somewhat limited. At a maximum possible concentration of the PEG monomer and the peptide crosslinker, the volume available in a 50 µl hydrogel for example is 26.8 µl for the nanoparticle solution. In order to maximise the amount of siRNA that could be loaded into a hydrogel at a 20:1 N:P ratio a range of siRNA concentrations were assayed. A maximal dosage of siRNA was considered necessary at it should maximise any release of nanoparticles from a gel and increase the probability of an invading cells encountering nanoparticles.

The relative cytotoxicity of nanoparticles formed at a range of concentrations of siRNA was initially assessed using negative control siRNA (section 3.1.3). None of the concentrations were found to be significantly cytotoxic (Figure 6a).

The optimal concentration with which to form nanoparticles for transfection (which would then be used for entrapment) was determined using AllStars Hs Cell Death Control siRNA as was previously done for earlier efficacy experiments (section 3.1.4). Nanoparticle complexes were formed at a range of concentrations of siRNA from 0.75 - 7.5 µM. While various concentrations of siRNA were used to treat cells, the absolute amount of siRNA for transfection was maintained at 0.075 µM siRNA per treated well. As the concentration at which the nanoparticles were formed increased there was a trend towards a decrease in efficacy (Figure 6b). Nanoparticles formed at an siRNA concentration of 0.75 µM achieved the highest levels of cell death (61 ± 8% cell death). Higher concentrations maintained this level of transfection until a concentration of 7.75 µM siRNA was used. Here there was a significant decrease in the efficacy relative to 0.75 µM siRNA nanoparticles ($p < 0.05$). Indeed no significant difference was observed for this concentration relative to untreated cells.

It has previously been shown that due to charge interactions over time, PEI nanoparticles can form aggregates[273]. These aggregates are too large to gain cell entry and are therefore ineffective at nucleic acid delivery. Both PEI and siRNA are charged molecules which enables their interaction and spontaneous complexation into nanoparticles. With this there is a reduction in the charge difference and therefore a reduction in repulsion which over time can lead to particle aggregation. Under physiological conditions such a situation is worsened due to the repulsion forces being screened[265,272]. Sharma *et al*[273]., conducted a mechanistic study of PEI/DNA complex aggregation. They reported on various conditions which would affect aggregation including that at higher concentrations complexes are more likely to aggregate over time. The lack of transfection efficiency at higher concentrations observed here most likely reflects the influence of this concentration induced aggregation.

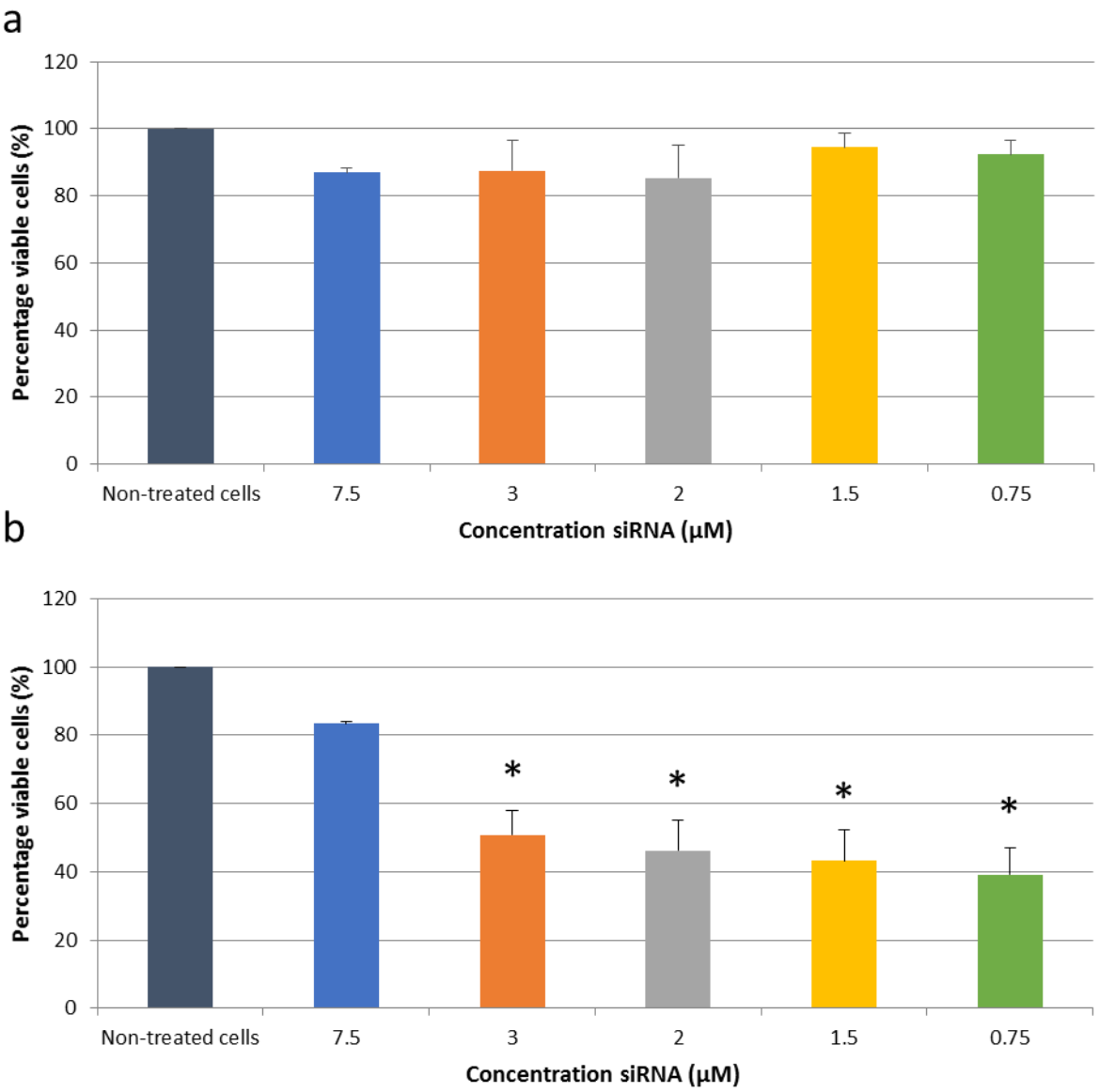

Figure 6: Effect on cytotoxicity and efficacy of different concentrations of PEI/siRNA nanoparticle complexes. *HT1080 cells were treated with various concentrations of siRNA while maintaining the same N:P ratio of 20:1. (a) Cytotoxicity of various concentrations of siRNA nanoparticles. (b) Efficacy of siRNA nanoparticles formed at different concentrations (*p < 0.05 versus non-treated cells). n = 3 (3 technical repeats per biological repeat).*

Potential particle aggregation was further examined by heparin dissociation. Complex stability for the range of siRNA concentrations was assessed using anionic heparin (Figure 7). Each of the various concentrations of siRNA were exposed to heparin at a range of concentrations (0 – 5 U/ml). Heparin can cause the dissociation of nanoparticles by competing with the siRNA binding to PEI[144,274]. It was hypothesised that if the nanoparticles were aggregating, heparin would be unable to fully compete and dissociate siRNA from the PEI.

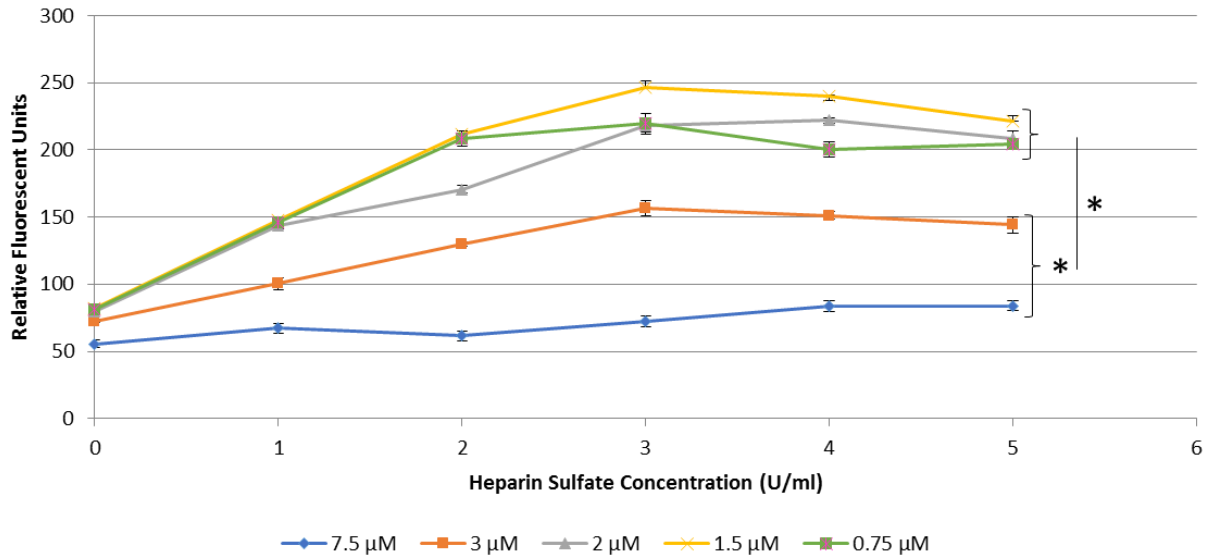

Figure 7: Stability of various concentrations of siRNA nanoparticles in heparin sulfate. *Nanoparticles formed at a range of siRNA concentrations and exposed to increasing concentrations of anionic heparin sulfate. Nanoparticles formed at a concentration of 7.5 and 3 µM were significantly less dissociated compared to nanoparticles formed at higher concentrations. The nanoparticles formed at 3 µM were also significantly more dissociated compared to the concentration of 7.5 µM (*p < 0.05).*

Nanoparticle complexes formed at higher concentrations (3 and 7.5 µM siRNA) were harder to dissociate with heparin than lower concentrations (0.75 – 2 µM). At 5 U/ml heparin nanoparticles formed at a concentration of 3 and 7.5 µM siRNA were significantly less dissociated than nanoparticle complexes formed at a concentration of 0.75, 1.5 and 2 µM ($p < 0.05$). There was also a significant difference between the nanoparticles formed at an siRNA concentration of 3 µM and 7.5 µM ($p < 0.05$).

The inability of complexes to dissociate at higher concentrations could be part of why siRNA efficacy (Figure 6b) was ineffective at these concentrations. Nanoparticles are required to release the siRNA upon entering the cell. The heparin dissociation assay gives an indication of the ability of the complexes to release the siRNA once the complexes have entered the cell[270]. The formation of aggregates may have compromised the ability of heparin to compete equally with the siRNA to bind PEI resulting in a lack of dissociation. The formation of large nanoparticle aggregates could therefore effect efficacy in two aspects. Firstly, larger aggregates are unlikely to be endocytosed due to their size and secondly the complexes inability to release siRNA if it was endocytosed would be deleterious for effective transfection.

A siRNA concentration of 2 µM for formation of nanoparticles was selected for future experiments. The 7.5 µM concentration was discarded due to the marked impairment in transfection efficacy and the reduced heparin driven dissociation observed for the 3 µM siRNA concentration raised concerns.

It should be noted that the finding of a concentration related decrease in efficacy may be specific to branched PEI. Nguyen *et al*[206]., formed nanoparticles with linear PEI modified with GMA at 37 µM siRNA and did not report any transfection complications.

3.2.2 Entrapment of nanoparticles

Nanoparticles were formulated at an optimal N:P ratio and siRNA concentration of 20:1 and 2 µM siRNA prior to being entrapped within an 8-arm PEG hydrogel and imaged. The confocal micrograph illustrates nanoparticle entrapment within the hydrogels (Figure 8). The compressed Z-stack allows for the visualisation of nanoparticles throughout the stack in 2D (Figure 8a). A 3D rendering also illustrates the distribution of the nanoparticle and demonstrates the even distribution of the nanoparticles throughout the depth of the hydrogel (Figure 8b). Having an even distribution of complexes is important for invading cells to ensure an equal likelihood that all cells invading encounter nanoparticle complexes. The entrapped nanoparticles appear to be sterically entrapped however further analysis was needed to confirm this.

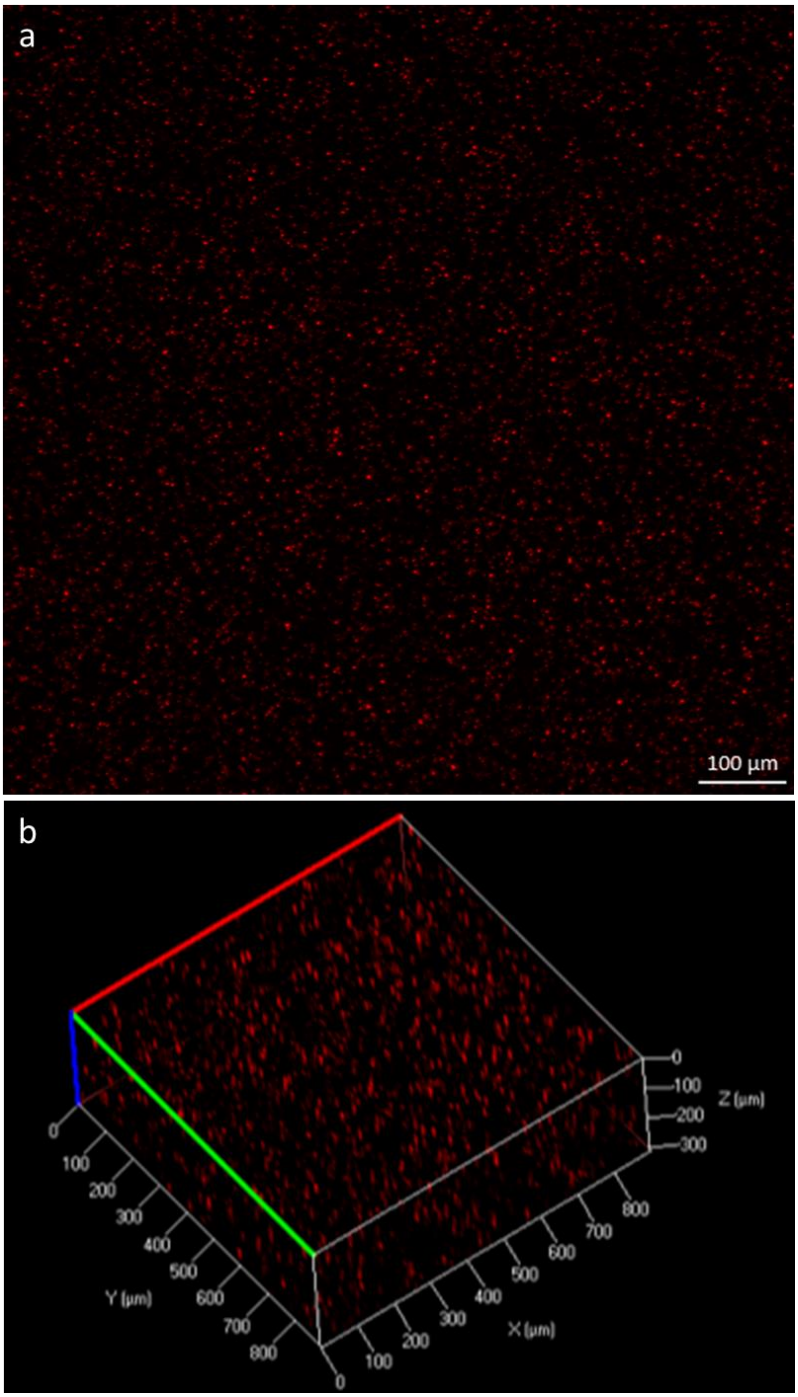

Figure 8: Nanoparticles (formed with Alexa 555 labelled siRNA) entrapment within an 8-arm PEG hydrogel. *Maximum intensity projections of nanoparticle suspended within a gel. (a) Compressed Z-stack of nanoparticles in a PEG hydrogel. (b) 3D rendered image of Z-stack.*

3.4 RNase protection within a PEG hydrogel

The potential for PEI/siRNA nanoparticle entrapment within PEG to provide additional protection to siRNA was investigated. Any additional protection from degradation from ribonucleases present in the serum would be beneficial for controlled release *in vivo* over a period of time where nanoparticles would be exposed to RNases. To our knowledge this has not previously been assessed although it has previously been proposed that scaffolds could provide additional protection from RNase degradation[226]. A novel RNase protection assay was developed by building upon experiments previously conducted for section 3.1.2. Eight-arm PEG hydrogels with entrapped nanoparticles were placed in FBS and hydrogels removed at various time points over 7 days. To analyse entrapped complexes after incubation in serum, Proteinase K was used to digest hydrogels. This digestion was carried out in the presence of SDS which enhances Proteinase K activity, dissociates the siRNA from PEI, and along with the Proteinase K would have also served to denature any ribonuclease that may still have been present in the sample. The digests were analysed by agarose gel electrophoresis.

Degradation of siRNA can be seen to occur in both nanoparticles and nanoparticles encapsulated in PEG hydrogel when incubated in serum (Figure 9a and b). However, upon quantification a significant decrease in degradation was observed for encapsulated nanoparticles relative to nanoparticles alone in serum at 24 hours ($p < 0.05$) (Figure 9c). Though no longer significant, the protection appeared to be maintained for 5 days. By 7 days the additional protection was lost.

Though a relatively minor protection (0 ± 3% vs 17 ± 3% degraded for encapsulated and nanoparticle alone respectively at 24 hours), this finding does indicate the potential of hydrogel encapsulation to deliver additional protection against RNase attack. It might be that these types of hydrogels with mesh size in the 10-20 nm range[202] are more protective than hydrogels with less potential for steric hindrance such as collagen. This aspect requires further examination.

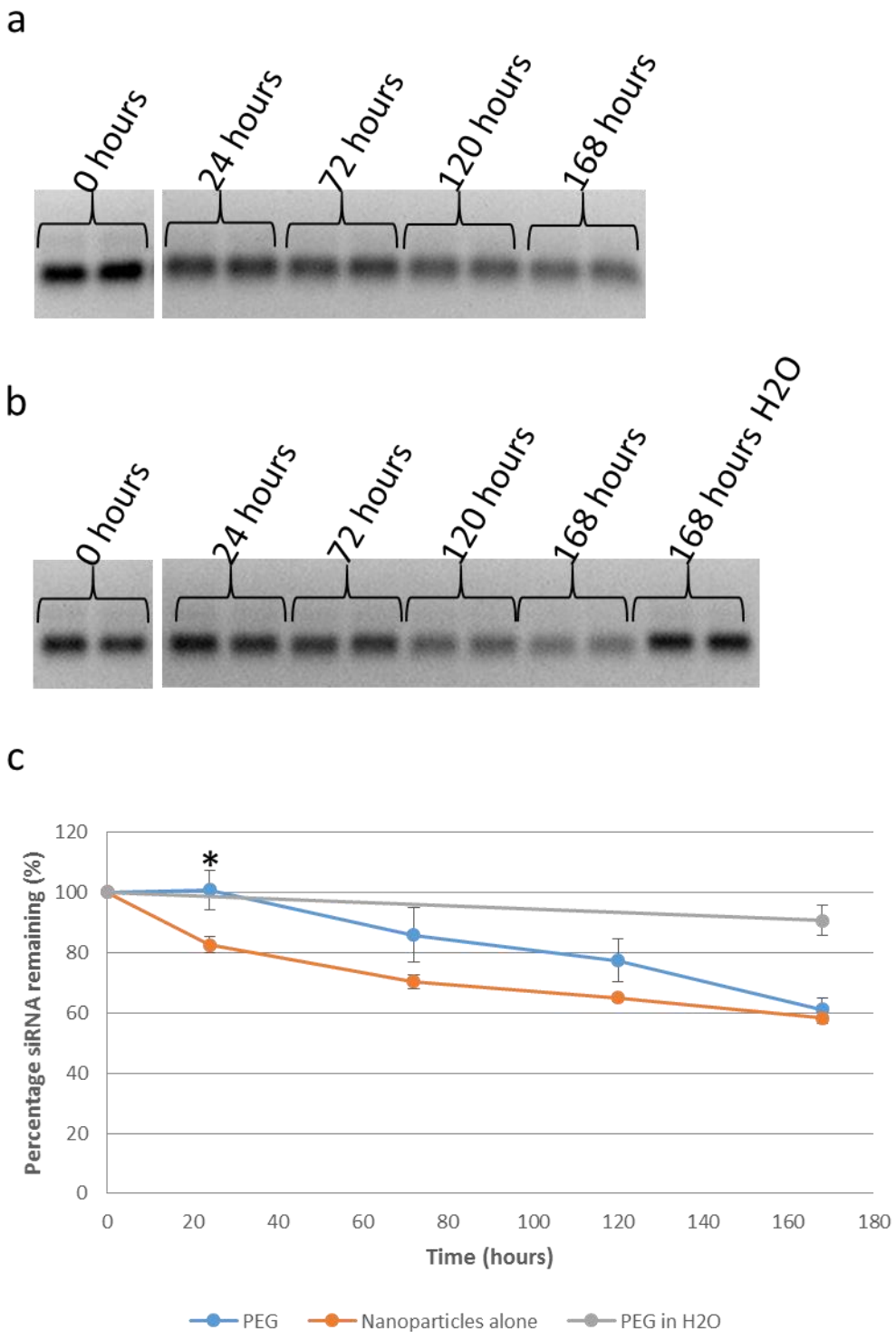

Figure 9: Ability of PEG hydrogel to protect encapsulated and complexed siRNA from degradation by RNases. *Nanoparticles entrapped within a hydrogel and free nanoparticles, were incubated in FBS concurrently or DEPC treated H_2O. (a) 20:1 nanoparticle complexes alone resolved on a 4% agarose gel. (b) 20:1 nanoparticles entrapped within in an 8-arm PEG hydrogel resolved on a 4% agarose gel. (c) Densitometric quantification 20:1 nanoparticles alone in FBS, 20:1 nanoparticles entrapped within PEG hydrogels placed in FBS and 20:1 nanoparticles entrapped within PEG hydrogels placed in DEPC treated H_2O. Extent of digestion was normalised to T = 0 samples. There was a significant difference in protection at 24 hours between entrapped nanoparticles (in FBS) and non-entrapped nanoparticles (in FBS) (*$p < 0.05$). n=5 (2 technical repeats per biological repeat).*

3.5 Hydrogel Release of Nanoparticles

If scaffold based delivery is to be successful, an important aspect of its success is maintaining the bioactivity of the entrapped siRNA. Another aspect to consider is the release profile. A sustained release rather than a sudden burst release of siRNA would be desirable, in order to have a prolonged silencing effect in surrounding tissue[275].

It is hypothesized that due to a mesh size in the 10-20 nm range[202], these hydrogels are able to sterically entrap nanoparticles and therefore may be unable to elute siRNA nanoparticles unaided by enzymatic degradation. It was therefore necessary to conduct a release experiment to confirm this hypothesis.

Initially, 8-arm PEG hydrogels were used to entrap either naked siRNA or siRNA complexed with PEI at a ratio of 20:1. The gels were placed in elution buffer, and samples from the various time points stored at -65°C until the completion of the experiment. After the experiment had run its course, nanoparticles were dissociated with SDS. Non-complexed siRNA which was entrapped within the 8-arm hydrogels appeared to have eluted extensively in the first 24 hours (Figure 10a) and densitometric analysis (Figure 10b) confirmed that essentially 100% had eluted in that period. No siRNA was visible in elution aliquots from hydrogels containing PEI/siRNA nanoparticles over the duration of the experiment and none could be detected by densitometry.

A 4-arm PEG hydrogel was then also assessed for release in the same way as the 8-arm hydrogel. The 4-arm hydrogel used here has larger mesh size than the 8-arm version (20 vs 10 nm for 4 and 8-arm respectively[202] (personal communication from the Polymer Unit)) and would therefore be more likely to allow elution of the nanoparticles. Once again however, the PEI/siRNA nanoparticles were entrapped for the duration of the experiment within the hydrogel while the uncomplexed siRNA eluted within 24 hours (Figure 10a and b).

It is however possible that a negligible amount of nanoparticles had in fact eluted but this would have been below the detection limit of the assay (< 2.5% siRNA loaded). These results confirm that the nanoparticle complexes were firmly entrapped within the hydrogels and that without complex formation the siRNA alone will elute out of the gel. It is probable that this is due to increased steric hindrance as PEG gels have minimal ionic charge and the nanoparticle size of 57 nm does exceed the mesh size.

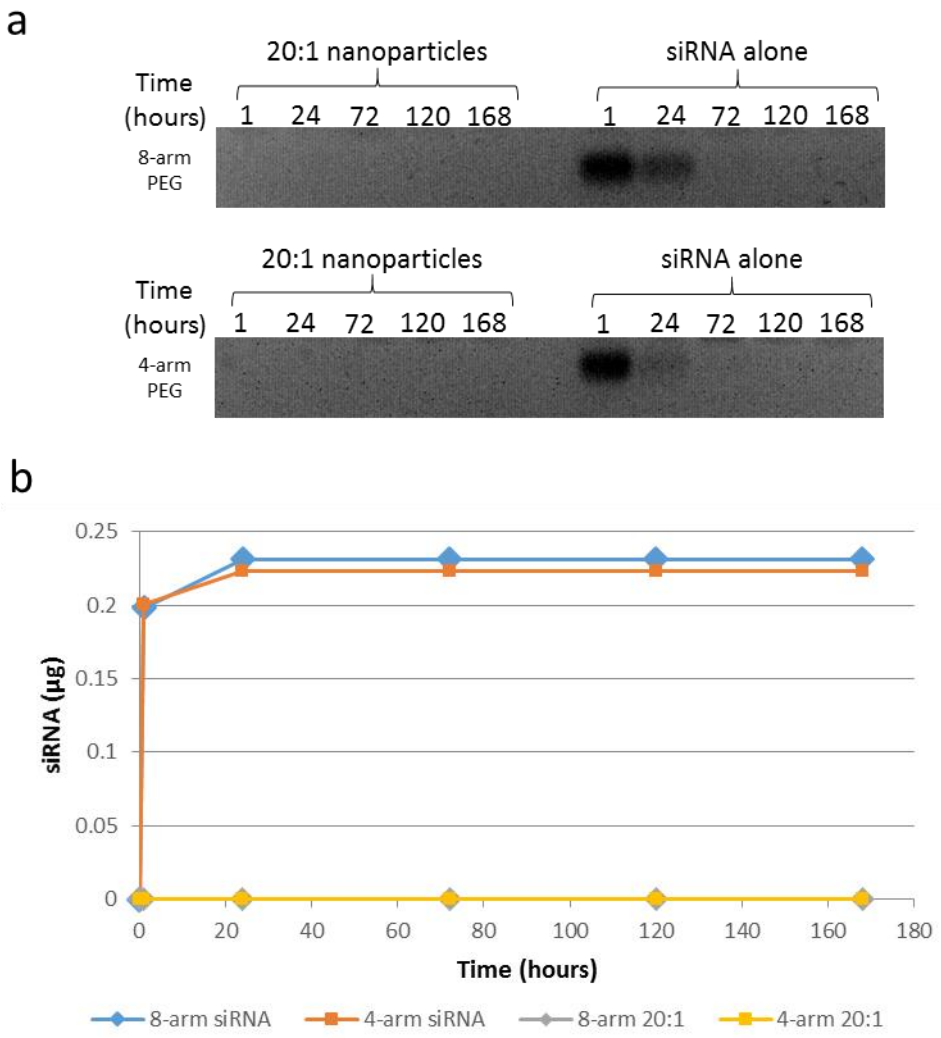

Figure 10: siRNA and nanoparticle release from 4- and 8-arm PEG hydrogels. *Hydrogels were incubated in a 25 mM HBS elution buffer. At 1, 24, 72, 120 and 168 hours hydrogels were placed in fresh elution buffer. Hydrogels were digested and along with elution samples were assessed for the presence siRNA and PEI/siRNA nanoparticles. (a) Elution buffer samples resolved on a 4% agarose gel. (b) Densitometric analysis of elution buffer samples. For quantification samples were run with a standard curve.*

3.5.1 PEI/siRNA nanoparticle release from PEG hydrogels to assess bioactivity

A possible approach to overcome the lack of release observed above (section 3.4) was to digest hydrogels using Proteinase K in order to assess the bioactivity of the entrapped nanoparticles. Unlike for the release experiment and RNase protection assays however, SDS could not be used as it dissociates the PEI/siRNA nanoparticles and is toxic to cells.

Proteinase K works optimally at 37°C and digests the hydrogels over a number of hours. Due to concerns regarding the increase in aggregation of PEI nanoparticles seen over time at higher temperatures[273], a time course study was conducted to determine if a limitation of digestion time might be required such that a reduction in efficacy of nanoparticles would not occur. Nanoparticles

were formed using Cell Death siRNA (2 µM), and were incubated at room temperature (RT) and at 37°C before being used for transfection experiments. Freshly prepared complexes were used as controls and surviving cell levels were normalised to non-treated cells. A drop in transfection efficacy could be observed within 1 hour at RT with a further drop at 2 hours (Figure 11). Incubation at 37°C resulted in a drop to levels equivalent to 2 hours at RT within 1 hour and this remained at 2 hours. This is in agreement with the previously cited study that found nanoparticles aggregation increased over time with an increase in temperature[273] and suggests that the drop in transfection seen here is due to aggregation. Though this experiment was carried out at the concentration of particles at which they were formed, it strongly indicated that digestion of hydrogels in Proteinase K should be carried out as rapidly as possible.

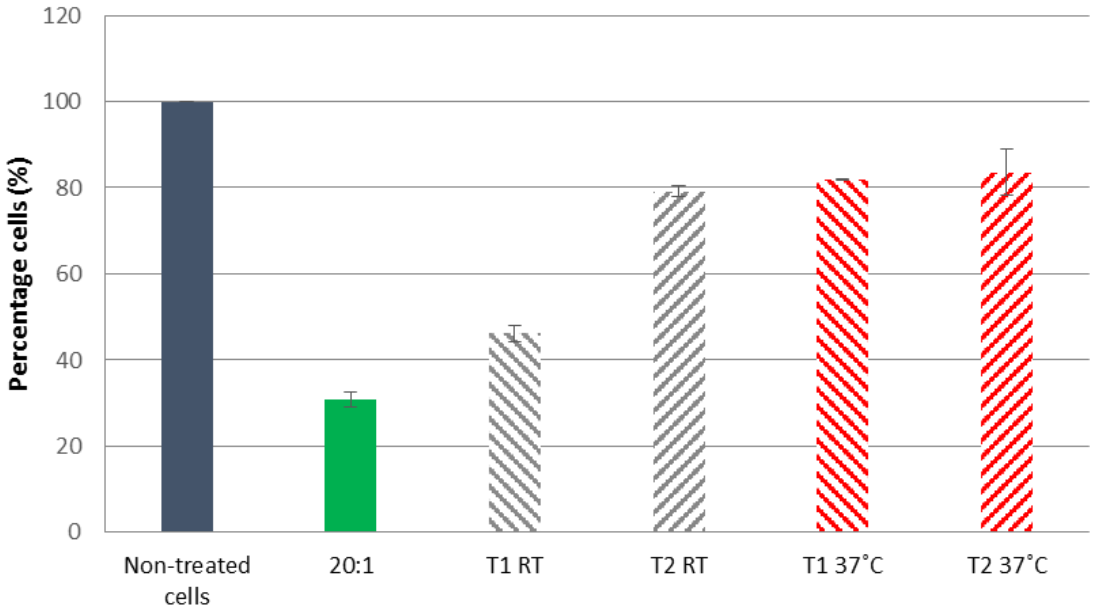

Figure 11: Transfection of HT1080 cells using complexes incubated for various lengths of time at room temperature and at 37°C. *Cells were normalised to non-treated cells. T = Time in hours. RT = Room temperature. n = 3 (technical repeats).*

It was deemed ideal if a concentration of Proteinase K that could digest the PEG hydrogels within 1 - 2 hours could be determined. Proteinase K is a relatively non-specific serine protease and as such its activity affects cell adhesion[276]. Unfortunately difficulties were encountered when attempting to digest the gels in this amount of time. High concentrations of proteinase K (1 mg/ml) were needed in order to digest the hydrogels in 2 hours (Figure 12a and b). When HT1080 cells were treated with digested gel solutions, complete lifting of all cells was observed within 10 minutes. This was also observed in the presence of 20% (v/v) serum and in the presence of Pefabloc® Sc. Pefabloc® Sc is a specific, irreversible serine protease inhibitor that is the only one to our knowledge which is reported to be a non-cytotoxic inhibitor of proteinase K available. As a last resort gels were digested overnight

in 100 µg/ml Proteinase K. Substantial loss of cell adhesion and cell lifting was still observed at this lower concentration of Proteinase K. Thus, in our hands it was not possible to digest gels such that an adequately rapid release could be achieved without substantial to complete loss of cells.

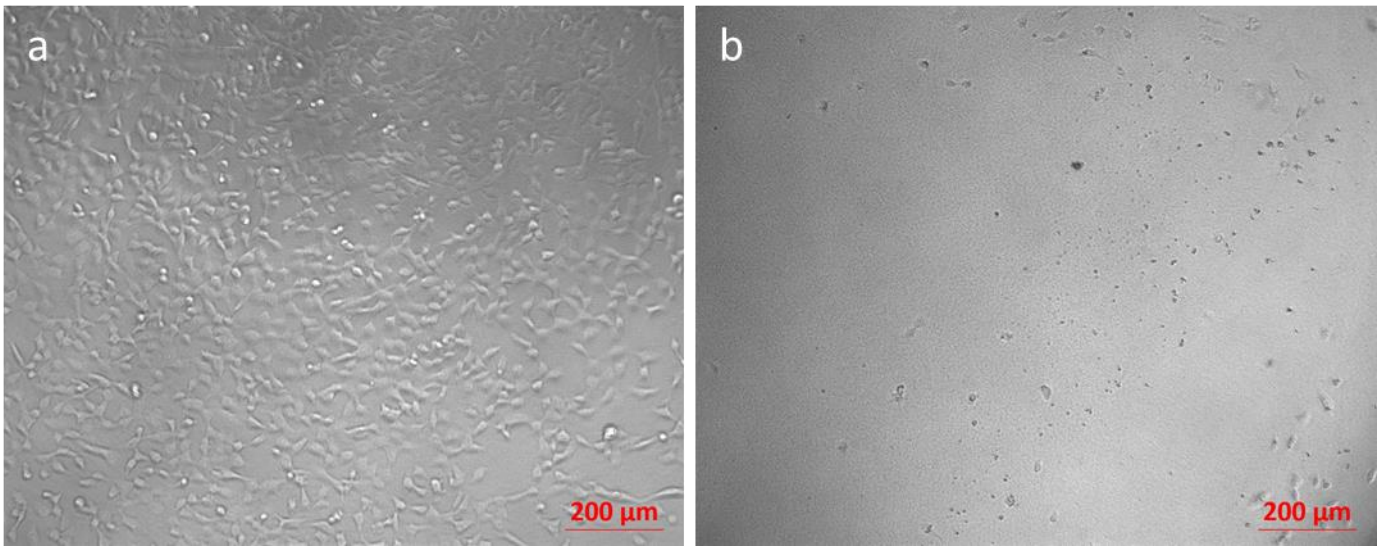

Figure 12: HT1080 cells treated with digested 1 mg/ml Proteinase K. *(a) Untreated HT1080 cells. (b) Cells treated with a digested PEG hydrogel. A large proportion of cells treated with Proteinase K lifted within 10 minutes of treatment.*

3.6 3D cell culture

As it was not possible to simply release nanoparticles for efficacy assessment, 3D cell invasion assays were explored. A 3D *in situ* assay which does not rely on release but rather cellular invasion is also a closer mimic of the *in vivo* scenario for these types of enzymatically degradable hydrogels.

3.6.1 Cells cultured in 3D with siRNA nanoparticles

In initial experiments to assess whether cells can take up encapsulated siRNA nanoparticles, hydrogels were formed containing both cells and nanoparticles dispersed throughout. This was achieved by polymerising gels with both cells and fluorescently labelled siRNA nanoparticles present. As can be observed in Figure 13, 100% of cells had been transfected by siRNA. Though this approach has been used by others[39,205,206,210], the high uptake of siRNA raised concern as cells are directly exposed to nanoparticles for a period of 20-30 minutes before complete polymerisation. During this time the nanoparticles and cells are in a relatively small volume (high concentration compared to normal transfections) and forced into contact. This situation may greatly enhance transfection efficacy and reinforces the need for a model that initially isolates the cells from the siRNA containing nanoparticles.

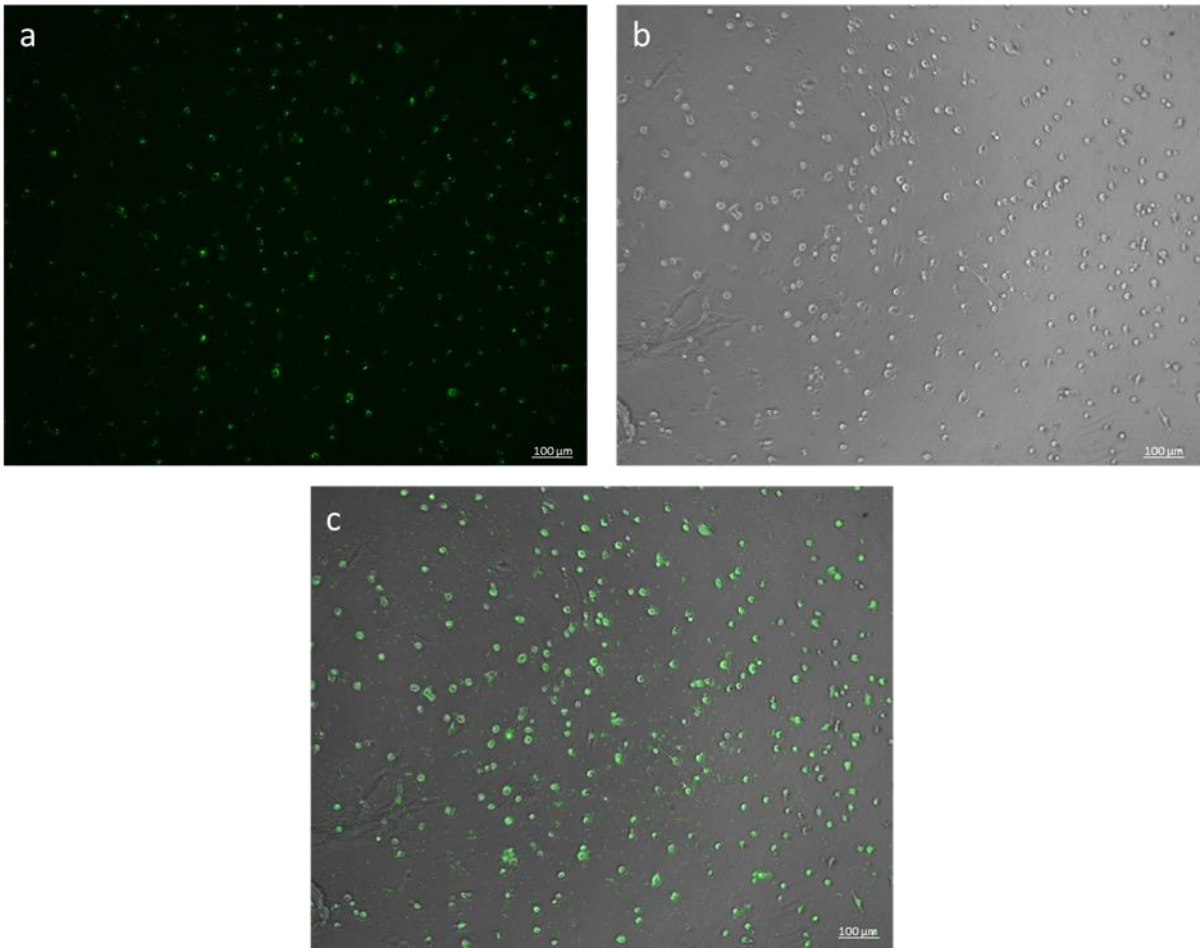

Figure 13: Photomicrographs of HT1080 cells encapsulated in an 8-arm PEG hydrogel with Alexa 488 labelled siRNA used to form nanoparticle complexes. *Images were taken on a LSM510 Confocal Microscope. (a) Fluorescent image of transfected cells. (b) Phase contrast image of the transfected cells seen in image (a). (c) Image overlay of (a) and (b).*

3.6.2 3D cellular invasion

It was important that nanoparticles and cells are separated prior to polymerisation, in order to more closely mimic an *in vivo* environment, whereby cells would need to invade an injected enzymatically degradable hydrogel after it has polymerised. Two 3D *in vitro* cell invasion assays were developed in order to determine the ability of invading cells to be transfected by the entrapped nanoparticles.

Cells were entrapped within an 8-arm PEG hydrogel which was centred in a siliconized 96-well plate and polymerised. Siliconizing the surface of the well creates a hydrophobic coat which aids in creating a well-defined hemisphere shape for gels polymerised on such a surface. After the cell containing hydrogel had formed a concise hemisphere, a second PEG hydrogel containing nanoparticles was polymerised onto the first hydrogel to form concentric hemispheres (Figure 14a). After polymerisation, a stimulatory media containing 10% FBS and EGF (100 ng/ml) was added. Minimal

invasion was observed to occur into the hydrogel by the cells (Figure 14b and c). Thus, this approach with a PEG gel within a PEG gel, though simple in application, was not suitable.

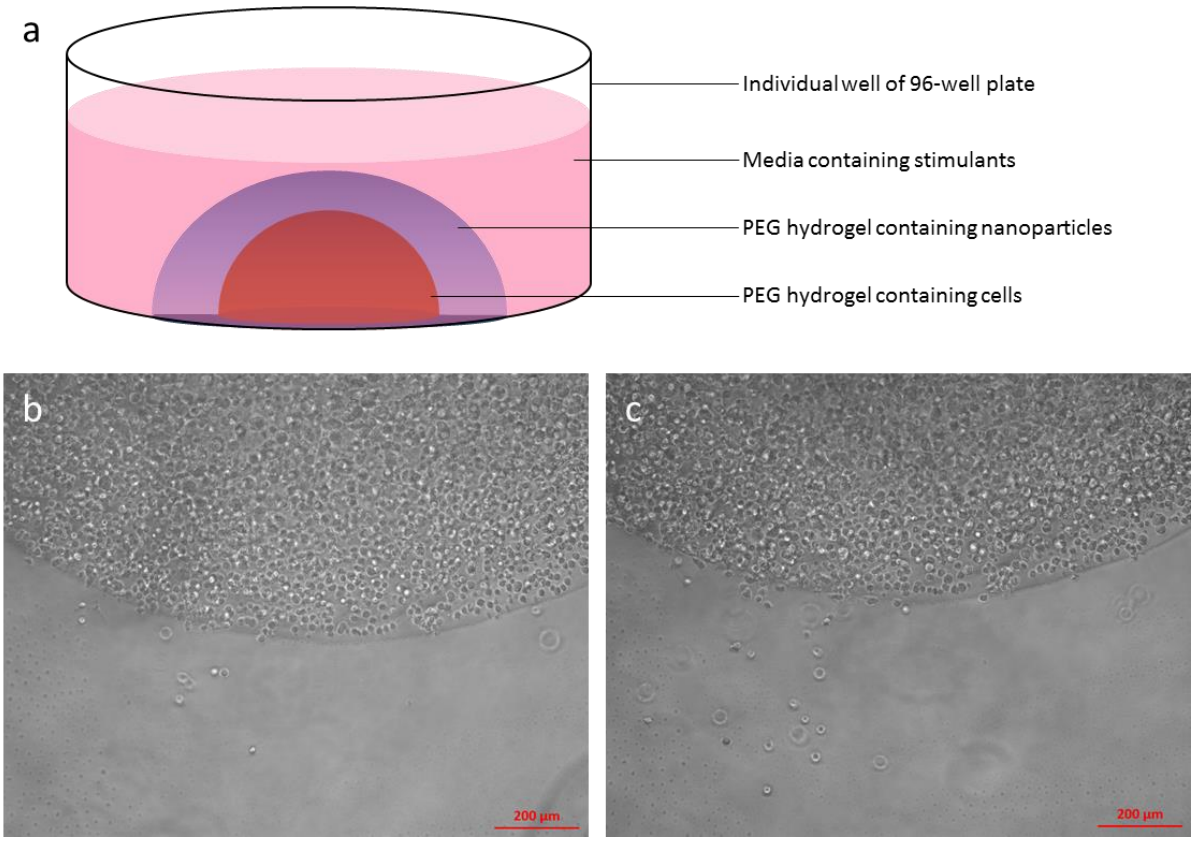

Figure 14: HT1080 cells migrating from a 2% PEG hydrogel into another 2% PEG hydrogel. *(a) Schematic of hydrogel setup. (b) Migration after 24 hours. (c) Migration after 96 hours. EGF (100 ng/ml) was added to the media on alternate days.*

3.6.2.1 Dermal equivalents for implantation into PEG hydrogels

The potential of combining PEG with another hydrogel was assayed. Examination of the literature indicated that an approach used by Grinnell *et al*[277]*.,* might allow for enhanced invasion. A nested collagen matrices protocol[277], which involves the preparation and implantation of dermal equivalents into a collagen hydrogel, was adapted for use with PEG hydrogels (Figure 15). Dermal equivalents are collagen gels which have been condensed over time by encapsulated cells into a tissue-like structure[278]. They were first developed as a model to study wound healing and fibroblast function *in vitro*[279] and later used in skin grafting *in vivo*[280]. Cells which have not first been incorporated into dermal equivalents, but rather seeded directly onto the surface of a 3D scaffold were shown to migrate very slowly into the interior[281–283]. Cells migrating from the contracted collagen matrices have been found to have a much more invasive phenotype and migrate more rapidly into the surrounding matrix[277].

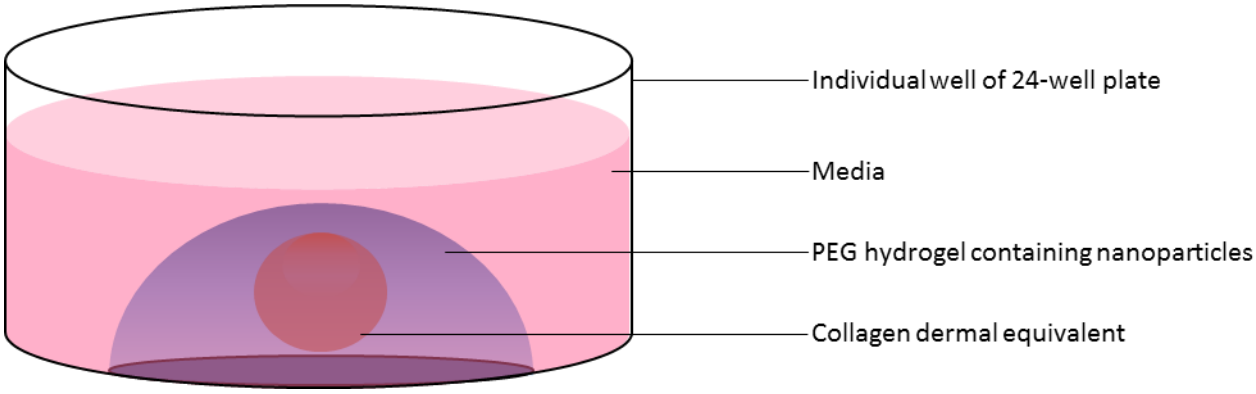

Figure 15: Schematic of dermal equivalent in a PEG hydrogel. *Dermal equivalents which had condensed were carefully placed into polymerizing PEG hydrogels so that dermal equivalent did not sink to the well floor.*

Here, tissue culture-treated 24-well plates which had been scored with a specially made surgical punch and siliconized were used to monitor cellular ingrowth. Scoring the well helped localise the hydrogels to the centre of the wells. Once formed, dermal equivalents were embedded in a PEG hydrogel as per diagram in Figure 15. After 48 hours of incubation, dermal equivalents formed using HT1080 cells were seen to be elongated (Figure 16). This "tissue-like" behaviour indicates that HT1080 fibrosarcoma cells behave similarly to fibroblasts[279].

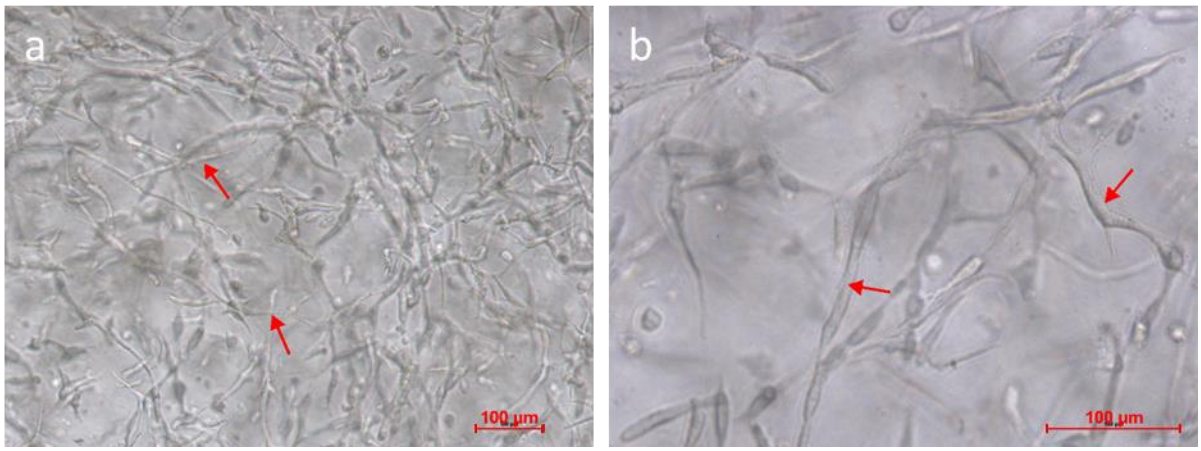

Figure 16: Annotated images of dermal equivalent showing the formation of the tissue-like lattice after incubation. *HT1080 cells were used to form the dermal equivalents. (a) 10X objective magnification of area in dermal equivalent. (b) 20X magnification of area in dermal equivalent. The red arrows point to examples of cells which have become elongated during 3D cell culture.*

In initial studies, HT1080 containing dermal equivalents were embedded in 3.5% 8- or 4-arm PEG hydrogels (Figure 17a and b). By imaging dermal equivalents which were prepared at the same time and placed in either hydrogel it was possible to compare migration. Dermal equivalents placed in a 4-arm PEG hydrogel were able to migrate substantially further than those placed in 8-arm PEG hydrogels over the same period of time and under the same conditions. Cells migrated 455 µm in an 8-arm PEG hydrogel while they migrated 1232.5 µm in the 4-arm over 7 days (Figure 17a and b). The cells of

dermal equivalents embedded in the 4-arm PEG hydrogel also appeared to be more spread out compared to those entrapped within the 8-arm PEG hydrogel. In the 8-arm PEG hydrogel it was harder to distinguish between individual cells. Thus, it was decided to use 4-arm hydrogels for future cellular invasion experiments.

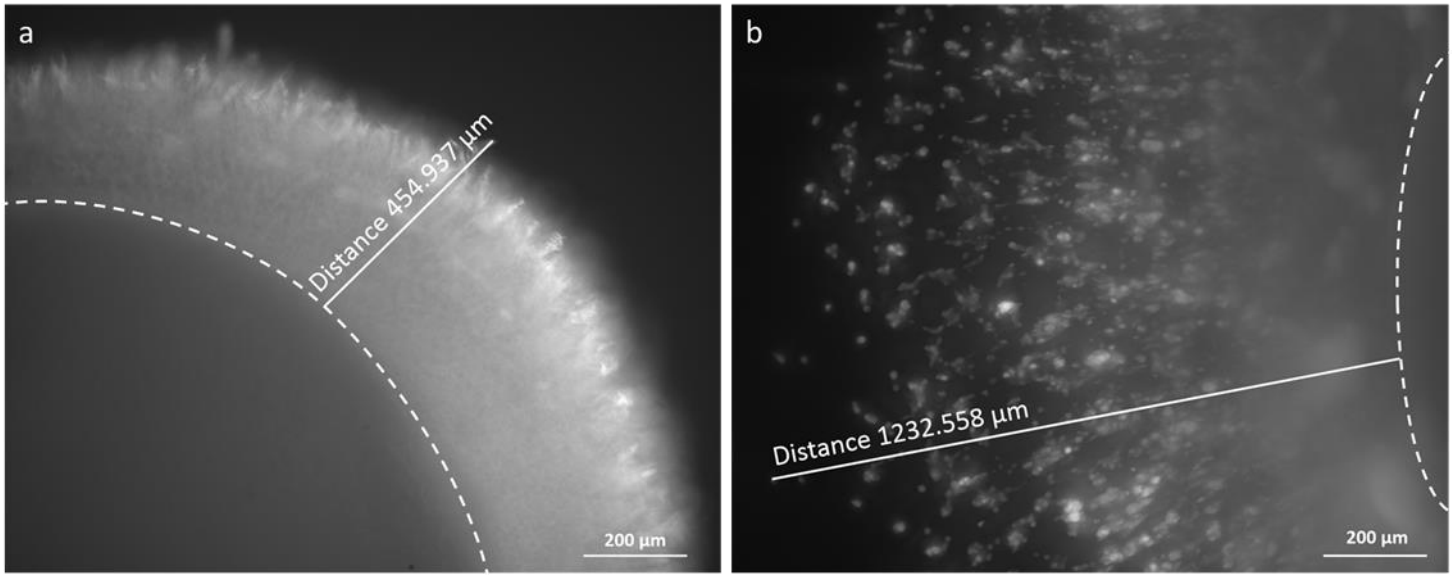

Figure 17: HT1080 cellular invasion using 4-arm versus 8-arm PEG hydrogels. *Dermal equivalents were placed in either a 4- or 8-arm hydrogel and incubated for 7 days after which time they were imaged. The distance migrated of the furthest cell was measured. Dashed lines represent dermal equivalent edge. (a) HT1080 cells invading a 8-arm PEG hydrogel. (b) HT1080 cells invading a 4-arm PEG hydrogel.*

3.6.2.2 Quantitation of cellular invasion rate

The 4-arm PEG hydrogel which has previously been used in this laboratory for spheroid assays and shown to allow cellular ingrowth[202] was further assessed with respect to cellular invasion from dermal equivalents. Cell migration was monitored over 7 days and imaged (Figure 18a - d). Migration was quantified by measuring the distance between the edge of the dermal equivalent and cells which had migrated furthest from the dermal edge. The average distance that the leading cells had migrated was 1129.5 ± 34 µm away from the dermal equivalent edge after 7 days (Figure 18e). The rate of migration was highest during the initial 24 hours in which the cells were monitored (17 µm/hour). This rate then slowed to 5 µm/hour between 24 and 168 hours (7 days). This rate of cellular invasion was judged to be sufficient to assess cellular internalisation of PEI/siRNA nanoparticles.

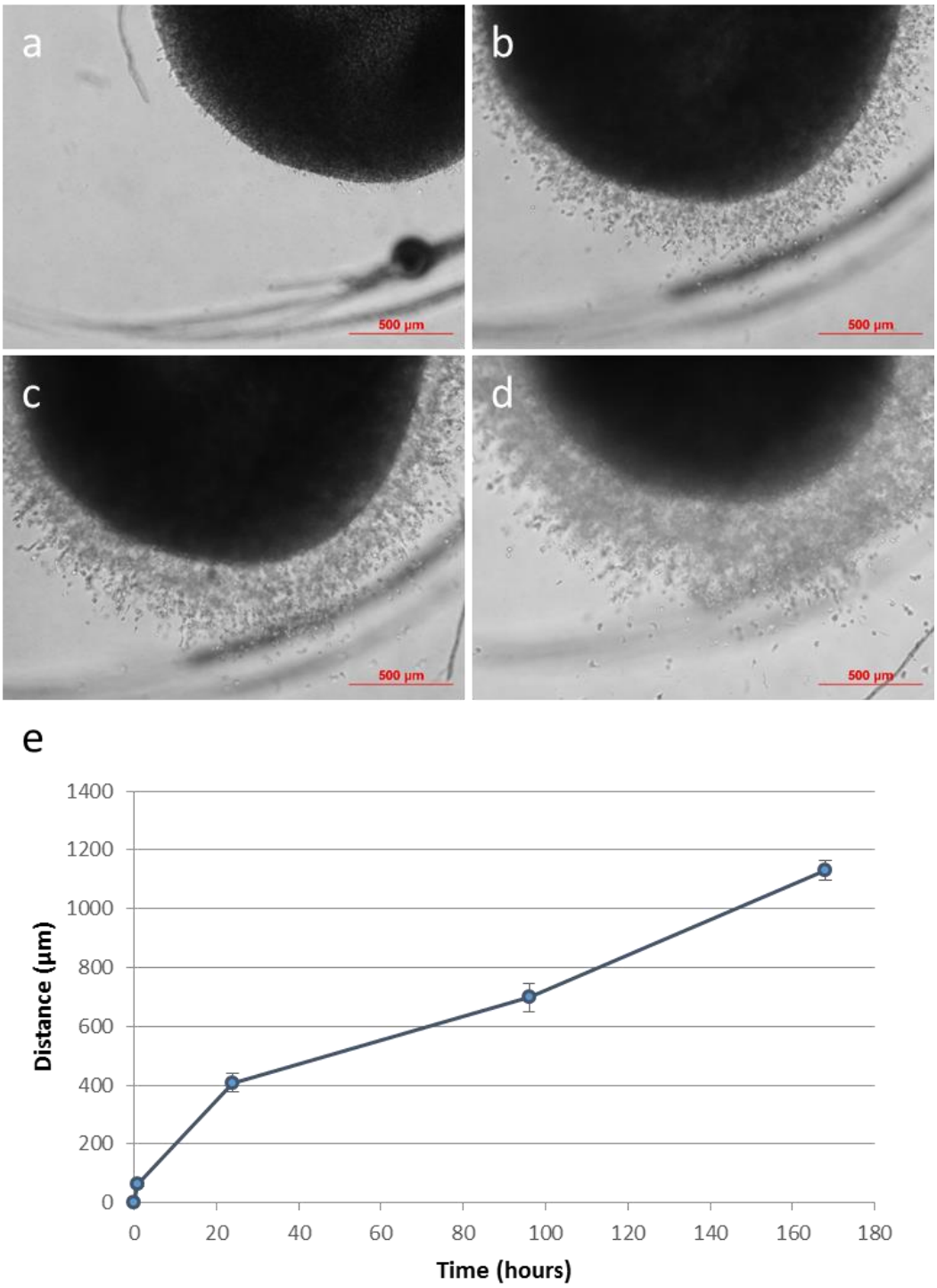

Figure 18: Cellular invasion from dermal equivalents into 3.5% 4-arm PEG hydrogels imaged over 7 days. *Representative photomicrographs of invading cells imaged over 7 days. (a) Time = 1 hour (b) Time = 24 hours (c) 96 hours (d) 168 hours (e) Distance cells migrated from edge of dermal equivalent. n=2 (3 technical repeats per biological repeat).*

3.6.3 Cellular invasion into a PEG hydrogel containing fluorescently tagged siRNA nanoparticles

In initial analyses of cellular uptake of encapsulated nanoparticles, GFP expressing HT1080 cells were used to form dermal equivalents and embedded within a PEG hydrogel containing Alexa 555 labelled scrambled siRNA. It was hypothesised that this would allow for determination of cellular internalisation of siRNA. After 3 days, tile-scan combined with Z-stacking images were taken using the Zeiss LSM510 confocal microscope. This allowed for a significant proportion of the invading cells to be captured. A single layer from the central region of the tiled Z-stack is shown in Figure 19. Nanoparticles can be seen throughout with arrows indicating examples of cells that appear to have internalised the siRNA. These were examined more closely utilising the orthogonal projection modality.

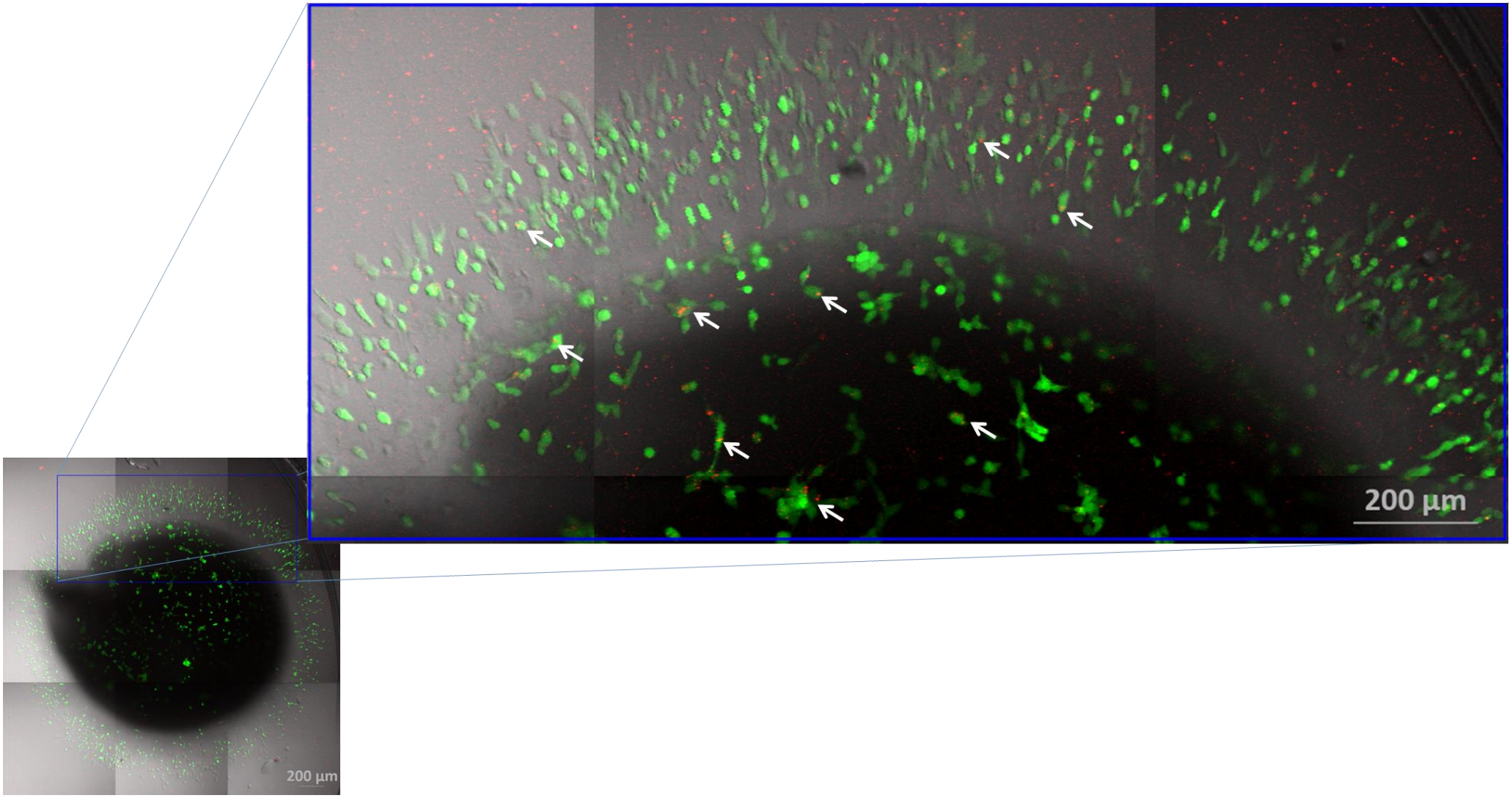

Figure 19: Enlarged view of HT1080 cells stably transfected with GFP invading a 4-arm 3.5% PEG hydrogel containing nanoparticles formed with Alexa555 siRNA (Time = 72 hour). *Displayed image is from a single layer of a Z-stack. Image is representative of other areas. Arrows are pointing to examples of cells which have internalised the siRNA.*

In order to confirm that the cells in Figure 19 had been transfected by the entrapped nanoparticles it was necessary to view an orthogonal projection (Figure 20). The orthogonal projection displays multiple views of an object at right angles to each other. For a Z-stack, this allows the user to view the x, y and z co-ordinate of a point simultaneously in 2D. The larger field of view (blue border) of the orthogonal projection represents a single layer of a Z-stack as if it was viewed from above. The red and green lines which intersect are the y- and x-axis respectively and are also represented by the red and green boxes (above and to the right respectively). The boxes are a side-on view along the lines of the x- and y-axis (as if one were viewing the entire z-stack from the side) (Figure 20a). An analogy of this would be if one had to view the cover of a book or individual pages, the large area would be an individual page. If one had to draw a line across the width (x-axis) of the book and then cut it along that line and view the book from the side, the green box would represent the area now exposed by cutting the book along that line. The blue line running across the green box represents the individual Z-stack layer or "page" that is being viewed in the larger box. In a similar manner the red box is the area that would be created if one had to draw a line along the length of the book (y-axis) and view the book from the side of the freshly cut page edges. Figure 19b is a drawing to aid in visualising the above description. The colours of Figure 20b correspond to the border colours seen in Figure 20a.

The nanoparticles in the cell (indicated by white arrows) examined in Figure 20a show that they are within the green fluorescence of the GFP expressing cell in all planes strongly suggesting uptake. However, this approach is extremely labour intensive limiting its applicability as a screening tool in part due to the fluorescence of the nanoparticles in the gel. It was hoped that unquenching in the cell would have resulted in a greater increase in fluorescence intensity.

The levels of transfection seen here are not necessarily all that high. This is probably due to the environment into which the cells are invading. Due to previously discussed constraints surrounding concentration of entrapped nanoparticles, the number of possible nanoparticles which cells can encounter is dramatically reduced compared to if there was a higher concentration of nanoparticles per hydrogel. This could be a possible reason for the low levels of transfection seen. In 2D based experiments the siRNA nanoparticle blanket the cells seeded in the tissue culture plate whereas for 3D experiments cells have to physically encounter nanoparticles.

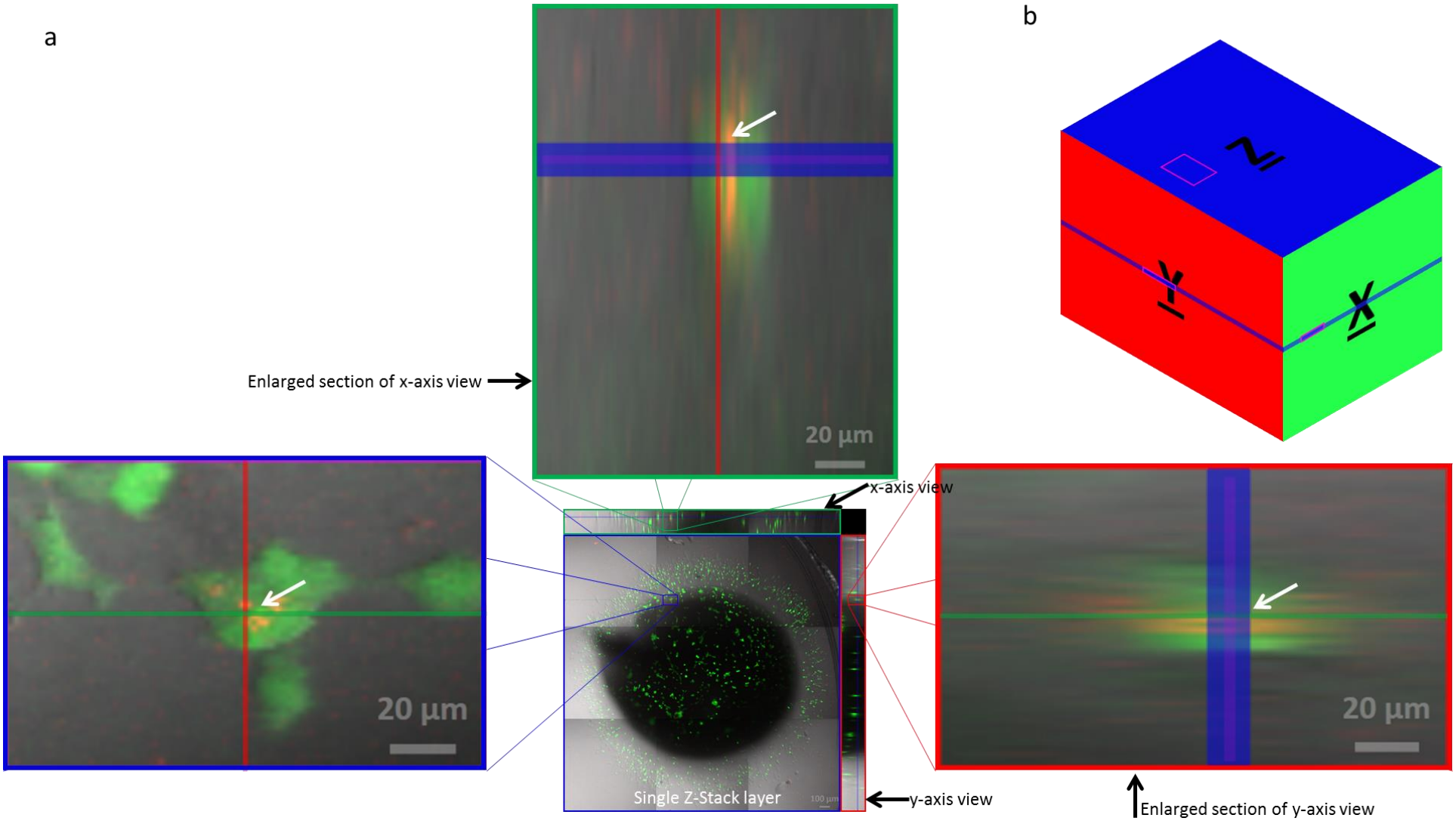

Figure 20: Orthogonal projection of an area of invading cells. *(a) Orthogonal projection with enlarged areas. Blue: z-view / z-cut line. Green: x-view / y-cut line. Red: y-view / x-cut line. (b) Illustration to help in understanding the orthogonal protection. The different perspectives of the same cell indicating cellular internalisation of fluorescently labelled siRNA (white arrows). The large area which is flanked by a red box on the right and a green above is a view of the Z-stack if one was looking from above. The different boxes indicate the same region from different viewing perspectives. The green box corresponds to the green line (x-axis) and is a side on view. The red box corresponds to the red line and is a side view of the y -axis. The blue line represents the layer in the Z-stack which is being viewed from above in the blue box. The blue line within the smaller of the two green and red boxes is the areas highlighted by the small blue box.*

3.6.4 Cell invasion into PEG hydrogel containing AllStars Hs Cell Death siRNA.

In order to assay the bioactivity of the entrapped PEI/siRNA nanoparticles, dermal equivalents were placed in 4-arm PEG hydrogels containing nanoparticle complexes which were formed using AllStars Hs Cell Death siRNA. A LIVE/DEAD™ Cell Viability Assay was used to assess efficacy. This assay enables the differentiation between populations of live and dead cells based on plasma membrane activity and esterase activity whereby live cells are stained green and dead cells are stained red.

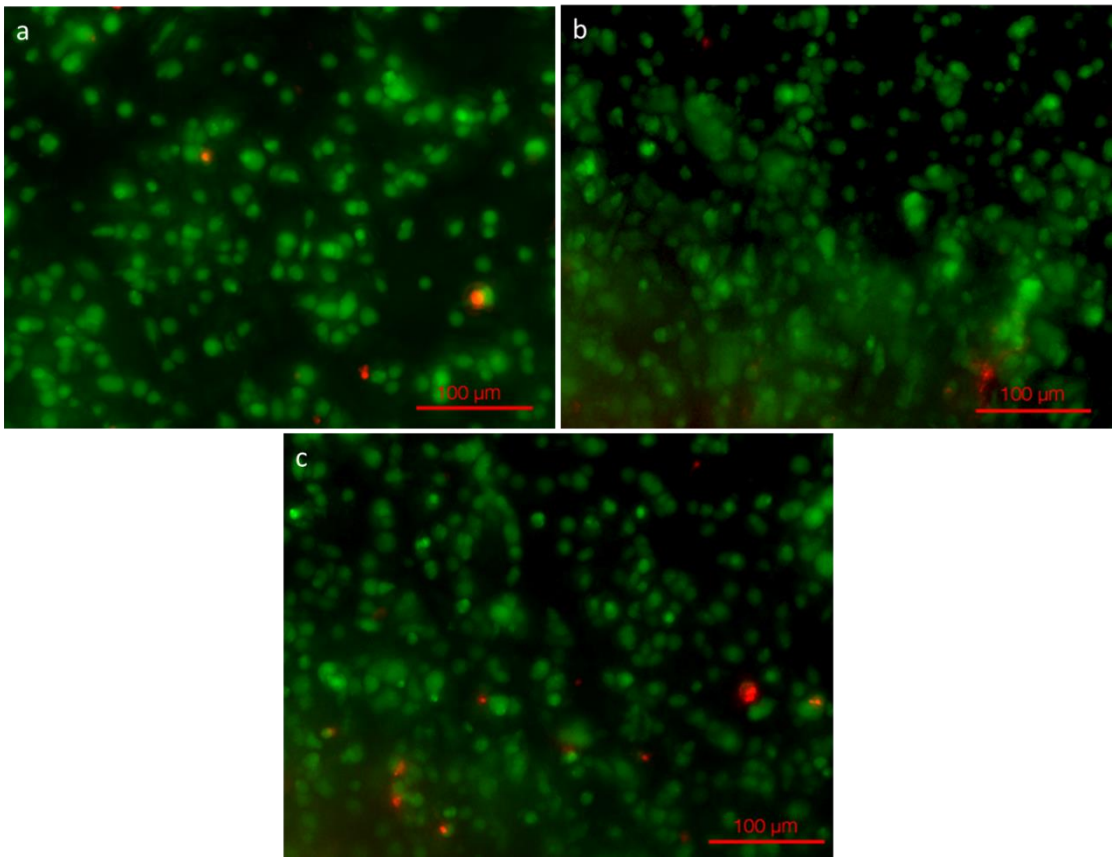

Figure 21: Compressed z-stacks of LIVE/DEAD™ cell staining within PEG. *(a) Non-treated cells. (b) Cells treated with negative control siRNA. (c) Cells treated with Cell Death siRNA.*

Figure 21 displays representative compressed Z-stack images of the quantified results. It was clear that the number of dead cells relative to the number of live cells was low. It was not possible to accurately count the number of living cells due to the lack of availability of a confocal microscope during this period. A Zeiss Axiovert fluorescent microscope was used to take these images. While the microscope is capable of acquiring Z-stack images the sections are coarser than what they would have been had a confocal been used instead. None-the-less careful attention was paid to selecting a region using the green channel (living cells) to capture images in order to avoid bias region selection. When

quantifying the number of dead cells per image, each layer of the Z-stack was manually examined. Attention was given to not count the same dead cells when moving between the layers.

Dead cells were manually counted and results were normalised to non-treated wells (Figure 22). There was an increase in number of dead cells in the cell death treated wells but this was not significantly different to the non-treated and negative control siRNA treated wells. There was an indication of a possible trend with cell death treated cells having a $p = 0.065$ versus untreated cells whilst negative control siRNA treated cells had a $p = 0.7$ versus the untreated cells.

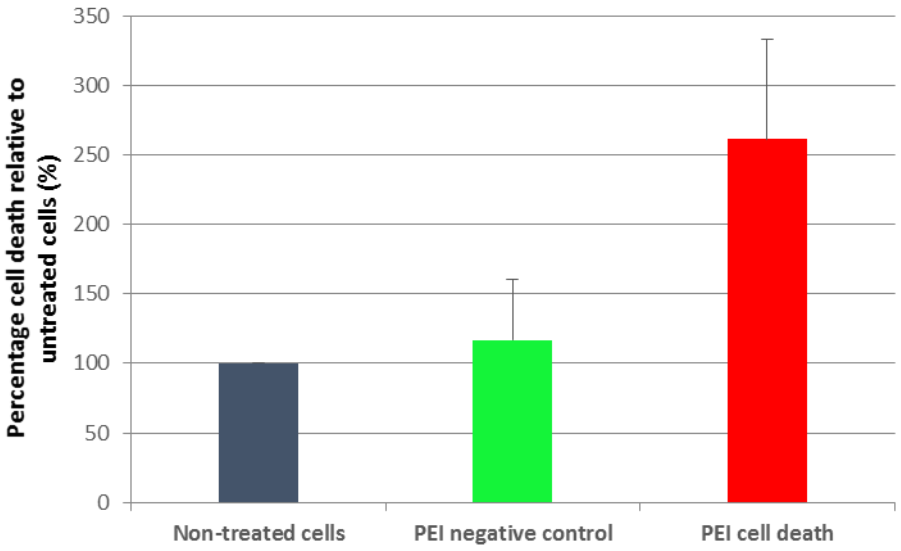

Figure 22: Percentage Cell Death relative to untreated cells. *Cells were normalised to non-treated wells a percentage cell death relative to that was calculated. Significant levels of cell death were achieved between untreated cells and those treat with cell death siRNA. n = 4 (2 technical repeats per biological repeat).*

These results are similar in nature to that observed for siRNA internalisation in the previous section (3.6.3) suggesting poor uptake of PEI/siRNA nanoparticles. A number of possible issues may have played a role. Due to the limited concentration of siRNA achievable when forming nanoparticles, and the limited available volume that can be added to a hydrogel, the likelihood of cells encountering nanoparticles may have been very low. This could potentially be overcome via the use of alternative delivery vehicles that might allow for higher siRNA concentrations during nanoparticle formation. Alternatively modifications of the PEI polymer itself may allow for an increase in siRNA concentration. Such modifications would need to maintain or improve efficacy in 2D but more importantly prevent nanoparticle aggregation. The apparent very tight encapsulation of nanoparticles achieved could have potentially exacerbated the lack of interaction with cells. The lack of release (Figure 10) achieved suggest minimal movement by the nanoparticles in the hydrogel which would limit the probability of a nanoparticle reaching a cell. In this hydrogel system it has been shown that the activity of cellular

proteases is localised to the invading cell minimising the possibility of cleavage of sites remote to the invading that would allow for release of nanoparticles. Here the introduction of hydrolytic cleavage sites in addition to enzymatically degradable sites might allow for greater movement of nanoparticles within and form the hydrogel. In studies where PEI nanoparticles were encapsulated throughout a hydrolytically degradable PEG hydrogels (either 8-arm PEG mono(2-acryloyloxyethyl) succinate or PEG acrylate), sustained release was obtained and reasonable levels of transfection were obtained. It cannot be entirely excluded that encapsulation of the nanoparticles has not damaged them in some fashion though it is not clear how this might occur. The PEI may have been covalently coupled into the hydrogel via the vinyl sulfone moiety. Though the latter has a very high specificity for thiols, it may be possible that it binds to amines. However, as pegylation of PEI is a common modification this seems unlikely to have caused significant issues with transfection. Certainly, when the PEG monomer was incubated with the nanoparticles prior to transfection no reduction in efficacy was observed (Figure A5.1, Appendix A5).

It was originally hoped that this assay would allow for the simple evaluation of PEI/siRNA nanoparticles in an environment which more closely mimics the i*n vivo* structure. Although this assay proved to be unsuccessful in assessing the bioactivity of entrapped nanoparticles, an *in vitro* milieu was created that resembles an *in vivo* scenario. It could be envisaged that with a more potent particle, that cell death could be monitored by simple analyses of this model that could include cell loss and reduced migration of the invading cell front.

4. Conclusion

RNAi has great potential for treatment for numerous pathological conditions. Targeted delivery to desired regions of interest in the body has impeded its progress to the clinic. Localised delivery from injectable hydrogel based scaffolds are one possible way to optimise delivery. Here, various existing assays were established in our laboratory as well as assays developed to assess *in vitro* the feasibility of using cationic PEI polymers and a PEG hydrogel system as a therapeutic siRNA delivery vehicle.

The 20:1 ratio was found to be the optimal ratio of nitrogen in PEI to phosphate in siRNA. This ratio achieved full complexation, while maintaining siRNA integrity of at least 50% over 7 days. This ratio was non-cytotoxic and efficacious at mRNA knock-down. The size and zeta potential of the 20:1 ratio was determined to be 74 nm and 57 mV respectively. Both of which are within the optimal range for RNAi delivery.

An siRNA concentration of 2 μM was determined to be the optimal concentration at which to form nanoparticles for encapsulation in a hydrogel. At higher concentrations the efficacy of the siRNA was found to be decreased which was possibly due to aggregation. This limits dosages achievable with PEI based nanoparticles in PEG hydrogel systems such as the one employed here.

It was found that nanoparticles entrapped within a PEG hydrogel had significantly higher levels of protection compared to non-encapsulated siRNA nanoparticles within the initial 24 hours which persisted up to 5 days. Though the additional RNA protection was lost after 7 days incubation in serum, this indicates that PEG hydrogels may be desirable in this context as localised delivery vehicles.

Both 4-arm and 8-arm PEG hydrogels were assessed for nanoparticle and naked siRNA release. Naked siRNA eluted within 24 hours whereas the complexed siRNA remained entrapped for at least 7 days. This apparent tight entrapment may not be an optimal parameter of the PEG hydrogel system as controlled release to surrounds as well as interaction with invading cells would probably be substantially reduced.

When hydrogels were polymerised with nanoparticles and cells together, 100% of cells were observed to take up siRNA. It was postulated that this may have resulted from initial uptake whilst reagents were in solution and motivated the desire to design models that more closely mimicked the *in vivo* scenario. Cellular invasion experiments where siRNA was initially sequestrated away from the cell containing hydrogels were conducted with either PEG/PEG or PEG/collagen combinations. Cells

invading from PEG to PEG were shown to only move minimally into the siRNA hydrogel. Cells invasion and migration from collagen (dermal equivalents) into either 8-arm or 4-arm PEG hydrogels was far more extensive with 4-arm PEG hydrogel allowing maximal 3D cellular migration.

Internalisation of siRNA into invading cells was assayed with a fluorescently labelled siRNA. Successful uptake was confirmed by confocal microscopy but level of uptake appeared low and quantification was challenging. Thus, an approach which might allow for both simpler quantification and efficacy to be determined was developed. Here siRNA sequences that cause cell death were employed in conjunction with an assay that can detect dead cells in 3D. Cell death levels achieved were very limited, which complicated aspects of quantification, but cell death levels in the experimental group (though non-significant) indicated possible successful transfection.

In conclusion, PEI based siRNA nanoparticles have been established in this laboratory as well as assays needed for optimisation of PEI and other nanoparticle formulations. An assay determining the ability of a scaffold based delivery system to confer additional protection from RNase degradation was also developed. A 3D cell invasion that gets closer to the in vivo scenario was established and could be easily adapted for use with other hydrogel siRNA formulations.

5. References

1. Kanasty, R., Dorkin, J. R., Vegas, A. & Anderson, D. Delivery materials for siRNA therapeutics. *Nat. Mater.* **12,** 967–977 (2013).
2. Napoli, C., Lemieux, C. & Jorgensen, R. Introduction of a Chimeric Chalcone Synthase Gene into Petunia Results in Reversible Co-Suppression of Homologous Genes in trans. *Plant Cell* **2,** 279–289 (1990).
3. Fire, A. *et al.* Potent and specific genetic interference by double-stranded RNA in Caenorhabditis elegans. *Nature* **391,** 806–11 (1998).
4. Deng, Y. *et al.* Therapeutic potentials of gene silencing by RNA interference: Principles, challenges, and new strategies. *Gene* **538,** 217–227 (2014).
5. Christopher, A. *et al.* MicroRNA therapeutics: Discovering novel targets and developing specific therapy. *Perspect. Clin. Res.* **7,** 68 (2016).
6. Bartel, D. P. MicroRNAs; genomics, biogenesis, mechanism, and function. *Cell* **116,** 281–297 (2004).
7. Guo, Y. *et al.* Effect of vector-expressed shRNAs on hTERT expression. *World J. Gastroenterol.* **11,** 2912–2915 (2005).
8. Kurreck, J. RNA interference: from basic research to therapeutic applications. *Angew. Chem. Int. Ed. Engl.* **48,** 1378–98 (2009).
9. Amendola, M. *et al.* Regulated and multiple miRNA and siRNA delivery into primary cells by a lentiviral platform. *Mol. Ther.* **17,** 1039–1052 (2009).
10. Wang, L. L. & Burdick, J. A. Engineered hydrogels for local and sustained delivery of RNA-interference therapies. *Adv. Healthc. Mater.* **6,** 1601041 (2017).
11. Liu, J. Argonaute2 is the catalytic engine of mammalian RNAi. *Science (80-.).* **305,** 1437–1441 (2004).
12. Valencia-Sanchez, M. A., Liu, J., Hannon, G. J. & Parker, R. Control of translation and mRNA degradation by miRNAs and siRNAs. *Genes Dev.* **20,** 515–524 (2006).
13. Lam, J. K. W., Chow, M. Y. T., Zhang, Y. & Leung, S. W. S. siRNA versus miRNA as therapeutics for gene silencing. *Mol. Ther. Acids* **4,** e252 (2015).
14. Kim, V. N., Han, J. & Siomi, M. C. Biogenesis of small RNAs in animals. *Nat. Rev. Mol. Cell Biol.* **10,** 126–139 (2009).
15. Huntzinger, E. & Izaurralde, E. Gene silencing by microRNAs: contributions of translational repression and mRNA decay. *Nat. Rev. Genet.* **12,** 99–110 (2011).
16. Carthew, R. W. & Sontheimer, E. J. Origins and mechanisms of miRNAs and siRNAs. *Cell* **136,**

642–655 (2009).

17. Elbashir, S. M. *et al.* Duplexes of 21-nucleotide RNAs mediate RNA interference in cultured mammalian cells. *Nature* **411,** 494–8 (2001).
18. Cullen, B. R. RNAi the natural way. *Nat. Genet.* **37,** 1163–1165 (2005).
19. Whitehead, K. A., Langer, R. & Anderson, D. G. Knocking down barriers: advances in siRNA delivery. *Nat. Rev. Drug Discov.* **8,** 129–138 (2009).
20. Tokatlian, T. & Segura, T. siRNA applications in nanomedicine. *Wiley Interdiscip. Rev. Nanomedicine Nanobiotechnology* **2,** 305–315 (2010).
21. Xu, C. & Wang, J. Delivery systems for siRNA drug development in cancer therapy. *Asian J. Pharm. Sci.* **10,** 1–12 (2015).
22. Bartlett, D. W. & Davis, M. E. Physicochemical and Biological Characterization of Targeted, Nucleic Acid-Containing Nanoparticles. *Bioconjug. Chem.* **18,** 456–468 (2007).
23. Braasch, D. A. *et al.* Biodistribution of phosphodiester and phosphorothioate siRNA. *Bioorg. Med. Chem. Lett.* **14,** 1139–43 (2004).
24. Watts, J. K. & Corey, D. R. Clinical status of duplex RNA. *Bioorg. Med. Chem. Lett.* **20,** 3203–7 (2010).
25. Judge, A. & MacLachlan, I. Overcoming the innate immune response to small interfering RNA. *Hum. Gene Ther.* **19,** 111–24 (2008).
26. Hornung, V. *et al.* Sequence-specific potent induction of IFN-alpha by short interfering RNA in plasmacytoid dendritic cells through TLR7. *Nat. Med.* **11,** 263–270 (2005).
27. Judge, A. D. *et al.* Sequence-dependent stimulation of the mammalian innate immune response by synthetic siRNA. *Nat Biotechnol* **23,** 457–462 (2005).
28. Sioud, M. Induction of inflammatory cytokines and interferon responses by double-stranded and single-stranded siRNAs is sequence-dependent and requires endosomal localization. *J. Mol. Biol.* **348,** 1079–1090 (2005).
29. Soutschek, J. *et al.* Therapeutic silencing of an endogenous gene by systemic administration of modified siRNAs. *Nature* **432,** 173–8 (2004).
30. Matyjaszewski, K., Berry, G. C., O'Rorke, S., Keeney, M. & Pandit, A. Non-viral polyplexes: Scaffold mediated delivery for gene therapy. *Prog. Polym. Sci.* **35,** 441–458 (2010).
31. Eulalio, A. *et al.* Functional screening identifies miRNAs inducing cardiac regeneration. *Nature* **492,** 376–81 (2012).
32. Burnett, J. C., Rossi, J. J. & Tiemann, K. Current progress of siRNA/shRNA therapeutics in clinical trials. *Biotechnol. J.* **6,** 1130–46 (2011).
33. Digiusto, D. L. *et al.* RNA-based gene therapy for HIV with lentiviral vector-modified CD34(+)

cells in patients undergoing transplantation for AIDSrelated lymphoma. *Sci. Transl. Med.* **2,** 36–43 (2010).

34. DiGiusto, D. L. *et al.* Development of hematopoietic stem cell based gene therapy for HIV-1 infection: considerations for proof of concept studies and translation to standard medical practice. *Viruses* **5,** 2898–919 (2013).
35. Thomas, C. E., Ehrhardt, A. & Kay, M. a. Progress and problems with the use of viral vectors for gene therapy. *Nat. Rev. Genet.* **4,** 346–58 (2003).
36. Nguyen, T., Menocal, E. M., Harborth, J. & Fruehauf, J. H. RNAi therapeutics: an update on delivery. *Curr. Opin. Mol. Ther.* **10,** 158–67 (2008).
37. Hacein-Bey-Abina, S. *et al.* Sustained correction of X-linked severe combined immunodeficiency by ex vivo gene therapy. *N. Engl. J. Med.* **346,** 1185–1193 (2002).
38. Hacein-bey-abina, S. & Schmidt, M. Correspondence: A serious adverse event after successful gene therapy for X-linked severe combined immunodeficiency. *N. Engl. J. Med.* **348,** 255–266 (2003).
39. Krebs, M. D. & Alsberg, E. Localized, targeted, and sustained siRNA delivery. *Chem. - A Eur. J.* **17,** 3054–3062 (2011).
40. McCaffrey, A. P. *et al.* Gene expression: RNA interference in adult mice. *Nature* **418,** 38–39 (2002).
41. Lewis, D. L., Hagstrom, J. E., Loomis, A. G., Wolff, J. a & Herweijer, H. Efficient delivery of siRNA for inhibition of gene expression in postnatal mice. *Nat. Genet.* **32,** 107–108 (2002).
42. Song, E. *et al.* RNA interference targeting Fas protects mice from fulminant hepatitis. *Nat Med* **9,** 347–351 (2003).
43. Zender, L. *et al.* Caspase 8 small interfering RNA prevents acute liver failure in mice. *Proc. Natl. Acad. Sci.* **100,** 7797–7802 (2003).
44. Bonamassa, B., Hai, L. & Liu, D. Hydrodynamic gene delivery and its applications in pharmaceutical research. *Pharm. Res.* **28,** 694–701 (2011).
45. Rust, C. & Gores, G. J. Apoptosis and liver disease. *Am. J. Med.* **108,** 567–574 (2000).
46. Adamis, A. P. *et al.* Increased vascular endothelial growth factor levels in the vitreous of eyes with proliferative diabetic retinopathy. *Am. J. Opthalmology* **118,** 445–450 (1994).
47. Pierce, E. A. *et al.* Vascular endothelial growth factor/vascular permeability factor expression in a mouse model of retinal neovascularization. *Biochemistry* **92,** 905–909 (1995).
48. Reich, S. J. *et al.* Small interfering RNA (siRNA) targeting VEGF effectively inhibits ocular neovascularization in a mouse model. *Mol. Vis.* **9,** 210–6 (2003).
49. Tolentino, M. J. *et al.* Intravitreal injection of vascular endothelial growth factor small

interfering RNA inhibits growth and leakage in a nonhuman primate, laser-induced model of choroidal neovascularization. *Retina* **24,** 132–8 (2004).

50. Kim, B. *et al.* Inhibition of ocular angiogenesis by siRNA targeting vascular endothelial growth factor pathway genes. *Am. J. Pathol.* **165,** 2177–2185 (2004).
51. Kaiser, P. K. *et al.* RNAi-based treatment for neovascular age-related macular degeneration by siRNA-027. *Am. J. Ophthalmol.* **150,** 33–39.e2 (2010).
52. Deleavey, G. F. & Damha, M. J. Designing chemically modified oligonucleotides for targeted gene silencing. *Chem. Biol.* **19,** 937–954 (2012).
53. Bruno, K. Using drug-excipient interactions for siRNA delivery. *Adv. Drug Deliv. Rev.* **63,** 1210–26 (2011).
54. Monaghan, M. & Pandit, A. RNA interference therapy via functionalized scaffolds. *Adv. Drug Deliv. Rev.* **63,** 197–208 (2011).
55. Morrissey, D. V. *et al.* Activity of stabilized short interfering RNA in a mouse model of hepatitis B virus replication. *Hepatology* **41,** 1349–1356 (2005).
56. Tros de Ilarduya, C., Sun, Y. & Düzgüneş, N. Gene delivery by lipoplexes and polyplexes. *Eur. J. Pharm. Sci.* **40,** 159–170 (2010).
57. Mo, R. H., Zaro, J. L. & Shen, W.-C. Comparison of cationic and amphipathic cell penetrating peptides for siRNA delivery and efficacy. *Mol. Pharm.* **9,** 299–309 (2012).
58. Frankel, A. D. & Pabo, C. O. Cellular uptake of the tat protein from human immunodeficiency virus. *Cell* **55,** 1189–1193 (1988).
59. Green, M., Ishino, M. & Loewenstein, P. M. Mutational analysis of HIV-1 Tat minimal domain peptides: Identification of trans-dominant mutants that suppress HIV-LTR-driven gene expression. *Cell* **58,** 215–223 (1989).
60. Tai, W. & Gao, X. Functional peptides for siRNA delivery. *Advanced Drug Delivery Reviews* **110–111,** 157–168 (2017).
61. Bechara, C. & Sagan, S. Cell-penetrating peptides: 20 years later, where do we stand? *FEBS Lett.* **587,** 1693–1702 (2013).
62. Koren, E. & Torchilin, V. P. Cell-penetrating peptides: breaking through to the other side. *Trends Mol. Med.* **18,** 385–393 (2012).
63. Song, E. *et al.* Antibody mediated in vivo delivery of small interfering RNAs via cell-surface receptors. *Nat. Biotechnol.* **23,** 709–17 (2005).
64. Freire, J. M. *et al.* siRNA-cell-penetrating peptides complexes as a combinatorial therapy against chronic myeloid leukemia using BV173 cell line as model. *J. Control. Release* **245,** 127–136 (2017).

65. Kumar, P. *et al.* T cell-specific siRNA delivery suppresses HIV-1 infection in humanized mice. *Cell* **134,** 577–586 (2008).

66. Welch, J. J., Swanekamp, R. J., King, C., Dean, D. A. & Nilsson, B. L. Functional delivery of siRNA by disulfide-constrained cyclic amphipathic peptides. *ACS Med. Chem. Lett.* **7,** 584–589 (2016).

67. Moschos, S. A. *et al.* Lung delivery studies using siRNA conjugated to TAT(48−60) and penetratin reveal peptide induced reduction in gene expression and induction of innate immunity. *Bioconjug. Chem.* **18,** 1450–1459 (2007).

68. Meade, B. R. & Dowdy, S. F. Exogenous siRNA delivery using peptide transduction domains/cell penetrating peptides. *Adv. Drug Deliv. Rev.* **59,** 134–140 (2007).

69. Endoh, T. & Ohtsuki, T. Cellular siRNA delivery using cell-penetrating peptides modified for endosomal escape. *Adv. Drug Deliv. Rev.* **61,** 704–709 (2009).

70. Crombez, L., Morris, M. C., Heitz, F. & Divita, G. in *Biochemical Society Transactions* **35,** 59–73 (2011).

71. Gooding, M., Browne, L. P., Quinteiro, F. M. & Selwood, D. L. siRNA delivery: from lipids to cell-penetrating peptides and their mimics. *Chem. Biol. Drug Des.* **80,** 787–809 (2012).

72. Felgner, P. L. *et al.* Lipofection: a highly efficient, lipid-mediated DNA-transfection procedure. *Proc. Natl. Acad. Sci. U. S. A.* **84,** 7413–7417 (1987).

73. Li, W. & Szoka, F. C. Lipid-based nanoparticles for nucleic acid delivery. *Pharm. Res.* **24,** 438–449 (2007).

74. Rezaee, M., Oskuee, R. K., Nassirli, H. & Malaekeh-Nikouei, B. Progress in the development of lipopolyplexes as efficient non-viral gene delivery systems. *J. Control. Release* **236,** 1–14 (2016).

75. Xia, Y., Tian, J. & Chen, X. Effect of surface properties on liposomal siRNA delivery. *Biomaterials* **79,** 56–68 (2016).

76. Payne, C. K., Jones, S. A., Chen, C. & Zhuang, X. Internalization and trafficking of cell surface proteoglycans and proteoglycan-binding ligands. *Traffic* **8,** 389–401 (2007).

77. Mislick, K. a & Baldeschwieler, J. D. Evidence for the role of proteoglycans in cation-mediated gene transfer. *Proc. Natl. Acad. Sci. U. S. A.* **93,** 12349–12354 (1996).

78. Mounkes, L. C., Zhong, W., Cipres-Palacin, G., Heath, T. D. & Debs, R. J. Proteoglycans mediate cationic liposome-DNA complex-based gene delivery in Vitro and in Vivo. *J. Biol. Chem.* **273,** 26164–26170 (1998).

79. Tseng, Y. C., Mozumdar, S. & Huang, L. Lipid-based systemic delivery of siRNA. *Adv. Drug Deliv. Rev.* **61,** 721–731 (2009).

80. Rehman, Z. U., Hoekstra, D. & Zuhorn, I. S. Mechanism of polyplex- and lipoplex-mediated delivery of nucleic acids: Real-time visualization of transient membrane destabilization without

endosomal lysis. *ACS Nano* **7,** 3767–3777 (2013).

81. Sheng, R. *et al.* Cationic nanoparticles assembled from natural-based steroid lipid for improved intracellular transport of siRNA and pDNA. *Nanomaterials* **6,** 69 (2016).
82. Warashina, S. *et al.* A lipid nanoparticle for the efficient delivery of siRNA to dendritic cells. *J. Control. Release* **225,** 183–91 (2016).
83. Lee, J. *et al.* Mono-arginine cholesterol-based small lipid nanoparticles as a systemic sirna delivery platform for effective cancer therapy. *Theranostics* **6,** 192–203 (2016).
84. Kim, W. J. *et al.* Cholesteryl oligoarginine delivering vascular endothelial growth factor siRNA effectively inhibits tumor growth in colon adenocarcinoma. *Mol. Ther.* **14,** 343–350 (2006).
85. Namiki, Y. *et al.* A novel magnetic crystal–lipid nanostructure for magnetically guided in vivo gene delivery. *Nat. Nanotechnol.* **4,** 598–606 (2009).
86. Li, S.-D., Chen, Y.-C., Hackett, M. J. & Huang, L. Tumor-targeted delivery of siRNA by self-assembled nanoparticles. *Mol. Ther.* **16,** 163–9 (2008).
87. Yanagi, T. *et al.* Lipid nanoparticle-mediated siRNA transfer against PCTAIRE1/PCTK1/Cdk16 inhibits *in vivo* cancer growth. *Mol. Ther. - Nucleic Acids* **5,** e327 (2016).
88. Palliser, D. *et al.* An siRNA-based microbicide protects mice from lethal herpes simplex virus 2 infection. *Nature* **439,** 89–94 (2006).
89. Sørensen, D. R., Leirdal, M. & Sioud, M. Gene silencing by systemic delivery of synthetic siRNAs in adult mice. *J. Mol. Biol.* **327,** 761–766 (2003).
90. Zimmermann, T. S. *et al.* RNAi-mediated gene silencing in non-human primates. *Nature* **441,** 111–4 (2006).
91. Sioud, M. & Sørensen, D. R. Cationic liposome-mediated delivery of siRNAs in adult mice. *Biochem. Biophys. Res. Commun.* **312,** 1220–1225 (2003).
92. Wu, G. & Wu, C. Receptor-mediated in vitro gene transformation by a soluble DNA carrier system [published erratum appears in J Biol Chem 1988 Jan 5;263(1):588]. *J. Biol. Chem.* **262,** 4429–4432 (1987).
93. Akinc, A., Thomas, M., Klibanov, A. M. & Langer, R. Exploring polyethylenimine-mediated DNA transfection and the proton sponge hypothesis. *J. Gene Med.* **7,** 657–663 (2005).
94. Grayson, A. C. R., Doody, A. M. & Putnam, D. Biophysical and structural characterization of polyethylenimine-mediated siRNA delivery in vitro. *Pharm. Res.* **23,** 1868–76 (2006).
95. Madaan, K., Kumar, S., Poonia, N., Lather, V. & Pandita, D. Dendrimers in drug delivery and targeting: Drug-dendrimer interactions and toxicity issues. *J. Pharm. Bioallied Sci.* **6,** 139–50 (2014).
96. Dominska, M. & Dykxhoorn, D. M. Breaking down the barriers: siRNA delivery and endosome

escape. *J. Cell Sci.* **123,** 1183–1189 (2010).

97. Cavallaro, G., Sardo, C., Craparo, E. F., Porsio, B. & Giammona, G. Polymeric nanoparticles for siRNA delivery: Production and applications. *Int. J. Pharm.* **525,** 313–333 (2017).
98. Shukla, R. S., Qin, B. & Cheng, K. Peptides used in the delivery of small noncoding RNA. *Mol. Pharm.* **11,** 3395–3408 (2014).
99. Mokhtarzadeh, A. *et al.* Biodegradable nano-polymers as delivery vehicles for therapeutic small non-coding ribonucleic acids. *J. Control. Release* **245,** 116–126 (2017).
100. Kano, A. *et al.* Grafting of poly(ethylene glycol) to poly-lysine augments its lifetime in blood circulation and accumulation in tumors without loss of the ability to associate with siRNA. *J. Control. Release* **149,** 2–7 (2011).
101. Hartono, S. B. *et al.* Poly-L-lysine functionalized large pore cubic mesostructured silica nanoparticles as biocompatible carriers for gene delivery. *ACS Nano* **6,** 2104–2117 (2012).
102. Watanabe, K. *et al.* In vivo siRNA delivery with dendritic poly(L-lysine) for the treatment of hypercholesterolemia. *Mol. Biosyst.* **5,** 1306–1310 (2009).
103. Patil, M. L., Zhang, M. & Minko, T. Multifunctional triblock nanocarrier (PAMAM-PEG-PLL) for the efficient intracellular siRNA delivery and gene silencing. *ACS Nano* **5,** 1877–1887 (2011).
104. Buyens, K. *et al.* Monitoring the disassembly of siRNA polyplexes in serum is crucial for predicting their biological efficacy. *J. Control. Release* **141,** 38–41 (2010).
105. Tomalia, D. A. *et al.* A new class of polymers: starburst-dendritic macromolecules. *Polym. J.* **17,** 117–132 (1985).
106. Tang, Y. *et al.* Efficient in vitro siRNA delivery and intramuscular gene silencing using PEG-modified PAMAM dendrimers. *Mol. Pharm.* **9,** 1812–1821 (2012).
107. Akhtar, S. & Benter, I. F. Nonviral delivery of synthetic siRNAs in vivo. *J. Clin. Invest.* **117,** 3623–3632 (2007).
108. Davis, M. E. The first targeted delivery of siRNA in humans via a self-assembling, cyclodextrin polymer-based nanoparticle: From concept to clinic. *Mol. Pharm.* **6,** 659–668 (2009).
109. Gonzalez, H., Hwang, S. J. & Davis, M. E. New class of polymers for the delivery of macromolecular therapeutics. *Bioconjug. Chem.* **10,** 1068–1074 (1999).
110. Davis, M. E. *et al.* Evidence of RNAi in humans from systemically administered siRNA via targeted nanoparticles. *Nature* **464,** 1067–70 (2010).
111. Chaturvedi, K. *et al.* Cyclodextrin-based siRNA delivery nanocarriers: a state-of-the-art review. *Expert Opin. Drug Deliv.* **8,** 1455–1468 (2011).
112. Mishra, S., Heidel, J. D., Webster, P. & Davis, M. E. Imidazole groups on a linear, cyclodextrin-containing polycation produce enhanced gene delivery via multiple processes. *J. Control.*

Release **116,** 179–191 (2006).

113. Mishra, S., Webster, P. & Davis, M. E. PEGylation significantly affects cellular uptake and intracellular trafficking of non-viral gene delivery particles. *Eur. J. Cell Biol.* **83,** 97–111 (2004).
114. Hu-Lieskovan, S., Heidel, J. D., Bartlett, D. W., Davis, M. E. & Triche, T. J. Sequence-specific knockdown of EWS-FLI1 by targeted, nonviral delivery of small interfering RNA inhibits tumor growth in a murine model of metastatic Ewing's sarcoma. *Cancer Res.* **65,** 8984–8992 (2005).
115. Guo, J. *et al.* Antibody-targeted cyclodextrin-based nanoparticles for siRNA delivery in the treatment of acute myeloid leukaemia – physicochemical characteristics, in vitro mechanistic studies and ex vivo patient derived therapeutic efficacy. *Mol. Pharm.* acs.molpharmaceut.6b01150 (2017). doi:10.1021/acs.molpharmaceut.6b01150
116. Guo, J., Ogier, J. R., Desgranges, S., Darcy, R. & O'Driscoll, C. Anisamide-targeted cyclodextrin nanoparticles for siRNA delivery to prostate tumours in mice. *Biomaterials* **33,** 7775–7784 (2012).
117. Fitzgerald, K. A. *et al.* The use of collagen-based scaffolds to simulate prostate cancer bone metastases with potential for evaluating delivery of nanoparticulate gene therapeutics. *Biomaterials* **66,** 53–66 (2015).
118. McCarthy, J. *et al.* Gene silencing of TNF-alpha in a murine model of acute colitis using a modified cyclodextrin delivery system. *J. Control. Release* **168,** 28–34 (2013).
119. Godinho, B. M. D. C., Ogier, J. R., Darcy, R., O'Driscoll, C. M. & Cryan, J. F. Self-assembling modified β-cyclodextrin nanoparticles as neuronal siRNA delivery vectors: Focus on huntington's disease. *Mol. Pharm.* **10,** 640–649 (2013).
120. O'Mahony, A. M. *et al.* Click-Modified Cyclodextrins as Nonviral Vectors for Neuronal siRNA Delivery. *ACS Chem. Neurosci.* **3,** 744–752 (2012).
121. McMahon, A. *et al.* Targeted gene delivery to hepatocytes with galactosylated amphiphilic cyclodextrins. *J. Pharm. Pharmacol.* **64,** 1063–1073 (2012).
122. Horton, S. J. & Huntly, B. J. P. Recent advances in acute myeloid leukemia stem cell biology. *Haematologica* **97,** 966–74 (2012).
123. Zuber, J. *et al.* RNAi screen identifies Brd4 as a therapeutic target in acute myeloid leukaemia. *Nature* **478,** 524–528 (2011).
124. Wang, J. J. *et al.* Recent advances of chitosan nanoparticles as drug carriers. *Int. J. Nanomedicine* **6,** 765–774 (2011).
125. Borzacchiello, A. *et al.* Chitosan-based hydrogels: synthesis and characterization. *J. Mater. Sci. Mater. Med.* **12,** 861–4 (2001).
126. Chen, M. *et al.* Chitosan/siRNA nanoparticles encapsulated in PLGA nanofibers for siRNA

delivery. *ACS Nano* **6,** 4835–44 (2012).

127. Katas, H. & Alpar, H. O. Development and characterisation of chitosan nanoparticles for siRNA delivery. *J. Control. Release* **115,** 216–225 (2006).
128. Mao, S., Sun, W. & Kissel, T. Chitosan-based formulations for delivery of DNA and siRNA. *Adv. Drug Deliv. Rev.* **62,** 12–27 (2010).
129. Lee, M. K. *et al.* The use of chitosan as a condensing agent to enhance emulsion-mediated gene transfer. *Biomaterials* **26,** 2147–2156 (2005).
130. Shu, X. . & Zhu, K. . The influence of multivalent phosphate structure on the properties of ionically cross-linked chitosan films for controlled drug release. *Eur. J. Pharm. Biopharm.* **54,** 235–243 (2002).
131. Sadio, A. *et al.* Modified-chitosan/siRNA nanoparticles downregulate cellular CDX2 expression and cross the gastric mucus barrier. *PLoS One* **9,** (2014).
132. Sadreddini, S. *et al.* Chitosan nanoparticles as a dual drug/siRNA delivery system for treatment of colorectal cancer. *Immunol. Lett.* **181,** 79–86 (2017).
133. Van Woensel, M. *et al.* Development of siRNA-loaded chitosan nanoparticles targeting Galectin-1 for the treatment of glioblastoma multiforme via intranasal administration. *J. Control. Release* **227,** 71–81 (2016).
134. Matokanovic, M., Barisic, K., Filipovic-Grcic, J. & Maysinger, D. Hsp70 silencing with siRNA in nanocarriers enhances cancer cell death induced by the inhibitor of Hsp90. *Eur. J. Pharm. Sci.* **50,** 149–158 (2013).
135. Yang, J. *et al.* Induction of apoptosis by chitosan/HPV16 E7 siRNA complexes in cervical cancer cells. *Mol. Med. Rep.* **7,** 998–1002 (2013).
136. Xia, H., Jun, J., Wen-ping, L., Yi-feng, P. & Xiao-ling, C. Chitosan nanoparticle carrying small interfering RNA to platelet-derived growth factor B mRNA inhibits proliferation of smooth muscle cells in rabbit injured arteries. *Vascular* **21,** 301–306 (2013).
137. Mittnacht, U. *et al.* Chitosan/siRNA nanoparticles biofunctionalize nerve implants and enable neurite outgrowth. *Nano Lett.* **10,** 3933–9 (2010).
138. Malmo, J., Sandvig, A., Vårum, K. M. & Strand, S. P. Nanoparticle mediated P-glycoprotein silencing for improved drug delivery across the blood-brain barrier: A siRNA-chitosan approach. *PLoS One* **8,** (2013).
139. Ragelle, H., Vandermeulen, G. & Préat, V. Chitosan-based siRNA delivery systems. *J. Control. Release* **172,** 207–218 (2013).
140. Aspden, T. J. *et al.* Chitosan as a nasal delivery system: The effect of chitosan solutions on *in vitro* and *in vivo* mucociliary transport rates in human turbinates and volunteers. *J. Pharm. Sci.*

86, 509–513 (1997).

141. Baldrick, P. The safety of chitosan as a pharmaceutical excipient. *Regulatory Toxicology and Pharmacology* **56,** 290–299 (2010).
142. Boussif, O. *et al.* A versatile vector for gene and oligonucleotide transfer into cells in culture and in vivo: polyethylenimine. *Proc. Natl. Acad. Sci. U. S. A.* **92,** 7297–301 (1995).
143. Werth, S. *et al.* A low molecular weight fraction of polyethylenimine (PEI) displays increased transfection efficiency of DNA and siRNA in fresh or lyophilized complexes. *J. Control. Release* **112,** 257–70 (2006).
144. Kwok, A. & Hart, S. L. Comparative structural and functional studies of nanoparticle formulations for DNA and siRNA delivery. *Nanomedicine* **7,** 210–9 (2011).
145. Wang, F. *et al.* A Neutralized noncharged polyethylenimine-based system for efficient delivery of siRNA into heart without toxicity. *ACS Appl. Mater. Interfaces* **8,** 33529–33538 (2016).
146. Dheur, S. *et al.* Polyethylenimine but not cationic lipid improves antisense activity of 3'-capped phosphodiester oligonucleotides. *Antisense Nucleic Acid Drug Dev* **9,** 515–525 (1999).
147. Lungwitz, U., Breunig, M., Blunk, T. & Göpferich, A. Polyethylenimine-based non-viral gene delivery systems. *Eur. J. Pharm. Biopharm.* **60,** 247–266 (2005).
148. Patnaik, S. & Gupta, K. C. Novel polyethylenimine-derived nanoparticles for in vivo gene delivery. *Expert Opin. Drug Deliv.* **10,** 215–228 (2013).
149. Lei, Y. *et al.* Incorporation of active DNA/cationic polymer polyplexes into hydrogel scaffolds. *Biomaterials* **31,** 9106–9116 (2010).
150. Parhamifar, L., Larsen, A. K., Hunter, A. C., Andresen, T. L. & Moghimi, S. M. Polycation cytotoxicity: a delicate matter for nucleic acid therapy—focus on polyethylenimine. *Soft Matter* **6,** 4001 (2010).
151. Parhamifar, L., Larsen, A. K., Hunter, A. C., Andresen, T. L. & Moghimi, S. M. Polycation cytotoxicity: a delicate matter for nucleic acid therapy—focus on polyethylenimine. *Soft Matter* **6,** 4001 (2010).
152. Wiethoff, C. M. & Middaugh, C. R. Barriers to nonviral gene delivery. *J. Pharm. Sci.* **92,** 203–217 (2003).
153. Kong, L. *et al.* Multifunctional PEI-entrapped gold nanoparticles enable efficient delivery of therapeutic siRNA into glioblastoma cells. *Biomater. Sci.* **5,** 258–266 (2017).
154. Liu, S. *et al.* Inhibition of murine breast cancer growth and metastasis by survivin-targeted siRNA using disulfide cross-linked linear PEI. *Eur. J. Pharm. Sci.* **82,** 171–182 (2016).
155. Schiffelers, R. M. *et al.* Cancer siRNA therapy by tumor selective delivery with ligand-targeted sterically stabilized nanoparticle. *Nucleic Acids Res.* **32,** e149 (2004).

156. Park, K., Lee, M.-Y., Kim, K. S. & Hahn, S. K. Target specific tumor treatment by VEGF siRNA complexed with reducible polyethyleneimine–hyaluronic acid conjugate. *Biomaterials* **31,** 5258–5265 (2010).

157. Chiu, S.-J., Ueno, N. T. & Lee, R. J. Tumor-targeted gene delivery via anti-HER2 antibody (trastuzumab, Herceptin®) conjugated polyethylenimine. *J. Control. Release* **97,** 357–369 (2004).

158. Wang, L. *et al.* Highly efficient Gab2 siRNA delivery to ovarian cancer cells mediated by chitosan–polyethyleneimine nanoparticles. *J. Mater. Chem. B* **4,** 273–281 (2016).

159. Abdallah, B. *et al.* A powerful nonviral vector for in vivo gene transfer into the adult mammalian brain: polyethylenimine. *Hum. Gene Ther.* **7,** 1947–54 (1996).

160. Goula, D. *et al.* Size, diffusibility and transfection performance of linear PEI/DNA complexes in the mouse central nervous system. *Gene Ther.* **5,** 712–7 (1998).

161. Gautam, a, Densmore, C. L., Xu, B. & Waldrep, J. C. Enhanced gene expression in mouse lung after PEI-DNA aerosol delivery. *Mol. Ther.* **2,** 63–70 (2000).

162. Xie, Y. *et al.* Targeted delivery of siRNA to activated T cells via transferrin-polyethylenimine (Tf-PEI) as a potential therapy of asthma. *J. Control. Release* **229,** 120–129 (2016).

163. Kim, D. *et al.* Anti-apoptotic cardioprotective effects of SHP-1 gene silencing against ischemia-reperfusion injury: Use of deoxycholic acid-modified low molecular weight polyethyleneimine as a cardiac siRNA-carrier. *J. Control. Release* **168,** 125–134 (2013).

164. Hong, J. *et al.* Cardiac RNAi therapy using RAGE siRNA/deoxycholic acid-modified polyethylenimine complexes for myocardial infarction. *Biomaterials* **35,** 7562–7573 (2014).

165. Urban-Klein, B., Werth, S., Abuharbeid, S., Czubayko, F. & Aigner, a. RNAi-mediated gene-targeting through systemic application of polyethylenimine (PEI)-complexed siRNA in vivo. *Gene Ther.* **12,** 461–6 (2005).

166. Lecocq, M., Wattiaux-De Coninck, S., Laurent, N., Wattiaux, R. & Jadot, M. Uptake and intracellular fate of polyethylenimine *in vivo*. *Biochem. Biophys. Res. Commun.* **278,** 414–418 (2000).

167. Goula, D. *et al.* Polyethylenimine-based intravenous delivery of transgenes to mouse lung. *Gene Ther.* **5,** 1291–5 (1998).

168. Howard, K. A. *et al.* RNA interference in vitro and in vivo using a novel chitosan/siRNA nanoparticle system. *Mol. Ther.* **14,** 476–84 (2006).

169. Clamme, J. P., Azoulay, J. & Mély, Y. Monitoring of the formation and dissociation of polyethylenimine/DNA complexes by two photon fluorescence correlation spectroscopy. *Biophys. J.* **84,** 1960–8 (2003).

170. Clamme, J. P., Krishnamoorthy, G. & Mély, Y. Intracellular dynamics of the gene delivery vehicle polyethylenimine during transfection: Investigation by two-photon fluorescence correlation spectroscopy. *Biochim. Biophys. Acta - Biomembr.* **1617,** 52–61 (2003).

171. Boeckle, S. *et al.* Purification of polyethylenimine polyplexes highlights the role of free polycations in gene transfer. *J. Gene Med.* **6,** 1102–1111 (2004).

172. Höbel, S. & Aigner, A. Polyethylenimines for siRNA and miRNA delivery in vivo. *Wiley Interdisciplinary Reviews: Nanomedicine and Nanobiotechnology* **5,** 484–501 (2013).

173. Dominska, M. & Dykxhoorn, D. M. Breaking down the barriers: siRNA delivery and endosome escape. *J. Cell Sci.* **123,** 1183–1189 (2010).

174. Caffrey, D. R. *et al.* siRNA Off-Target Effects Can Be Reduced at Concentrations That Match Their Individual Potency. *PLoS One* **6,** e21503 (2011).

175. Williams, D. F. On the nature of biomaterials. *Biomaterials* **30,** 5897–909 (2009).

176. Andersen, M., Howard, K. A., Paludan, S. R., Besenbacher, F. & Kjems, J. Delivery of siRNA from lyophilized polymeric surfaces. *Biomaterials* **29,** 506–512 (2008).

177. Takahashi, H., Wang, Y. & Grainger, D. W. Device-based local delivery of siRNA against mammalian target of rapamycin (mTOR) in a murine subcutaneous implant model to inhibit fibrous encapsulation. *J. Control. Release* **147,** 400–407 (2010).

178. Zhang, X. *et al.* SiRNA-loaded multi-shell nanoparticles incorporated into a multilayered film as a reservoir for gene silencing. *Biomaterials* **31,** 6013–8 (2010).

179. Joddar, B. *et al.* Sustained delivery of siRNA from dopamine-coated stainless steel surfaces. *Acta Biomater.* **9,** 6753–6761 (2013).

180. Kent Leach, J., Kaigler, D., Wang, Z., Krebsbach, P. H. & Mooney, D. J. Coating of VEGF-releasing scaffolds with bioactive glass for angiogenesis and bone regeneration. *Biomaterials* **27,** 3249–3255 (2006).

181. Yang, K. *et al.* Polydopamine-mediated surface modification of scaffold materials for human neural stem cell engineering. *Biomaterials* **33,** 6952–6964 (2012).

182. Macdonald, M. L. *et al.* Tissue integration of growth factor-eluting layer-by-layer polyelectrolyte multilayer coated implants. *Biomaterials* **32,** 1446–1453 (2011).

183. Shah, N. J. *et al.* Tunable dual growth factor delivery from polyelectrolyte multilayer films. *Biomaterials* **32,** 6183–6193 (2011).

184. Santiago, F. S. *et al.* New DNA enzyme targeting Egr-1 mRNA inhibits vascular smooth muscle proliferation and regrowth after injury. *Nat. Med.* **5,** 1264–1269 (1999).

185. Castleberry, S. A. *et al.* Nanolayered siRNA delivery platforms for local silencing of CTGF reduce cutaneous scar contraction in third-degree burns. *Biomaterials* **95,** 22–34 (2016).

186. Chuva De Sousa Lopes, S. M. *et al.* Connective tissue growth factor expression and Smad signaling during mouse heart development and myocardial infarction. *Dev. Dyn.* **231,** 542–550 (2004).

187. Khorshidi, S. *et al.* A review of key challenges of electrospun scaffolds for tissue-engineering applications. *J. Tissue Eng. Regen. Med.* **10,** 715–738 (2016).

188. Cao, H., Jiang, X., Chai, C. & Chew, S. Y. RNA interference by nanofiber-based siRNA delivery system. *J. Control. Release* **144,** 203–12 (2010).

189. Rujitanaroj, P. on, Wang, Y. C., Wang, J. & Chew, S. Y. Nanofiber-mediated controlled release of siRNA complexes for long term gene-silencing applications. *Biomaterials* **32,** 5915–5923 (2011).

190. Low, W. C. *et al.* Nanofibrous scaffold-mediated REST knockdown to enhance neuronal differentiation of stem cells. *Biomaterials* **34,** 3581–3590 (2013).

191. Chong, J. A. *et al.* REST: A mammalian silencer protein that restricts sodium channel gene expression to neurons. *Cell* **80,** 949–957 (1995).

192. Schoenherr, C. J. & Anderson, D. J. The neuron-restrictive silencer factor (NRSF): a coordinate repressor of multiple neuron-specific genes. *Science (80-.).* **267,** 1360–3 (1995).

193. Saul, J. M. & Williams, D. F. in *Handbook of Polymer Applications in Medicine and Medical Devices* 279–302 (Elsevier, 2011). doi:10.1016/B978-0-323-22805-3.00012-8

194. Li, Y., Tang, Y., Narain, R., Lewis, A. L. & Armes, S. P. Biomimetic stimulus-responsive star diblock gelators. *Langmuir* **21,** 9946–54 (2005).

195. Wang, K., Fu, Q., Chen, X., Gao, Y. & Dong, K. Preparation and characterization of pH-sensitive hydrogel for drug delivery system. *RSC Adv.* **2,** 7772 (2012).

196. Mahkam, M. Novel pH-sensitive hydrogels for colon-specific drug delivery. *Drug Deliv.* **17,** 158–163 (2010).

197. Zisch, A. H. *et al.* Cell-demanded release of VEGF from synthetic, biointeractive cell ingrowth matrices for vascularized tissue growth. *FASEB J.* **17,** 2260–2 (2003).

198. De Laporte, L. & Shea, L. D. Matrices and scaffolds for DNA delivery in tissue engineering. *Adv. Drug Deliv. Rev.* **59,** 292–307 (2007).

199. Shea, L. D., Smiley, E., Bonadio, J. & Mooney, D. J. DNA delivery from polymer matrices for tissue engineering. *Nat. Biotechnol.* **17,** 551–554 (1999).

200. Drury, J. L. & Mooney, D. J. Hydrogels for tissue engineering: Scaffold design variables and applications. *Biomaterials* **24,** 4337–4351 (2003).

201. Lutolf, M. P. *et al.* Synthetic matrix metalloproteinase-sensitive hydrogels for the conduction of tissue regeneration: engineering cell-invasion characteristics. *Proc. Natl. Acad. Sci. U. S. A.*

100, 5413–8 (2003).

202. Bracher, M. *et al.* Cell specific ingrowth hydrogels. *Biomaterials* **34,** 6797–6803 (2013).
203. Goetsch, K. P., Bracher, M., Bezuidenhout, D., Zilla, P. & Davies, N. H. Regulation of tissue ingrowth into proteolytically degradable hydrogels. *Acta Biomater.* **24,** 44–52 (2015).
204. Wall, S. T., Walker, J. C., Healy, K. E., Ratcliffe, M. B. & Guccione, J. M. Theoretical impact of the injection of material into the myocardium: A finite element model simulation. *Circulation* **114,** 2627–2635 (2006).
205. Krebs, M. D., Jeon, O. & Alsberg, E. Localized and sustained delivery of silencing RNA from macroscopic biopolymer hydrogels. *J. Am. Chem. Soc.* **131,** 9204–6 (2009).
206. Nguyen, K., Dang, P. N. & Alsberg, E. Functionalized, biodegradable hydrogels for control over sustained and localized siRNA delivery to incorporated and surrounding cells. *Acta Biomater.* **9,** 4487–4495 (2013).
207. Wightman, L. *et al.* Different behavior of branched and linear polyethylenimine for gene delivery in vitro and in vivo. *J. Gene Med.* **3,** 362–72 (2001).
208. Gao, H., Shi, W. & Freund, L. B. Mechanics of receptor-mediated endocytosis. *Proc. Natl. Acad. Sci. U. S. A.* **102,** 9469–74 (2005).
209. Pantarotto, D. *et al.* Functionalized carbon nanotubes for plasmid DNA gene delivery. *Angew. Chemie* **116,** 5354–5358 (2004).
210. Nguyen, M. K., Jeon, O., Krebs, M. D., Schapira, D. & Alsberg, E. Sustained localized presentation of RNA interfering molecules from in situ forming hydrogels to guide stem cell osteogenic differentiation. *Biomaterials* **35,** 6278–6286 (2014).
211. Huynh, C. T. *et al.* Photocleavable hydrogels for light-triggered siRNA release. *Adv. Healthc. Mater.* **5,** 305–310 (2016).
212. Babincova, M., Novotny, J., Rosenecker, J. & Babinec, P. Remote radio-control of siRNA release from magnetite-hydrogel composite. *Optoelectron. Adv. Mater. Commun.* **1,** 644–647 (2007).
213. Liu, J. *et al.* [Synthesis and experimental study of a novel polymer/gene compound drug controlled release system for the treatment of erectile dysfunction]. *Zhonghua Nan Ke Xue* **19,** 771–5 (2013).
214. Han, H. D. *et al.* Chitosan hydrogel for localized gene silencing. *Cancer Biol. Ther.* **11,** 839–845 (2011).
215. Kim, Y. M., Park, M. R. & Song, S. C. Injectable polyplex hydrogel for localized and long-term delivery of siRNA. *ACS Nano* **6,** 5757–5766 (2012).
216. Kim, Y. M., Park, M. R. & Song, S. C. An injectable cell penetrable nano-polyplex hydrogel for localized siRNA delivery. *Biomaterials* **34,** 4493–4500 (2013).

217. Kim, Y. M. & Song, S. C. Targetable micelleplex hydrogel for long-term, effective, and systemic siRNA delivery. *Biomaterials* **35,** 7970–7977 (2014).

218. Kim, Y.-M., Kim, C.-H. & Song, S.-C. Injectable ternary nanocomplex hydrogel for long-term chemical drug/gene dual delivery. *ACS Macro Lett.* **5,** 297–300 (2016).

219. Peng, H. *et al.* Sustained delivery of siRNA/PEI complex from in situ forming hydrogels potently inhibits the proliferation of gastric cancer. *J. Exp. Clin. Cancer Res.* **35,** 57 (2016).

220. Laroui, H. *et al.* Targeting intestinal inflammation with CD98 siRNA/PEI–loaded nanoparticles. *Mol. Ther.* **22,** 69–80 (2014).

221. Browne, S. *et al.* Modulation of inflammation and angiogenesis and changes in ECM GAG-activity via dual delivery of nucleic acids. *Biomaterials* **69,** 133–147 (2015).

222. Zhao, R., Yan, Q., Huang, H., Lv, J. & Ma, W. Transdermal siRNA-TGFβ1-337 patch for hypertrophic scar treatment. *Matrix Biol.* **32,** 265–76 (2013).

223. Cao, C., Yan, C., Hu, Z. & Zhou, S. Potential application of injectable chitosan hydrogel treated with siRNA in chronic rhinosinusitis therapy. *Mol. Med. Rep.* **12,** 6688–6694 (2015).

224. Kanazawa, T. *et al.* Topical anti-nuclear factor-kappa B small interfering RNA with functional peptides containing sericin-based hydrogel for atopic dermatitis. *Pharmaceutics* **7,** 294–304 (2015).

225. Laroui, H. *et al.* Fab'-bearing siRNA TNFα-loaded nanoparticles targeted to colonic macrophages offer an effective therapy for experimental colitis. *J. Control. Release* **186,** 41–53 (2014).

226. Monaghan, M., Browne, S., Schenke-Layland, K. & Pandit, A. A Collagen-based scaffold delivering exogenous microRNA-29B to modulate extracellular matrix remodeling. *Mol. Ther.* **22,** 786–796 (2014).

227. Li, Y. *et al.* The promotion of bone regeneration through positive regulation of angiogenic–osteogenic coupling using microRNA-26a. *Biomaterials* **34,** 5048–5058 (2013).

228. Manaka, T. *et al.* Local delivery of siRNA using a biodegradable polymer application to enhance BMP-induced bone formation. *Biomaterials* **32,** 9642–9648 (2011).

229. Wang, Y., Malcolm, D. W. & Benoit, D. S. W. Controlled and sustained delivery of siRNA/NPs from hydrogels expedites bone fracture healing. *Biomaterials* **139,** 127–138 (2017).

230. San Juan, A. *et al.* Development of a functionalized polymer for stent coating in the arterial delivery of small interfering RNA. *Biomacromolecules* **10,** 3074–3080 (2009).

231. Wan, W. G. *et al.* Enhanced cardioprotective effects mediated by plasmid containing the short-hairpin RNA of angiotensin converting enzyme with a biodegradable hydrogel after myocardial infarction. *J. Biomed. Mater. Res. - Part A* **102,** 3452–3458 (2014).

232. Wang, L. L. *et al.* Injectable, guest–host assembled polyethylenimine hydrogel for siRNA delivery. *Biomacromolecules* **18,** 77–86 (2017).

233. Huang, L., Xu, A. M. & Liu, W. Transglutaminase 2 in cancer. *Am. J. Cancer Res.* **5,** 2756–2776 (2015).

234. Tekedereli, I. *et al.* Therapeutic silencing of Bcl-2 by systemically administered siRNA nanotherapeutics inhibits tumor growth by autophagy and apoptosis and enhances the efficacy of chemotherapy in orthotopic xenograft models of ER (−) and ER (+) breast cancer. *Mol. Ther. - Nucleic Acids* **2,** e121 (2013).

235. Thi, H. *et al.* CD98 expression modulates intestinal homeostasis , inflammation , and colitis-associated cancer in mice. *J. Clin. Invest.* **121,** 1–23 (2011).

236. Xue, F.-M. *et al.* CD98 positive eosinophils contribute to T helper 1 pattern inflammation. *PLoS One* **7,** e51830 (2012).

237. Yan, Y. *et al.* Temporal and spatial analysis of clinical and molecular parameters in dextran sodium sulfate induced colitis. *PLoS One* **4,** e6073 (2009).

238. Li, Z. *et al.* Biological Functions of miR-29b Contribute to Positive Regulation of Osteoblast Differentiation. *J. Biol. Chem.* **284,** 15676–15684 (2009).

239. Liu, Y. *et al.* Renal Medullary MicroRNAs in Dahl Salt-Sensitive Rats: miR-29b Regulates Several Collagens and Related Genes. *Hypertension* **55,** 974–982 (2010).

240. Roderburg, C. *et al.* Micro-RNA profiling reveals a role for miR-29 in human and murine liver fibrosis. *Hepatology* **53,** 209–218 (2011).

241. Cushing, L. *et al.* miR-29 Is a Major Regulator of Genes Associated with Pulmonary Fibrosis. *Am. J. Respir. Cell Mol. Biol.* **45,** 287–294 (2011).

242. van Rooij, E. *et al.* Dysregulation of microRNAs after myocardial infarction reveals a role of miR-29 in cardiac fibrosis. *Proc. Natl. Acad. Sci.* **105,** 13027–13032 (2008).

243. Kondiah, P. J. *et al.* A review of injectable polymeric hydrogel systems for application in bone tissue engineering. *Molecules* **21,** (2016).

244. PANYAM, J. Rapid endo-lysosomal escape of poly(DL-lactide-co-glycolide) nanoparticles: implications for drug and gene delivery. *FASEB J.* **16,** 1217–1226 (2002).

245. Panyam, J. & Labhasetwar, V. Biodegradable nanoparticles for drug and gene delivery to cells and tissue. *Adv. Drug Deliv. Rev.* **55,** 329–347 (2003).

246. Shu, L., Zhang, H., Boyce, B. F. & Xing, L. Ubiquitin E3 ligase Wwp1 negatively regulates osteoblast function by inhibiting osteoblast differentiation and migration. *J. Bone Miner. Res.* **28,** 1925–1935 (2013).

247. Katsaros, K. M. *et al.* Increased Restenosis Rate After Implantation of Drug-Eluting Stents in

Patients With Elevated Serum Activity of Matrix Metalloproteinase-2 and -9. *JACC Cardiovasc. Interv.* **3,** 90–97 (2010).

248. Monaghan, M. G. *et al.* Exogenous miR-29B Delivery Through a Hyaluronan-Based Injectable System Yields Functional Maintenance of the Infarcted Myocardium. *Tissue Eng. Part A* **0,** 1–11 (2017).
249. Mather, B. D., Viswanathan, K., Miller, K. M. & Long, T. E. Michael addition reactions in macromolecular design for emerging technologies. *Prog. Polym. Sci.* **31,** 487–531 (2006).
250. Lutolf, M. P., Tirelli, N., Cerritelli, S., Cavalli, L. & Hubbell, J. A. Systematic modulation of Michael-type reactivity of thiols through the use of charged amino acids. *Bioconjug. Chem.* **12,** 1051–1056 (2001).
251. Lutolf, M. P. & Hubbell, J. a. Synthesis and Physicochemical Characterization of End-Linked Poly(ethylene glycol)- co -peptide Hydrogels Formed by Michael-Type Addition. *Biomacromolecules* **4,** 713–722 (2003).
252. Lutolf, M. P. *et al.* Repair of bone defects using synthetic mimetics of collagenous extracellular matrices. *Nat. Biotechnol.* **21,** 513–8 (2003).
253. Dobner, S., Bezuidenhout, D., Govender, P., Zilla, P. & Davies, N. A Synthetic Non-degradable Polyethylene Glycol Hydrogel Retards Adverse Post-infarct Left Ventricular Remodeling. *J. Card. Fail.* **15,** 629–636 (2009).
254. Kadner, K. *et al.* The beneficial effects of deferred delivery on the efficiency of hydrogel therapy post myocardial infarction. *Biomaterials* **33,** 2060–2066 (2012).
255. Johnson, N. R. *et al.* Coacervate Delivery of Growth Factors Combined with a Degradable Hydrogel Preserves Heart Function after Myocardial Infarction. *ACS Biomater. Sci. Eng.* **1,** 753–759 (2015).
256. Gautam, A., Densmore, C. L., Xu, B. & Waldrep, J. C. Enhanced Gene Expression in Mouse Lung after PEI–DNA Aerosol Delivery. *Mol. Ther.* **2,** 63–70 (2000).
257. Huang, W. *et al.* Site-specific RNase A activity was dramatically reduced in serum from multiple types of cancer patients. *PLoS One* **9,** 3–10 (2014).
258. Shen, Y. *et al.* Efficient protection and transfection of small interfering RNA by cationic shell-crosslinked knedel-like nanoparticles. *Nucleic Acid Ther.* **23,** 95–108 (2013).
259. Bartlett, D. W. & Davis, M. E. Effect of siRNA nuclease stability on the in vitro and in vivo kinetics of siRNA-mediated gene silencing. *Biotechnol. Bioeng.* **97,** 909–921 (2007).
260. Corporation, P. CellTiter-Glo ® Luminescent Cell Viability Assay. (2012).
261. Crouch, S. P. M., Kozlowski, R., Slater, K. J. & Fletcher, J. The use of ATP bioluminescence as a measure of cell proliferation and cytotoxicity. *Journal of Immunological Methods* **160,** 81–88

(1993).

262. Ruoslahti, E. & Pierschbacher, M. New perspectives in cell adhesion: RGD and integrins. *Science (80-.).* **238,** 491–497 (1987).

263. Höbel, S. & Aigner, A. in (eds. Min, W.-P. & Ichim, T.) **623,** 283–297 (Humana Press, 2010).

264. Haupenthal, J., Baehr, C., Kiermayer, S., Zeuzem, S. & Piiper, A. Inhibition of RNAse A family enzymes prevents degradation and loss of silencing activity of siRNAs in serum. *Biochem. Pharmacol.* **71,** 702–710 (2006).

265. Gary, D. J., Puri, N. & Won, Y.-Y. Polymer-based siRNA delivery: Perspectives on the fundamental and phenomenological distinctions from polymer-based DNA delivery. *J. Control. Release* **121,** 64–73 (2007).

266. Banan, M. & Puri, N. The Ins and Outs of RNAi in Mammalian Cells. *Curr. Pharm. Biotechnol.* **5,** 441–450 (2004).

267. Shen, Y. *et al.* Efficient protection and transfection of small interfering RNA by cationic shell-crosslinked knedel-like nanoparticles. *Nucleic Acid Ther.* **23,** 95–108 (2013).

268. Moghimi, S. M. *et al.* A two-stage poly(ethylenimine)-mediated cytotoxicity: Implications for gene transfer/therapy. *Mol. Ther.* **11,** 990–995 (2005).

269. Fischer, D. *et al.* Copolymers of ethylene imine and N-(2-hydroxyethyl)-ethylene imine as tools to study effects of polymer structure on physicochemical and biological properties of DNA complexes. *Bioconjug. Chem.* **13,** 1124–1133 (2002).

270. Kwok, A. & Hart, S. L. Comparative structural and functional studies of nanoparticle formulations for DNA and siRNA delivery. *Nanomedicine* **7,** 210–9 (2011).

271. Bishop, N. E. An Update on Non-clathrin-coated Endocytosis. *Rev. Med. Virol.* **7,** 199--209 (1997).

272. Oupický, D., Konák, C., Ulbrich, K., Wolfert, M. A. & Seymour, L. W. DNA delivery systems based on complexes of DNA with synthetic polycations and their copolymers. *J. Control. Release* **65,** 149–71 (2000).

273. Sharma, V. K., Thomas, M. & Klibanov, A. M. Mechanistic studies on aggregation of polyethylenimine-DNA complexes and its prevention. *Biotechnol. Bioeng.* **90,** 614–620 (2005).

274. Sundaram, S., Viriyayuthakorn, S. & Roth, C. M. Oligonucleotide Structure Influences the Interactions between Cationic Polymers and Oligonucleotides. *Biomacromolecules* **6,** 2961–2968 (2005).

275. Sarett, S. M., Nelson, C. E. & Duvall, C. L. Technologies for controlled, local delivery of siRNA. *J. Control. Release* **218,** 94–113 (2015).

276. Nikolaev, Y. A. & Panikov, N. S. Extracellular protease as a reversible adhesion regulator in

Pseudomonas fluorescens. *Microbiology* **71,** 541–545 (2002).

277. Grinnell, F., B. Rocha, L., Iucu, C., Rhee, S. & Jiang, H. Nested collagen matrices: A new model to study migration of human fibroblast populations in three dimensions. *Exp. Cell Res.* **312,** 86–94 (2006).
278. Bell, E., Ivarsson, B. & Merrill, C. Production of a tissue-like structure by contraction of collagen lattices by human fibroblasts of different proliferative potential in vitro. *Proc. Natl. Acad. Sci.* **76,** 1274–1278 (1979).
279. Bell, E., Ivarsson, B. & Merrill, C. Production of a tissue-like structure by contraction of collagen lattices by human fibroblasts of different proliferative potential in vitro. *Proc. Natl. Acad. Sci. U. S. A.* **76,** 1274–8 (1979).
280. Bell, E., Ehrlich, H. P., Buttle, D. J. & Nakatsuji, T. Living tissue formed in vitro and accepted as skin-equivalent tissue of full thickness. *Science (80-.).* **211,** 1052 LP-1054 (1981).
281. Schor, S. L. Cell proliferation and migration on collagen substrata in vitro. *J. Cell Sci.* **41,** 159–75 (1980).
282. Sabeh, F. *et al.* Tumor cell traffic through the extracellular matrix is controlled by the membrane-anchored collagenase MT1-MMP. *J. Cell Biol.* **167,** 769–781 (2004).
283. Helary, C., Foucault-Bertaud, A., Godeau, G., Coulomb, B. & Giraud Guille, M. M. Fibroblast populated dense collagen matrices: Cell migration, cell density and metalloproteinases expression. *Biomaterials* **26,** 1533–1543 (2005).

6. Appendices

A1: Reagents and Equipment

Table A1.1: Reagents

Product	Producer / Supplier	Product Catalogue Number
Actin Red™ ReadyProbes® Reagent	Life Technologies	R37112 lot 174846
Agarose (SeaKem LE)	Lonza, Rockland, ME	50004 (500 g)
AllStars Negative Control siRNA AF488 20 nmol	Qiagen, Hilden, Germany	1027292
AllStars Negative Control siRNA AF555 20 nmol	Qiagen, Hilden, Germany	1027294
AllStars Hs Death siRNA 20 nmol	Qiagen, Hilden, Germany	1027299
Boric Acid	Sigma-Aldrich®, St Louis, MO	B0394-1KG
Cell Titre Glo® Luminescent Cell Viability Assay	Promega®, Madison, WI	G7571 (10 × 10 ml)
Diethyl Pyrocarbonate (DEPC)	Sigma-Aldrich®, St Louis, MO	D5758-100ML
Dimethyl Sulfoxide (DMSO)	Sigma-Aldrich®, St Louis, MO	D2650-5X1ML
DL-Dithiothreitol	Sigma-Aldrich®, St Louis, MO	D5545-1KG
DMEM	Sigma-Aldrich®, St Louis, MO	D5648-10X1L
EDTA – disodium salt dehydrate 99%	Sigma-Aldrich®, Germany	E5134-500G
EDTA – trisodium salt min. 95%	Sigma-Aldrich®, St Louis, MO	ED3SS-500G
Foetal Bovine Serum (FBS) (gamma irradiated) - 1	Gibco® by Life Technologies™, Paisley, UK	10499-044 (500 ml)
Foetal Bovine Serum (FBS) Superior (heat inactivated) - 2	Biochrom GmbH, Berlin, Germany	S0615 (500 ml)
Gel Red Nucleic Acid Gel Stain (10'000X in water)	Biotium, Hayward, CA	41003 (0.5 ml)
GoTaq® Flexi Buffer 5X	Promega, Madison, WI	M791B
Lipofectamine RNAi Max	ThermoFisher Scientific	13778030 (0.3 ml)
MCDB-131 Medium	Sigma-Aldrich, St Louis, MO	M8537
MMP-1 (GCREGPQGIWGQERCG, MW = 1732.91 g/mol)	GenScript USA Inc., Piscataway, NJ	U5878BB230-1 (100 mg per vile)
Negative control siRNA (this siRNA has a scrambled sequence and as such its presence no effect on cellular activity)	Bioneer Corp., Daedeok District, South Korea	SN-1015
Hepes (25g)	Sigma-Aldrich®, St Louis, MO	H4034-25G
Heparin NaCl	Sigma-Aldrich®, St Louis, MO	H3393-50KU
Hydrochloric acid (HCl), 25% w/v	Riedel-deHaën, Germany	30723 (2.5 L)
20PEG8-OH	Nektar Therapeutics AL, Coperration, AL	0J000P08
20PEG4-OH	Nektar Therapeutics AL, Coperration, AL	0J000P04
Penicillin Streptomycin (10 000 U penicillin and 10 mg streptomycin / ml)	Sigma-Aldrich®, St Louis, MO	P0781 (100X concentration)
Penicillin Streptomycin (10 000 U/ml / 10 000 µg/ml)	Gibco® by Life Technologies	15140-122 (100 ml)
Polyethylenimine (PEI) Branched 100ml 25 KDa,.	Sigma-Aldrich®, St Louis, MO	408727-100ML
RGD (GCGYGRGDSPG, MW = 1025.06g/mol)	GenicBio Synthetic Peptide, Shanghai, China	No catalogue number, 100mg
Sigmacote	Sigma-Aldrich®, St Louis, MO	SL2-25ML
Sodium Bicarbonate ($NaHCO_3$)	Sigma-Aldrich®, St Louis, MO	S-5761-1KG
Sodium Chloride (NaCl)	Sigma-Aldrich®, St Louis, MO	S-7653-1KG
Sodium Dodecyl Sulfate – SDS	Sigma-Aldrich®, St Louis, MO	L3771-100G

Sodium Hydroxide (NaOH)	Sigma-Aldrich®, St Louis, MO	S-5881-500G
Sodium Phosphate Dibasic Dodecahydrate ($Na_2HPO_4.12H_2O$) 500g	Sigma-Aldrich®, St Louis, MO	71649-500G
Sodium Phosphate Monobasic Monohydrate ($NaH_2PO_4.H_2O$)	Sigma-Aldrich®, St Louis, MO	S9638-500G
Triethanolamine (TEOA) 99%	Saarchem-Holpro Analytic, Krugersdorp, South Africa	6112040 (2.5 L)
Trypan Blue	Sigma-Aldrich®, St Louis, MO	T8154-100ML
Trizma Base® 500g	Sigma-Aldrich®, St Louis, MO	T6066-500G
Trypsin (2.5%) (10X) GI 100ml	Sigma-Aldrich®, St Louis, MO	59427C-100ML

Table A1.2: Consumables & Cells

Product	**Producer / Supplier**	**Product Catalogue Number**
24-well cell culture cluster, clear, flat bottomed, sterile tissue culture treated	Costar® by Corning Incorporated, NY	3524
96-well cell culture cluster, clear, flat bottomed, sterile	Costar by Corning Incorporated, NY	3595
96-well opaque flat bottomed non-sterile plate	Nunc® MicroWell, Roskilde, Denmark by Sigma,	Z688665 or P8616
96-well non-tc treated	Nunc® MicroWell Roskilde, Denmark by Sigma	260887
Cell culture flask, surface area 25 cm^2, canted neck, cap (vented)	Corning Inc. Corning, NY	CLS430639
Centrifuge tube (50 ml)	Falcon by BD Biosciences, San Jose, CA	352070
Centrifuge tube (15 ml)	Falcon by BD Biosciences, San Jose, CA	352096
Cuvette Pack of 100 with stoppers (40 µl)	Malvern Instruments LTD., Worcestershire, UK	ZEN0040
Filter, syringe filter unit (0.2 µm)	Abluo™, GVS Lifesciences, Sanford, ME	FJ25ASCCA002DL01
Filter, low-protein binding (0.22 µm PES, 250 ml) for cell culture media	Millipore® Stericup™ (polyethersulfone membrane, Millipore Express PLUS), Merck KGaA, Darmstadt, Germany	Z660493 – Sigma SCGPU02RE – Merck
Folded Capillary Cells – Pack of 10	Malvern Instruments LTD., Worcestershire, UK	DTS1061, now replaced by DTS1070
HT1080 cells	ATCC, Manassas, VA, USA	-
Micro centrifuge tube (with screw cap) for freeze-drying samples	Corning Incorporated, Nuevo Leon, Mexico	430909
Micro centrifuge tube (graduated) with flat cap (0.6 ml)	Thermo Scientific QSP, San Diego, CA	502-GRD-Q
Micro centrifuge tube (graduated) with flat cap (1.5 ml)	Thermo Scientific QSP, San Diego, CA	509-GRD-Q
Micro centrifuge tube (graduated) with flat locking cap (2 ml)	Thermo Scientific QSP, San Diego, CA	L-508GRD-Q
Parafilm M® 4 in. X 250 ft. roll	Bemis NA, Neenah, WI	PM 999

Table A1.3: Equipment and Software

Product	**Producer / Supplier**
AxioVision 4.8	Carl Zeiss Microscopy GmbH, Göttingen, Germany
Cary Eclips, Fluorescence Spectrophotometer	Varian, Palto Alto, CA
Centrifuge (Megafuge 1.0R)	Heraeus Sepatech, Hanau, Germany
Centrifuge 5415R (for micro centrifuge tubes)	Eppendorf, Hamburg, Germany
Freeze Dryer - Virtis	SP Industries, Gardiner, NY
GeneSys image capture and manipulation software with GeneTools software	Syngene, Cambridge, England
Glomax 96 Luminometer	Promega, Madison, WI
Haemocytometer	Improved Neubauer, Baxter Scientific
Mini Sub-Cell® GT Agarose Gel Electrophoresis system	Bio-Rad Laborities (PTY) LTD, Johannesburg, South Africa
MCO-175M, O_2/CO_2 Incubator	Osaka Sanyo Electric Co., Japan
Incubator (37 °C) for tissue culture	HERA cell by Heraeus, Hanau, Germany
	MCO-175M, O2/CO2 Incubator, Osaka Sanyo Electric Co., Japan
Laminar Flow Hood (Microbiological Safety Cabinet Class II, model 4B2)	Labaire Manufacturing Company, (Pty), Ltd, Mt Edgcombe, South Africa
Nikon Fluorescent Microscope (Nikon Eclipse90i DS-Ri1)	Nikon, Tokyo, Japan
Nikon Light microscope (Nikon Eclipse Ti-S)	Nikon, Tokyo Japan
pH meter (3510 pH meter)	Jenway by Bibby Scientific, Staffs, UK
Pipettes	Gilson, Inc. Middleton, WI
Power Pack	Bio-Rad Laboratories (PTY) LTD, Johannesburg, South Africa
Manual Gel Documentation (InGenius3)	Syngene, Cambridge, England
Mini Sub-Cell® GT Agarose Gel Electrophoresis system	Bio-Rad Laboratories (PTY) LTD, Johannesburg, South Africa
Motic Image Plus 2.0	Motic, Hongkong
NIS-Elements BR 2.30	Nikon instruments Inc, Melville, NY
Shaking incubator	IncoShake by Labotech, Cape Town, South Africa
Water Bath (Grant Y14 water bath)	Grant Instruments, Cambridge, England
Zeiss Axiovert 200M Inverted Fluorescent Microscope	Carl Zeiss Microscopy GmbH, Göttingen, Germany
Zeiss 510 LSM with MaiTai two photon laser	Carl Zeiss Microscopy GmbH, Göttingen, Germany
Zetasizer Nano-Zs (ZEN3600)	Malvern Instruments LTD., Worcestershire, UK
37°C incubator for tissue culture	MCO-175M, O2/CO2 Incubator, Osaka Sanyo Electric Co., Japan
	Heraeus, Hanau, Germany
-65°C freezer	Snijders Scientific, Holland

A2: Recipes and instructions for buffers and other reagents

Table A2.1: Components and recipes of various commonly used buffers and reagents.

Solution	Components	
Agarose gel – 4% (m/v)	4 g Agarose / 100 ml TBE Add ± 10 ml Barnstead Nanopure H_2O extra Microwave until agarose dissolved	
Calcium chloride ($CaCl_2$)	55.5 g $CaCl_2$ / 50 ml Nanopure H_2O (100 mM)	
DMEM, pH 7.4	13.4 g powdered DMEM medium, 3.7 g $NaHCO_3$ per 1 L Barnstead Nanopure H_2O	
DEPC treated Barnstead Nanopure Water	0.05% (v/v) solution Autoclave	
EDTA (ethylenediamine tetraacitic acid), pH 8.0	37.22 g $Na_2EDTA.2\ H_2O$ / 200 ml Barnstead Nanopure H_2O (0.5M)	
Isotonic Phosphate Buffered Saline (PBS) – Calcium and Magnesium free	2.9 g/L $Na_2HPO_4.12H_2O$ (8 mM), 0.2 g/L KH_2PO_4 (1.4 mM), 0.2 g/L KCl (2.7 mM), 8 g/L NaCl (137 mM)	
	Sterilise by autoclaving or by using a 0.22 µm cutoff low protein binding bottle top filter	
Iso-Osmotic PBS	Sol A: 20.7 g/L $NaH_2PO_4.H_2O$ (0.15M) Sol B: 53.7 g/L $Na_2HPO_4.12H_2O$ NaCl: 9 g/L NaCl (0.15M)	Combine 65 ml Sol A with 435 ml Sol B and 500 ml NaCl. pH using Sol A or B only. pH to 7.5
	Sterilise by autoclaving or by using a 0.22 µm cutoff low protein binding bottle top filter	
Hepes Buffered Saline (HBS) pH 7.4-7.5	0.595 g Hepes (25 mM), 0.82 g NaCl (140 mM) / 100 ml Barnstead Nanopure H_2O	
Loading dye	3 µl Gel Red was added to 1 ml 5X Green GoTaq® Flexi Buffer	
MCDB-131 Medium pH 7.4	11.6 g MCDB-131 powdered medium, 1.18 g $NaHCO_3$ / 1 L Sterilise using a 0.22 µm cutoff low protein binding bottle top filter - stored at 4˚C	
Penicillin / Streptomycin	Arrived pre-prepared, Stored 1 ml aliquots at -20°C	
Proteinase K – 10 mg/ml stock	25 mg Proteinase K allowed to defrost at room temperature Dissolve in 2.5 ml 10 mM Tris-Cl pH 7.3 Store in 100.2 µl aliquots at -65°C. Stored in non-activated form	
Sodium Hydroxide (NaOH) 10 M	39.997 g NaOH / 100 ml Barnstead Nanopure H_2O Dissolve NaOH in 100 ml H_2O overnight, on ice while being stirred.	
Sodium Dodecyl Sulfate (SDS) – 10 %	10 g SDS / 100 ml nanopure H_2O	
Triethanolamine (TEOA) – 0.3 M, pH 7.4	2.24 g 99% TEOA / 50 ml Barnstead Nanopure H_2O Highly viscous ∴ must dilute in same container it is weighed out in. pH to 7.4 with HCl	
Tris/borate/EDTA (TBE) electrophoresis buffer 10X, pH 8.3	108 g Trisma® base (890 mM), 55 g Boric acid (890 mM), 40 ml 0.5 M EDTA (pH 8.0) (0.02M) / 1 L Nanopure H_2O, Sterilise by autoclave	
TRIS	1.2114 g Trisma®-Base (100 mM) / 100 ml Barnstead Nanopure H_2O Do not pH	
TRIS-Cl –10 mM, pH 7.3	10 ml 100 mM Tris / 100 ml Nanopure H_2O (v/v), pH with 6 N & 1 N HCl to 7.3	
Trypan Blue	0.4% (m/v) in PBS. Arrived pre-prepared	
Trypsin / EDTA	100 ml Trypsin / EDTA was made up to 1 L with either Barnstead Nanopure H_2O or 1X PBS pH 7.4 depending on how it arrived Stored at -20°C in 12 ml aliquots.	

Table A2.2: Preparation for collagen hydrogels – components and recipes

Bovine collagen	Arrived in liquid form from the supplier therefore no preparation required. Store at 4°C.
Rat tail collagen	Arrived lyophilised and was resuspended sterile 0.2% acetic acid (v/v) overnight at room temperature. Special attention was made to not agitate the bottle. Once resuspended collagen was store at 4°C.
Acetic acid – 0.2% (v/v)	100.3 µl 99.7% acetic acid in 50 ml Barnstead Nanopure H_2O Sterilise using 0.2 µm syringe filters

DMEM - 10X, pH 7.4	13.4 g DMEM powder / 100 ml Barnstead Nanopure H_2O pH to 0.1-0.3 pH units below 7.4 with 1 N HCl or 1 N NaOH.
DMEM - 100ml, 1X, pH 10,	10 ml 10X DMEM (pH 7.4), 10 ml $NaHCO_3$ (23 mg / ml) pH to 10 with 1 N NaOH 80 ml nanopure H_2O
$NaHCO_3$ (23 mg / ml)	0.23 g $NaHCO_3$ / 10 ml nanopure H_2O
NaOH (0.36 M)	144 µl 10 M NaOH 3856 µl nanopure H_2O
	All reagents (except the collagen) were individually sterilised using separate 0.2 µm syringe filters. 10X DMEM and 1X DMEM were stored as 1 ml aliquots at -20°C. The $NaCHO_3$ and NaOH were stored at 4°C.

Table A2.3: Recipe and components of 6.68 mh/ml Proteinase K for PEG hydrogel digestion

	Volume
Proteinase K 10 mg / ml stock	100.2 µl
$CaCl_2$ 100 mM	10.02 µl
10 mM Tris pH	39.78 µl

*Proteinase K is activated in the presence of 1-5 mM Ca^{2+}.

Table A2.4: Table according to which PEG hydrogels were digested

	Volume
Hydrogel	20 µl
Proteinase K 6.68 mg/ml	10 µl
SDS 6.5%	5 µl

A3: Siliconized surfaces

Different surfaces were siliconized using Sigmacote®. Between 500 µl and 3 ml of Sigmacote® was used to cover the surface of a petri dish or tissue culture plate being siliconized. After 1 minute the Sigmacoate® was removed and the surface allowed to dry overnight. The surface was then rinsed 2X with DEPC treated H_2O and allowed to dry. Once dry the surface was polished with a lint free cloth. To remove any dust or in the case of tissue culture plates which had been score, a high pressure air hose was to remove any excess plastic or dust. Plate or petri dish was then sterillsed with ethylene oxide.

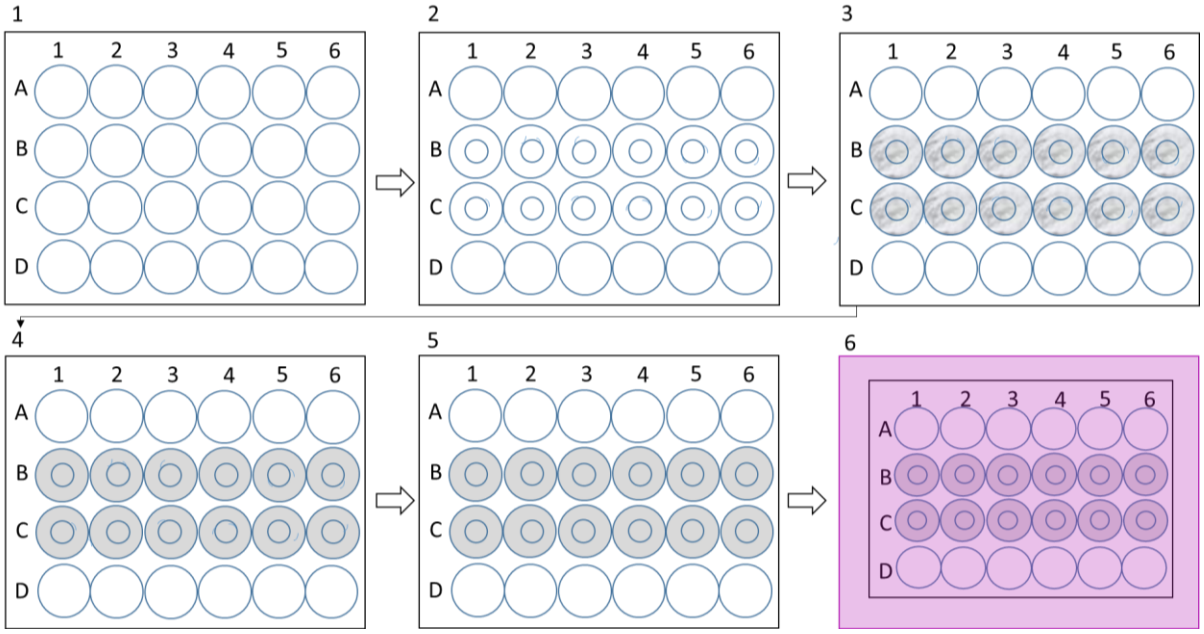

Figure A3.1: 24 well plate preparation. The plates were prepared in the laminar flow hood as much as possible to limit contamination. 1. Sterile 24 well plate. 2. Specially made surgical punch was used to score the centre of each well. 3. Wells were siliconised with Sigmacote®. 4. A lint free cloth was used to polish wells. 5. High pressure air hose was used to get rid of any plastic shards. 6. Plate was sterilised by gas (ethylene oxide).

A4: Size and Zeta Potential reports

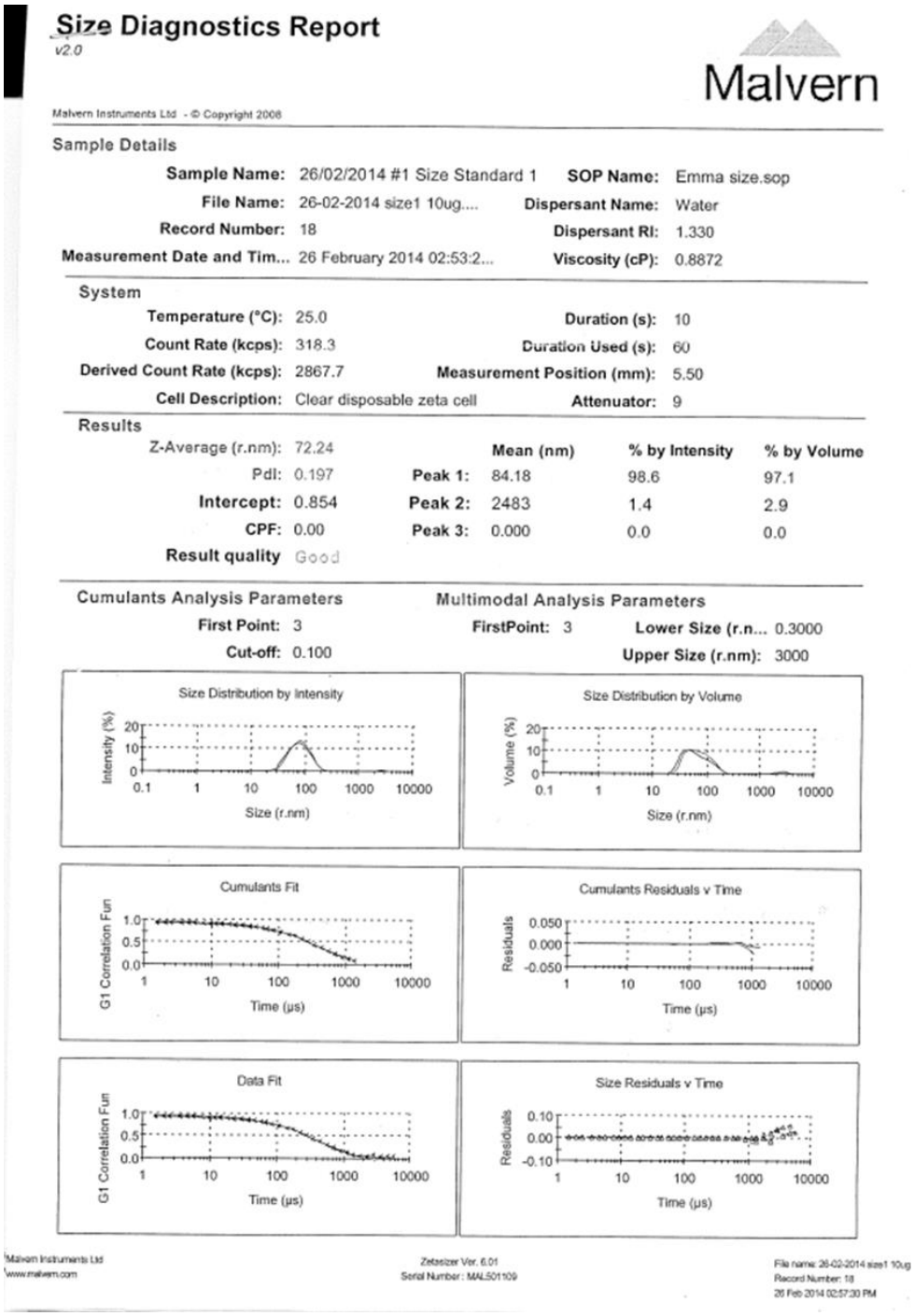

Size Diagnostics Report
v2.0

Malvern

Sample Details

Sample Name:	26/02/2014 #1 Size Standard 1	**SOP Name:**	Emma size.sop
File Name:	26-02-2014 size1 10ug....	**Dispersant Name:**	Water
Record Number:	18	**Dispersant RI:**	1.330
Measurement Date and Tim...	26 February 2014 02:53:2...	**Viscosity (cP):**	0.8872

System

Temperature (°C):	25.0	**Duration (s):**	10
Count Rate (kcps):	318.3	**Duration Used (s):**	60
Derived Count Rate (kcps):	2867.7	**Measurement Position (mm):**	5.50
Cell Description:	Clear disposable zeta cell	**Attenuator:**	9

Results

Z-Average (r.nm):	72.24		**Mean (nm)**	**% by Intensity**	**% by Volume**
PdI:	0.197	**Peak 1:**	84.18	98.6	97.1
Intercept:	0.854	**Peak 2:**	2483	1.4	2.9
CPF:	0.00	**Peak 3:**	0.000	0.0	0.0
Result quality	Good				

Cumulants Analysis Parameters

First Point: 3
Cut-off: 0.100

Multimodal Analysis Parameters

FirstPoint: 3 **Lower Size (r.n...** 0.3000
Upper Size (r.nm): 3000

Malvern Instruments Ltd
www.malvern.com

Zetasizer Ver. 6.01
Serial Number : MAL501109

File name: 26-02-2014 size1 10ug
Record Number: 18
26 Feb 2014 02:57:30 PM

...eta Potential Report

v2.2

Malvern

Sample Details

Sample Name: 20:1 08/08/2013 Zeta 1
SOP Name: Emma zeta.sop
General Notes:

File Name: 26-02-2014 size1 10ug.dts
Record Number: 25
Date and Time: 26 February 2014 03:13:03 PM
Dispersant Name: Water
Dispersant RI: 1.330
Viscosity (cP): 0.8872
Dispersant Dielectric Const... 78.5

System

Temperature (°C): 25.0
Count Rate (kcps): 36.5
Cell Description: Clear disposable zeta ...
Zeta Runs: 12
Measurement Position (mm): 2.00
Attenuator: 11

Results

			Mean (mV)	Area (%)	Width (mV)
Zeta Potential (mV):	56.7	**Peak 1:**	56.7	100.0	6.22
Zeta Deviation (mV):	6.22	**Peak 2:**	0.00	0.0	0.00
Conductivity (mS/c...	0.0301	**Peak 3:**	0.00	0.0	0.00
Result quality	Good				

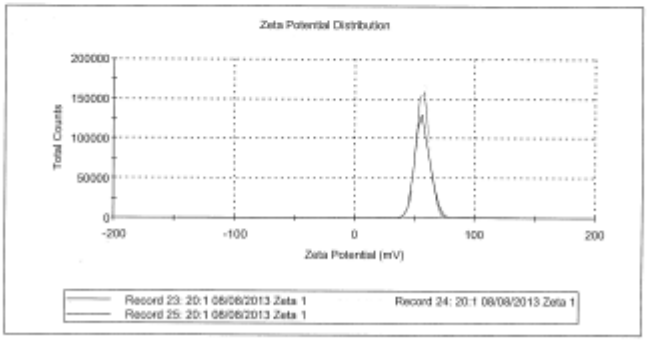

A5: Incubation of PEG monomer with 20:1 PEI/siRNA nanoparticles

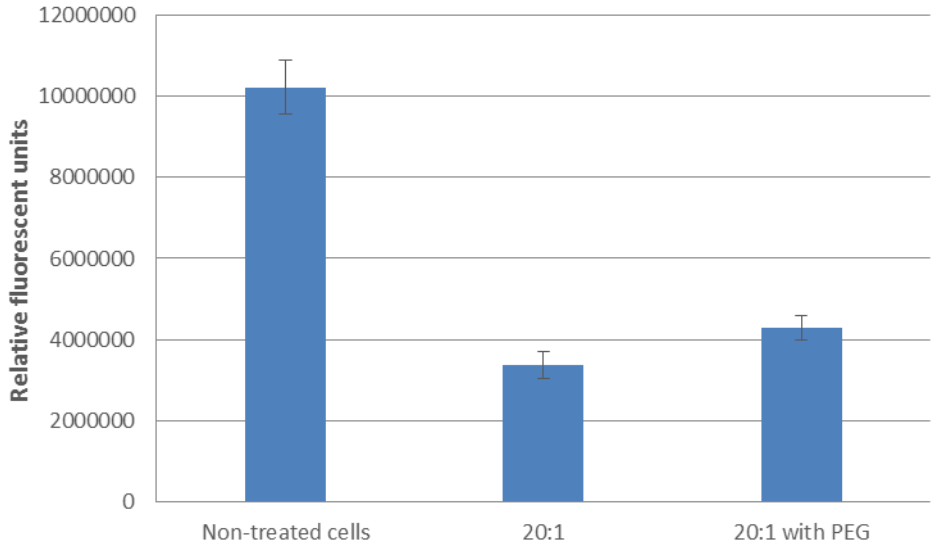

Figure A5.1: Incubation of PEG monomer with 20:1 PEI/siRNA nanoparticles. The PEG monomer was incubated for 30 minutes with the nanoparticles prior to transfection.